

LECTURE NOTES

ON

AEROSPACE PROPULSION

M.Tech I Semester

Prepared by

Mr. Shiva Prasad U,
Assistant Professor



AERONAUTICAL ENGINEERING

INSTITUTE OF AERONAUTICAL ENGINEERING

(Autonomous)

Dundigal, Hyderabad, Telangana -500 043

UNIT – I

AIR-BREATHING ENGINES

Propulsion

Propulsion (Lat. pro-pellere, push forward) is making a body to move (against natural forces), i.e. fighting against the natural tendency of relative-motion to decay. Motion is relative to an environment. Sometimes, propulsion is identified with thrust, the force pushing a body to move against natural forces, and one might say that propulsion is thrust (but thrust not necessary implies motion, as when pushing against a wall; on the other hand, propulsion implies thrust).

Sometimes a distinction is made from propulsion (pushing) to traction (pulling), but, leaving aside internal stresses in the system (compression in the first case and tension in the latter), push and pull motions produces the same effect: making a body to move against natural forces. In other occasions 'traction' is restricted to propulsion by shear forces on solid surfaces.

The special case of creating aerodynamic thrust to just balance gravitational attraction of a vehicle without solid contact (e.g. hovering helicopters, hovering VTOL-aircraft, hovering rockets, hovering hovercraft...), is often included as propulsion (it is usually based on the same engine), though its propulsion efficiency is zero.

Operational envelopes

Each engine type will operate only within a certain range of altitudes and Mach numbers (velocities). Similar limitations in velocity and altitude exist for airframes. It is necessary, therefore, to match airframe and propulsion system capabilities.

Figure 1.1 shows the approximate velocity and altitude limits, or corridor of flight, within which airlift vehicles can operate. The corridor is bounded by a lift limit, a temperature limit, and an aerodynamic force limit. The lift limit is determined by the maximum level-flight altitude at a given velocity. The temperature limit is set by the structural thermal limits of the material used in construction of the aircraft. At any given altitude, the maximum velocity attained is temperature-limited by aerodynamic heating effects. At lower altitudes, velocity is limited by aerodynamic force loads rather than by temperature.

The operating regions of all aircraft lie within the flight corridor. The operating region of a particular aircraft within the corridor is determined by aircraft design, but it is a very small portion of the overall corridor. Superimposed on "the flight corridor in Fig. 1.1 are the operational envelopes of various powered aircraft. The operational limits of each propulsion system are determined by limitations of the components of the propulsion system and are shown in Fig. 1.2.

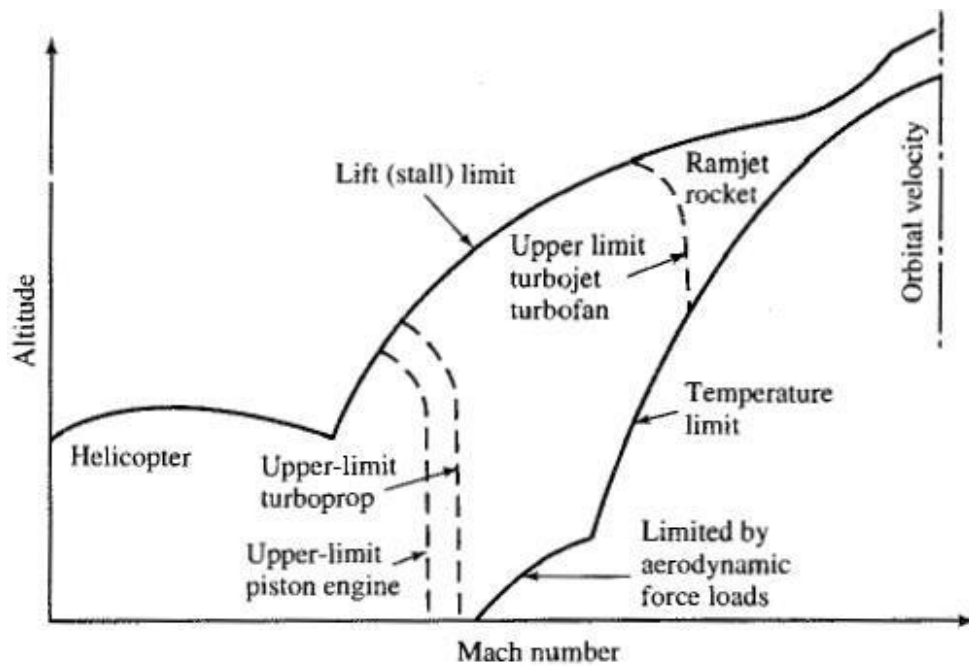


Fig.1.1: Flight limits.

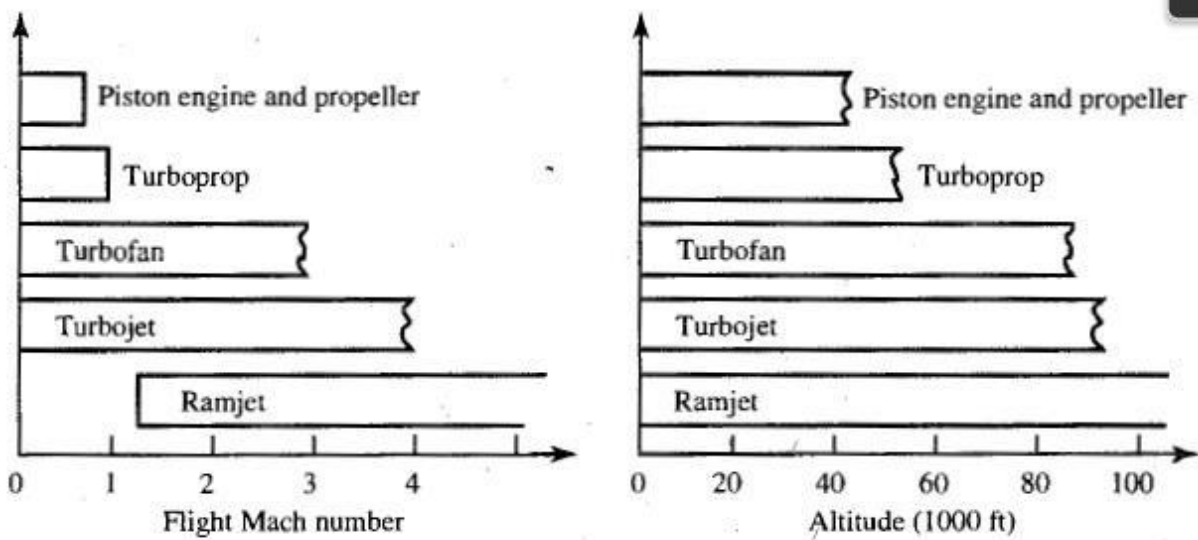


Fig.1.2: Engine operational limits.

Classification of air-breathing engine

The air-breathing engine classified into following types:

1. turbojet
2. turbofan
3. turboprop
4. turboshaft
5. ramjet
6. scramjet

Gas Generator

The "heart" of a gas turbine type of engine is the gas generator. A schematic diagram of a gas generator is shown in Fig. 1.3. The compressor, combustor, and turbine are the major components of the gas generator which is common to the turbojet, turbofan, turboprop, and turboshaft engines. The purpose of a gas generator is to supply high-temperature and high-pressure gas.

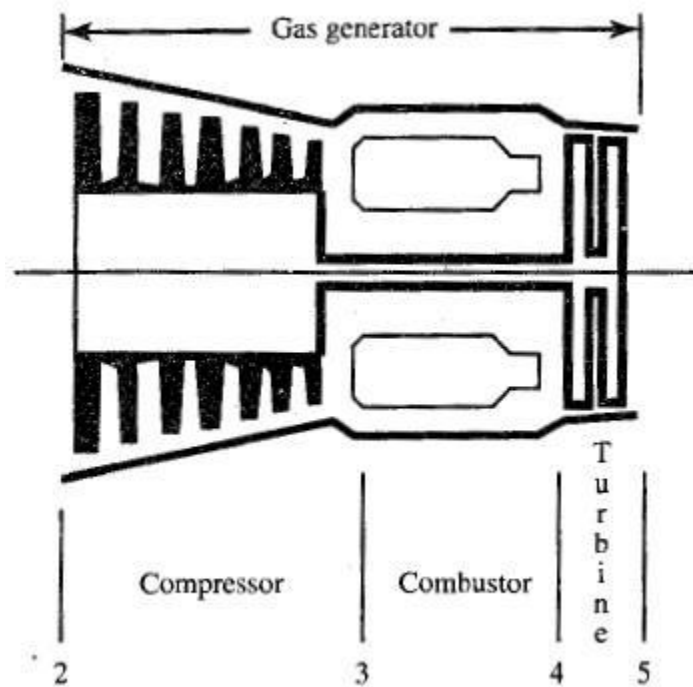


Fig.1.3:Schematic diagram of gas generator.

Turbojet engine

By adding an inlet and a nozzle to the gas generator, a turbojet engine can be constructed. A schematic diagram of a turbojet engine with an afterburner is shown in Fig. 1.4. The thrust of a turbojet is developed by compressing air in the inlet and compressor, mixing the air with fuel and burning in the combustor, and expanding the gas stream through the turbine and nozzle. The expansion of gas through the turbine supplies the power to turn the compressor. The net thrust delivered by the engine is the result of converting internal energy to kinetic energy.

The different processes in a turbojet cycle are the following:

- a-1: Air from far upstream is brought to the air intake (diffuser) with some acceleration/deceleration
- 1-2: Air is decelerated as it passes through the diffuser
- 2-3: Air is compressed in a compressor (axial or centrifugal)
- 3-4: The air is heated using a combustion chamber/burner
- 4-5: The air is expanded in a turbine to obtain power to drive the compressor
 - : The air may or may not be further heated in an afterburner by adding further fuel
- 6-7: The air is accelerated and exhausted through the nozzle to produce thrust.

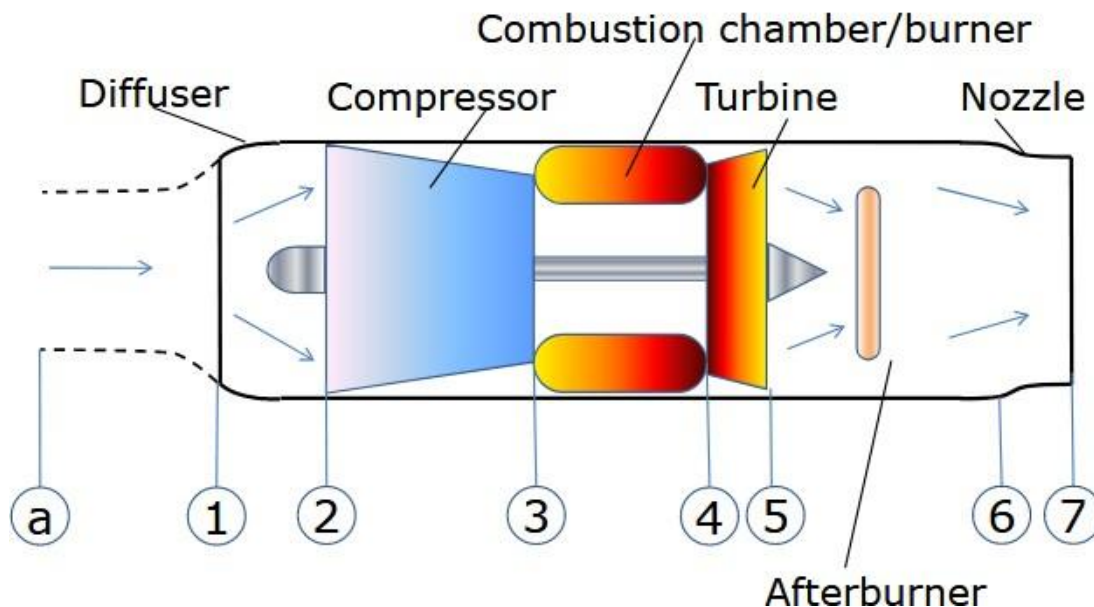


Fig.1.4: Turbo jet engine with after burner

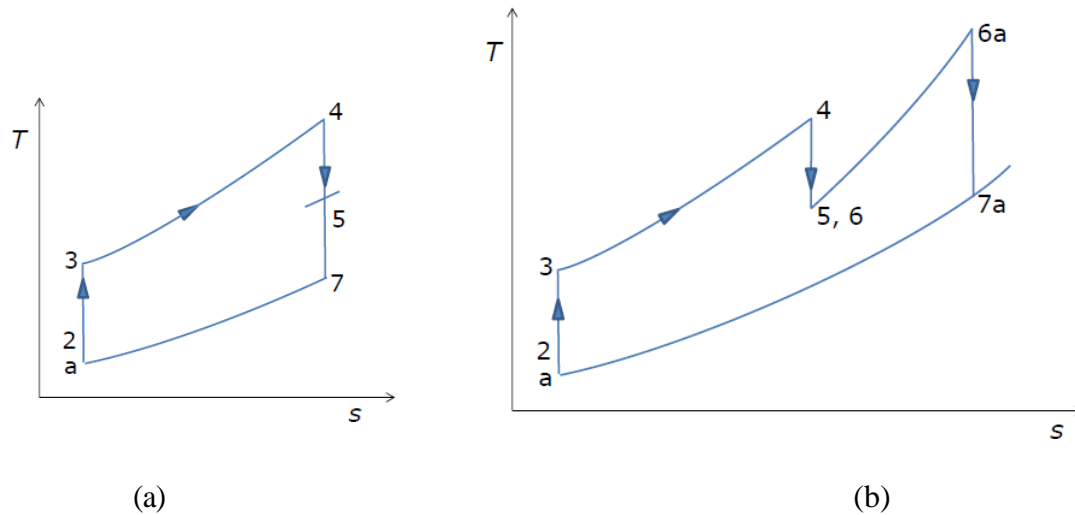


Fig.1.5: (a) Ideal turbojet cycle (without afterburning). (b) Ideal turbojet cycle with afterburning

Afterburning: used when the aircraft needs a substantial increment in thrust. For eg., To accelerate to and cruise at supersonic speeds. Since the air-fuel ratio in gas turbine engines are much greater than the stoichiometric values, there is sufficient amount of air available for combustion at the turbine exit. There are no rotating components like a turbine in the afterburner, the temperatures can be taken to much higher values than that at turbine entry.

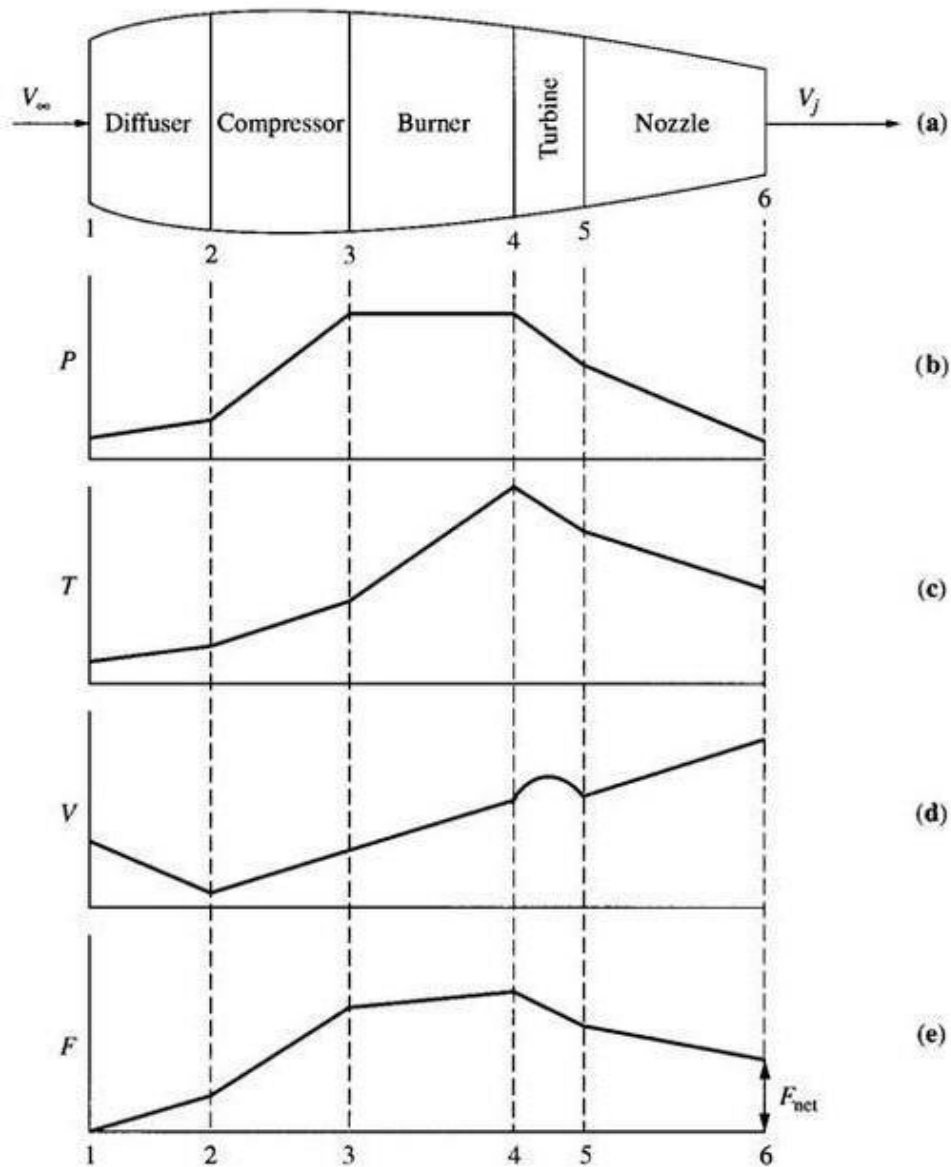


Fig.1.6: Variation of flow properties across turbojet engine

The pressure, temperature, and velocity variations through a jet engine are shown in Fig. 1.6. In the compressor section, the pressure and temperature increase as a result of work being done on the air. The temperature of the gas is further increased by burning in the combustor. In the turbine section, energy is being removed from the gas stream and converted to shaft power to turn the compressor. The energy is removed by an expansion process which results in a decrease of temperature and pressure. In the nozzle, the gas stream is further expanded to produce a high exit kinetic energy. All the sections of the engine must operate in such a way as to efficiently produce the greatest amount of thrust for a minimum of weight.

Turbo fan engine

The turbofan engine consists of an inlet, fan, gas generator, and nozzle. A schematic diagram of a turbofan is shown in Fig. 17. In the turbofan, a portion of the turbine work is used to supply power to the fan. Generally the turbofan engine is more economical and efficient than the turbojet engine in a limited realm of flight. The thrust specific fuel consumption (TSFC, or fuel mass flow rate per unit thrust) is lower for turbofans and indicates a more economical operation. The turbofan also accelerates a larger mass of air to a lower velocity than a turbojet for a higher propulsive efficiency. The frontal area of a turbofan is quite large compared to that of a turbojet, and for this reason more drag and more weight result. The fan diameter is also limited aerodynamically when compressibility effects occur.

Variation of flow properties across jet engine

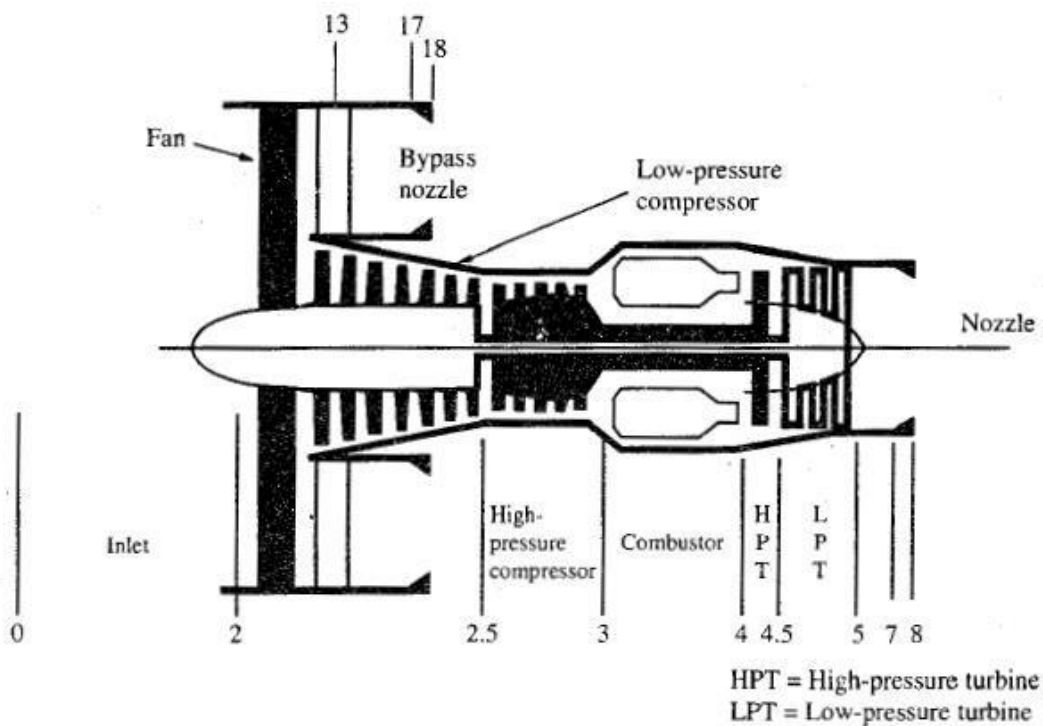


Fig.1.7: Schematic diagram of a high-bypass-ratio turbofan.

Bypass ratio

The bypass ratio (BPR) of a turbofan engine is the ratio between the mass flow rate of the bypass stream to the mass flow rate entering the core. A 10:1 bypass ratio, for example, means that 10 kg of air passes through the bypass duct for every 1 kg of air passing through the core.

The Turboprop and Turboshaft engine

A gas generator that drives a propeller is a turboprop engine. The expansion of gas through the turbine supplies the energy required to turn the propeller. A schematic diagram of the turboprop is shown in Fig. 1.8. The turboshaft engine is similar to the turboprop except that power is supplied to a shaft rather than a propeller. The turboshaft engine is used quite extensively for supplying power for helicopters. The turboprop engine may find application in VTOL (vertical takeoff and landing) transporters. The limitations and advantages of the turboprop are those of the propeller. For low-speed flight and, short-field takeoff, the propeller has a performance advantage. At speeds approaching the speed of sound, compressibility effects set in and the propeller loses its aerodynamic efficiency. Due to the rotation of the propeller, the propeller tip will approach the speed of sound before the vehicle approaches the speed of sound. This compressibility effect when one approaches the speed of sound limits the design of helicopter rotors and propellers. At high subsonic speeds, the turbofan engine will have a better aerodynamic performance than the turboprop since the turbofan is essentially a ducted turboprop. Putting a duct or shroud around a propeller increases its aerodynamic performance.

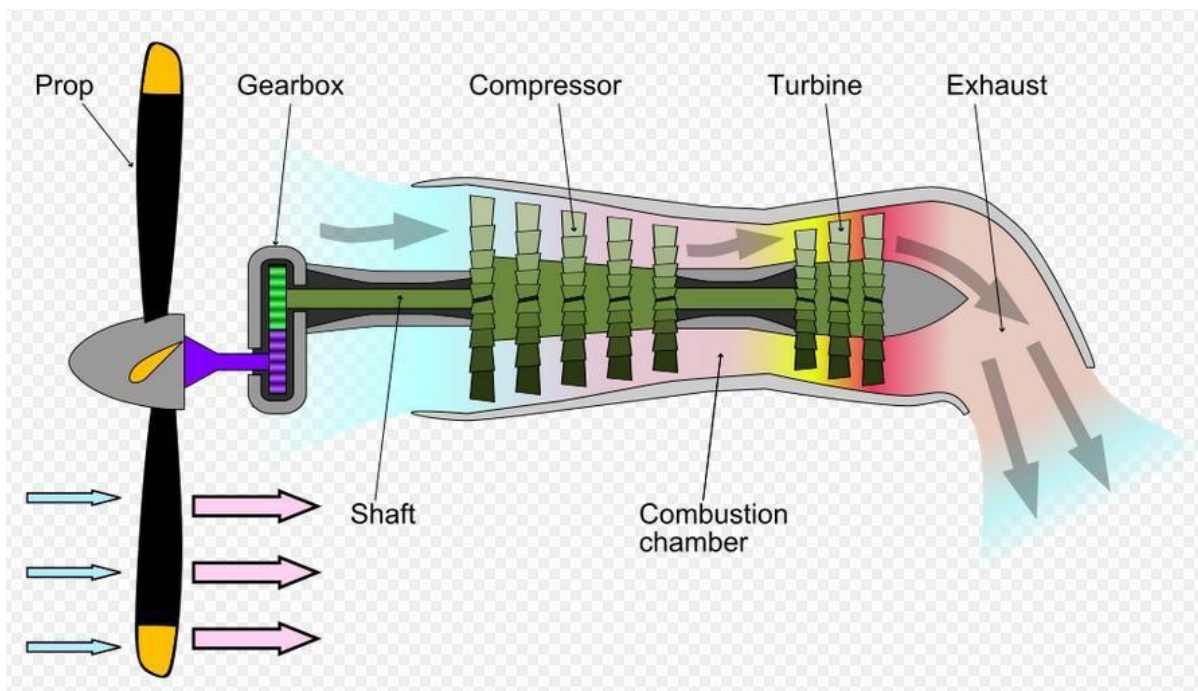


Fig.1.8:Schematic diagram of a turboprop.

The Ramjet

The ramjet engine consists of an inlet, a combustion zone, and a nozzle. A schematic diagram of a ramjet is shown in Fig. 1.9. The ramjet does not have the compressor and turbine as the turbojet does. Air enters the inlet where it is compressed and then enters the combustion zone where it is mixed with the fuel and burned. The hot gases are then expelled through the nozzle, developing thrust. The operation of the ramjet depends upon the inlet to decelerate the incoming air to raise the pressure in the combustion zone. The pressure rise makes it possible for the ramjet to operate. The higher the velocity of the incoming air, the greater the pressure rise. It is for this reason that the ramjet operates best at high supersonic velocities. At subsonic velocities, the ramjet is inefficient, and to start the ramjet, air at a relatively higher velocity must enter the inlet.

The combustion process in an ordinary ramjet takes place at low subsonic velocities. At high supersonic flight velocities, a very large pressure rise is developed that is more than sufficient to support operation of the ramjet. Also, if the inlet has to decelerate a supersonic high-velocity airstream to a subsonic velocity, large pressure losses can result. The deceleration process also produces a temperature rise, and at some limiting flight speed, the temperature will approach the limit set by the wall materials and cooling methods. Thus when the temperature increase due to deceleration reaches the limit, it may not be possible to burn fuel in the airstream.

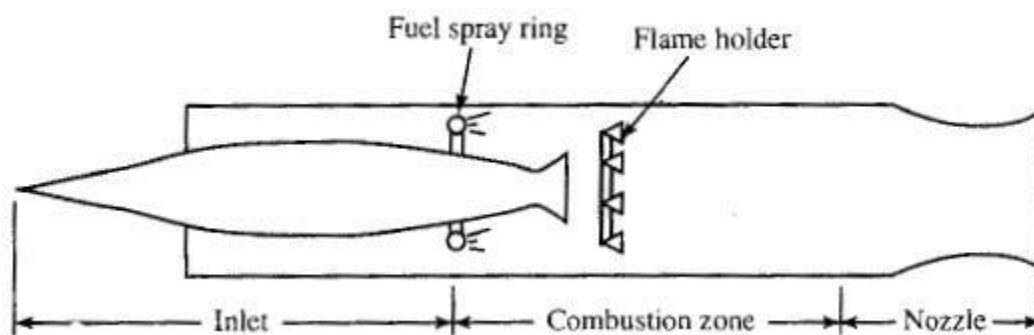


Fig.1.9:Schematic diagram of a ramjet.

SCRAMJET

The ramjet with supersonic combustion is known as the scramjet (supersonic combustion ramjet). By using a supersonic combustion process, the temperature rise and pressure loss due to deceleration in the inlet can be reduced.

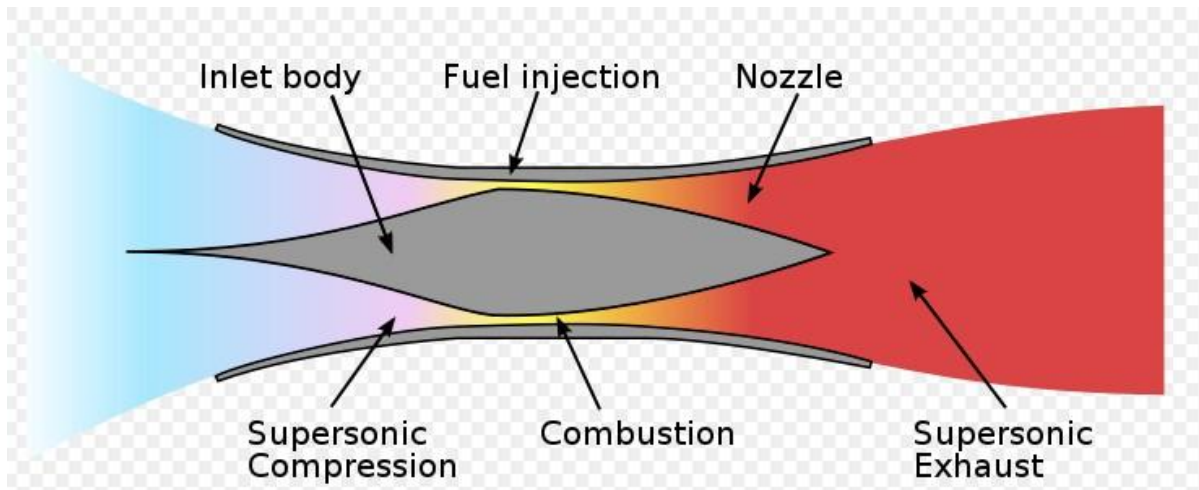


Fig.1.10:Schematic diagram of a Scramjet.

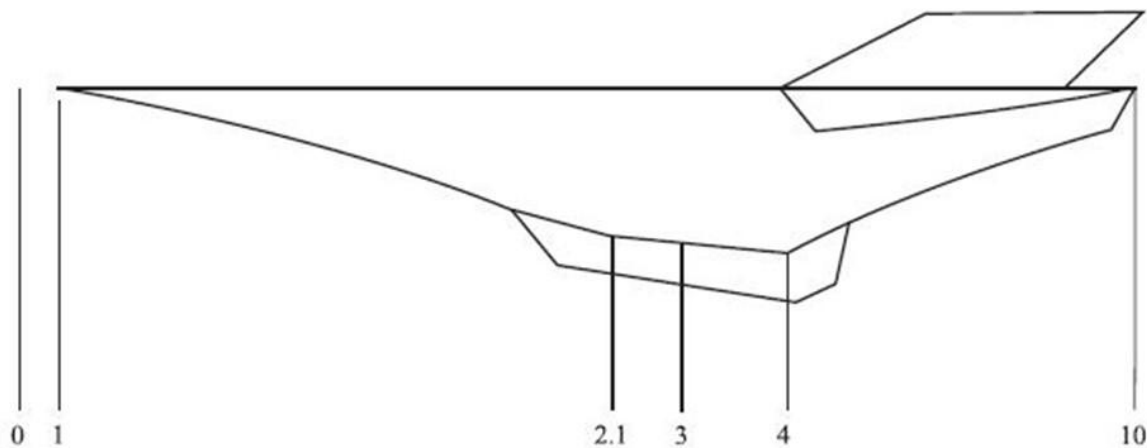


Fig.1.11:Schematic diagram of a Scramjet with station number.

The scramjet engine belongs to the family of Brayton cycles, which consist of two adiabatic and two constant-pressure processes. A simplified schematic of a scramjet equipped vehicle is shown above Fig.1.10.

Station 0 represents the free-stream condition.

Station 1 represents the beginning of the compression process. Hypersonic shock-wave angles are small, resulting in long compression ramps (or spikes if an axisymmetric configuration is used) that, in many of the suggested configurations, begin at the vehicle's leading edge. Additional compression takes place inside the inlet duct.

Station 2.1 represents the entrance into the isolator section. The role of the isolator is to separate the inlet from the adverse effects of a pressure rise that is due to combustion in the combustion chamber. The presence of a shock train in the isolator further compresses the air before arriving at the combustion chamber. Thermodynamically the isolator is not a desirable component, because it is a source of additional pressure losses, increases the engine cooling loads, and adds to the engine weight. However, operationally it is needed to include a shock train that adjusts such that it fulfills the role just described.

Station 3 is the combustion chamber entrance. Unlike the turbojet engine cycle, in which the air compression ratio is controlled by the compressor settings, in a fixed-geometry scramjet the pressure at the combustion chamber entrance varies over a large range.

Station 4 is the combustion chamber exit and the beginning of expansion.

Station 10 is the exit from the nozzle; because of the large expansion ratios the entire aft part of the vehicle may be part of the engine nozzle.

The thrust equation

The following assumptions are made:

1. The flow is steady within the control volume; thus all the properties within the control do not change with time.
2. The external flow is reversible; thus the pressures and velocities are constant over the control surface except over the exhaust area P_e of the engine.

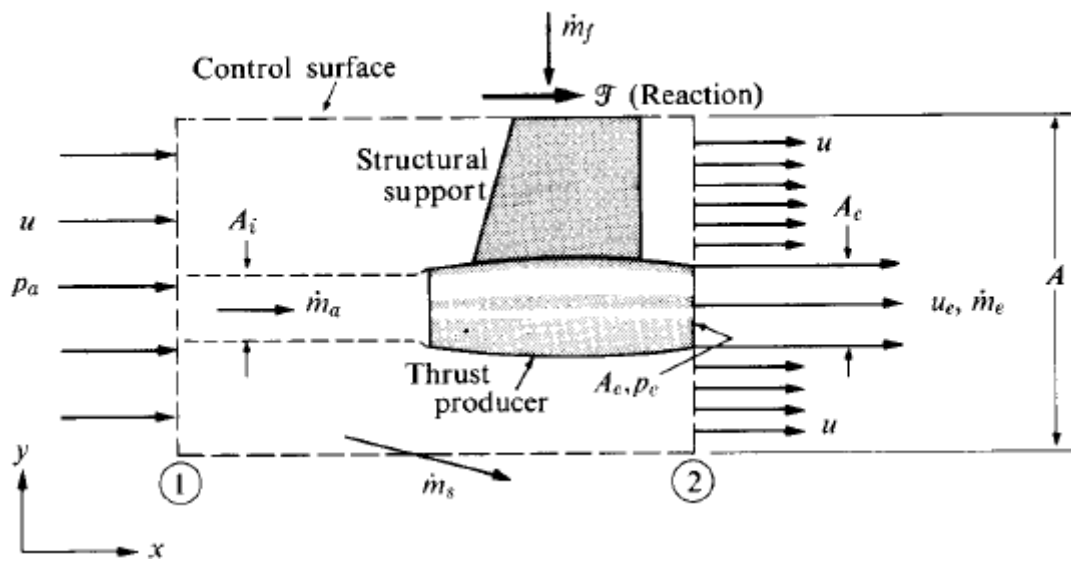


Fig.1.12: Generalized thrust producing device.

$$\mathcal{T} = \dot{m}_a[(1 + f)u_e - u] + (p_e - p_a)A_e.$$

Engine performance parameters

The engine performance is described by different efficiency definitions, thrust and the fuel consumption. The efficiency definitions that we shall now be discussing are applicable to an engine with a single propellant stream (turbojets or ramjets). For other types of jet engines (turbofan, turboprop) the equations need to be appropriately modified.

Thermal efficiency: The ratio of the rate of production of propellant kinetic energy to the total energy consumption rate.

$$\eta_{th} = \frac{\dot{m}_a[(1 + f)(u_e^2 / 2) - u^2 / 2]}{\dot{m}_f Q_R} = \frac{[(1 + f)(u_e^2 / 2) - u^2 / 2]}{f Q_R}$$

For a turboprop or turboshaft engine, the output is largely shaft power. In this case,

$$\eta_{th} = \frac{P_s}{\dot{m}_f Q_R}$$

Propulsion efficiency: The ratio of thrust power to the rate of production of propellant kinetic energy. The propulsive efficiency η_p can be defined as the ratio of the useful propulsive energy or thrust power ($F \cdot u$) to the sum of that energy and the unused kinetic energy of the jet.

$$\eta_p = \frac{F u}{\dot{m}_a \left[(1+f) \left(\frac{u_e^2}{2} \right) - \frac{u^2}{2} \right]}$$

If we assume that $f \ll 1$ and the pressure thrust term is negligible

$$\eta_p = \frac{(u_e - u)u}{u_e^2 / 2 - u^2 / 2} = \frac{2u / u_e}{1 + u / u_e}$$

Overall efficiency: The product of thermal efficiency and propulsion efficiency.

$$\eta_o = \eta_p \eta_{th}$$

Specific Thrust

Specific thrust is a term used in gas turbine engineering to show the relative thrust per air mass flow rate of a jet engine (e.g. turbojet, turbofan, etc.) and is defined as the ratio: net thrust/total intake airflow.

Why are we interested in specific thrust?

First, it is an indication of engine efficiency. Two different engines have different values of specific thrust. The engine with the higher value of specific thrust is more efficient because it produces more thrust for the same amount of airflow.

It gives us an easy way to "size" an engine during preliminary analysis. The result of our thermodynamic analysis is a certain value of specific thrust. The aircraft drag defines the required value of thrust. Dividing the thrust required by the specific thrust tells us how much airflow our engine must produce and this determines the physical size of the engine.

Specific impulse

Specific impulse (usually abbreviated I_{sp}) is a measure of how effectively a rocket uses propellant or jet engine uses fuel. By definition, it is the total impulse (or change in momentum) delivered per unit of propellant consumed.

$$I_{sp} \equiv \frac{F}{\dot{m}_p g}$$

Thrust Specific fuel consumption

TSFC or SFC for thrust engines (e.g. turbojets, turbofans, ramjets, rocket engines, etc.) is the mass of fuel needed to provide the net thrust for a given period. SFC varies with throttle setting, altitude and climate. For jet engines, flight speed also has a significant effect upon SFC; SFC is roughly proportional to air speed.

$$TSFC = \frac{\dot{m}_f}{\mathfrak{T}} \approx \frac{\dot{m}_f}{\dot{m}_a [(1+f)u_e - u]}$$

Component performance

Air intake performance

Inlet losses arise due to wall friction and shock waves (in a supersonic inlet).

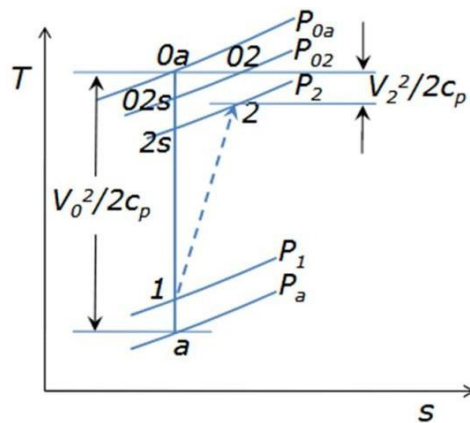
- These result in a reduction in total pressure.
- The flow is usually adiabatic as it flows through the intake.
- Performance of intakes are characterized using total pressure ratio and isentropic efficiency.

Isentropic efficiency, η_d , of the diffuser is

$$\eta_d = \frac{h_{02s} - h_a}{h_{0a} - h_a} \cong \frac{T_{02s} - T_a}{T_{0a} - T_a}$$

This efficiency can be related to the total pressure ratio (π_d) and Mach number

$$\eta_d = \frac{\left(1 + \frac{\gamma - 1}{2} M^2\right) \pi_d^{(\gamma - 1)/\gamma} - 1}{[(\gamma - 1)/2] M^2}$$

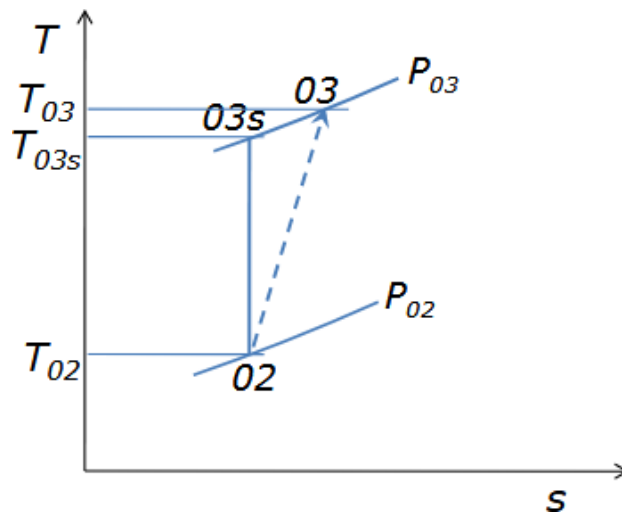


Compressor/fan performance

Compressors are to a high degree of approximation, adiabatic. Compressor performance is evaluated using the isentropic efficiency.

$$\eta_c = \frac{\text{Ideal work of compression for given pressure ratio}}{\text{Actual work of compression for given pressure ratio}}$$

$$= \frac{w_{ci}}{w_c} = \frac{h_{03s} - h_{02}}{h_{03} - h_{02}}$$



$$\begin{aligned}
\eta_c &= \frac{h_{03s} - h_{02}}{h_{03} - h_{02}} \approx \frac{T_{03s} - T_{02}}{T_{03} - T_{02}} \\
&= \frac{T_{03s}/T_{02} - 1}{T_{03}/T_{02} - 1} = \frac{(P_{03}/P_{02})^{(\gamma-1)/\gamma} - 1}{\tau_c - 1} \\
&= \frac{(\pi_c)^{(\gamma-1)/\gamma} - 1}{\tau_c - 1}
\end{aligned}$$

The isentropic efficiency is thus a function of the total pressure ratio and the total temperature ratio.

Combustion chamber performance

In a combustion chamber (or burner), there are two possibilities of losses, incomplete combustion and total pressure losses.

- Combustion efficiency can be defined by carrying out an energy balance across the combustor.
- Two different values of specific heat at constant pressure: one for fluid upstream of the combustor and the other for fluid downstream of the combustor

Combustion efficiency, η_b

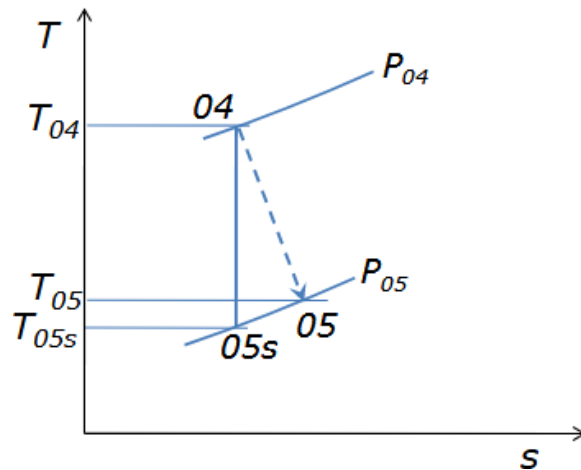
$$\begin{aligned}
\eta_b &= \frac{(\dot{m} + \dot{m}_f)h_{04} - \dot{m}h_{03}}{\dot{m}_f\dot{Q}_f} = \frac{(\dot{m} + \dot{m}_f)c_{p4}T_{04} - \dot{m}c_{p3}T_{03}}{\dot{m}_f\dot{Q}_f} \\
&= \frac{(\dot{m} + \dot{m}_f)c_{pg}T_{04} - \dot{m}c_{pa}T_{03}}{\dot{m}_f\dot{Q}_f}
\end{aligned}$$

Total pressure losses arise from two effects:

- viscous losses in the combustion chamber
- total pressure loss due to combustion at finite Mach number.

Turbine performance

The flow in a turbine is also assumed to be adiabatic, though in actual engines there could be turbine blade cooling. Isentropic efficiency of the turbine is defined in a manner similar to that of the compressor.

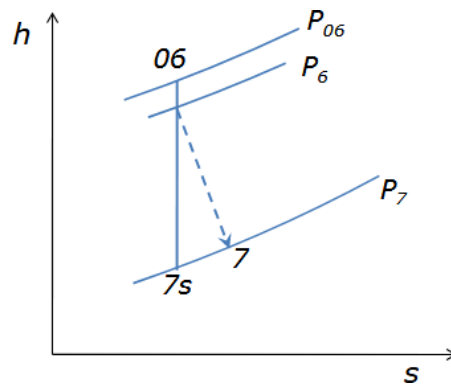


$$\eta_t = \frac{\text{Actual work of compression for given pressure ratio}}{\text{Ideal work of compression for given pressure ratio}}$$

$$= \frac{w_t}{w_{ti}} = \frac{h_{04} - h_{05}}{h_{04} - h_{05s}} = \frac{1 - \tau_t}{1 - \pi_t^{(\gamma-1)/\gamma}}$$

Nozzle performance

The flow in the nozzle is also adiabatic, however losses in a nozzle could occur due to incomplete expansion process (under or over-expansion). Friction may reduce the isentropic efficiency.



The efficiency is defined by

$$\eta_n = \frac{h_{06} - h_7}{h_{06} - h_{7s}}$$

Afterburner performance

Afterburner is thermodynamically similar to a combustion chamber. The performance parameters for an afterburner are thus the combustion efficiency and the total pressure loss. In case of engines with afterburning, the corresponding performance parameters for an afterburner need to be taken into account.

As stated above the propeller rotates at very low speed compared to its driving turbine. The speed reduction may be 1:15. This speed reduction is necessary owing to two reasons:

1. A large centrifugal force arises from the rotation of the large diameter (2–4 m or even more) propeller blades. These blades are fixed to the propeller hub in a cantilever fixed end configuration. Consequently, such a centrifugal force generates a large tensile stress at blade root. Stress limitations require that the large diameter propeller rotates at a much slower speed. It is a fact that no propeller can withstand the tensile force (and stress) that is generated when it is turned at the same speed of the turbine.
2. Owing to the rotation of the propeller, the relative velocity at the propeller tip will approach the speed of sound before the aircraft approaches the speed of sound. This compressibility effect when approaching the speed of sound limits the design of propellers. At high subsonic flight speeds ($M > 0.7$), the tips of blades may approach supersonic speeds. If this happens, the flow may separate and shock waves may form. As a consequence, the performance of turboprop engine deteriorates due to both the poor propeller efficiency and the decrease in air flow rate into the engine.

The propeller is pitch controlled to be suitable for a wider range of satisfactory applications.

If the shaft of a free turbine is used to drive something other than an aircraft propeller, the engine is called a turboshaft engine. This is one of the turboshaft engines that will be discussed later in this chapter. Turboshaft engines are similar to turboprop engines, except that the hot gases are expanded to a lower pressure in the turbine, thus providing greater shaft power and low exhaust velocity.

Examples of turboshaft engines are those used in helicopters.

Now, let us discuss the advantages of turboprop engines:

1. Turboprops have high fuel efficiency, even greater than turbofan engines. This is due to the small amount of air flow burned inside the engine. Turboprop engines can then generate a lot of thrust at low fuel consumption.
2. Turboprop engines may find application in vertical takeoff and landing (VTOL). The Osprey V-22 aircraft as shown in Figure 6.5 is one of the famous VTOL aircraft that is powered by a turboprop engine.
3. Turboprop engines have high takeoff thrust that enables aircraft to have a short field takeoff.
4. They have the highest propulsive efficiency for flight speeds of 400 mph compared to turbofan and turbojet engines.

However, turboprop engines have several disadvantages:

1. The noise and vibration produced by the propeller is a significant drawback.
1. Turboprop engines are limited to subsonic flights (< 400 mph) and low altitudes (below 30,000 ft).

2. The propeller and its pitch control mechanism as well as the power turbine contribute additional weight, so the turboprop engine may be 1.5 times as heavy as a conventional turbojet of the same gas generator size.

CLASSIFICATION OF TURBOPROP ENGINES

1. Based on engine–aircraft configuration

Turboprop engines may be either of the tractor (sometimes identified as puller) or pusher types. By the word puller (tractor) it is meant a turboprop engine with a propeller that precedes the intake and compressor. The thrust force (mostly generated by the propeller) is thus a pulling force. Most aircraft are powered by puller (tractor) configuration; Figure 1.13, for example. If the propeller is downstream the inlet and compressor then this turboprop is identified as pusher as shown in Figure 1.14.



Fig 1.13: Russian TU-95.



Fig 1.14: Pusher configuration of Jetcruzer 500, AASI airplane.

Advantages of pusher turboprop engines are as follows:

- A higher quality (clean) airflow prevails over the wing.
- Engine noise in the cabin area is reduced.
- The pilot's front field of view is improved.

Disadvantages are as follows:

- The heavy gearbox is at the back, which shifts the center of gravity rearward and thus reduces the longitudinal stability.
- Propeller is more likely to be damaged by flying debris at landing.
- Engine cooling problems are more severe.

The "pusher" configuration is not very common.

Problem 1: A gas turbine operating at a pressure ratio of 11.314 produces zero net work output when 473.35 kJ of heat is added per kg of air. If the inlet air temperature is 300 K and the turbine efficiency is 71%, find the compressor efficiency.

Since the net work output is zero

$$W_c = W_t$$

$$\text{or, } T_{02} - T_{01} = T_{03} - T_{04}$$

$$T_{03} - T_{02} = T_{04} - T_{01}$$

$$\frac{T_{02s}}{T_{01}} = \left(\frac{P_{02}}{P_{01}} \right)^{(\gamma-1)/\gamma} = 11.314^{0.4/1.4}$$

$$T_{02s} = 300 \times 11.314^{0.4/1.4} = 600K$$

Given that heat added = 476.35 kJ/kg

$$c_p(T_{03} - T_{02}) = 476.354$$

$$\text{or, } T_{03} - T_{02} = 474K$$

We know that

$$T_{04} = T_{01} + (T_{03} - T_{02}) = 300 + 474 = 774K$$

The turbine efficiency is 71%

$$0.71 = \frac{T_{03}(1 - T_{04}/T_{03})}{T_{04s}(T_{03}/T_{04s} - 1)} \text{ and } T_{03}/T_{04s} = 11.314^{0.4/1.4}$$

$$\therefore \frac{T_{04}}{T_{03}} = 1 - \frac{0.71}{2} = 0.645$$

$$\text{or, } T_{03} = 774 / 0.645 = 1200K \text{ and } T_{02} = 1200 - 474 = 726K$$

$$\therefore \eta = \frac{T_{02s} - T_{01}}{T_{02} - T_{01}} = \frac{600 - 300}{726 - 300} = 0.704 \text{ or } 70.4\%$$

Problem 2: An aircraft flies at a Mach number of 0.75 ingesting airflow of 80 kg/s at an altitude where the ambient temperature and pressure are 222 K and 10 kPa, respectively. The inlet design is such that the Mach number at the entry to the inlet is 0.60 and that at the compressor face is 0.40. The inlet has an isentropic efficiency of 0.95. Find (a) the area of the inlet entry (b) the inlet pressure recovery (c) the compressor face diameter.

Mach number is 0.75, hence, the flight speed is

$$u_a = M_a \sqrt{\gamma R T_a} = 0.75 \sqrt{1.4 \times 287 \times 222} = 224 \text{ m/s}$$

$$\rho_a = P_a / R T_a = 0.1569 \text{ kg/m}^3$$

$$\text{The total temperature, } T_{0a} = T_a \left(1 + \frac{\gamma - 1}{2} M_a^2 \right) = 246 \text{ K}$$

$$\text{Total pressure, } P_{0a} = P_a \left(1 + \frac{\gamma - 1}{2} M_a^2 \right)^{\gamma/(\gamma - 1)} = 14522.8 \text{ Pa}$$

∴ Static temperature at inlet entry,

$$T_1 = T_{0a} / \left(1 + \frac{\gamma - 1}{2} M_a^2 \right) = 230.4 \text{ K}$$

Static pressure at inlet entry,

$$P_1 = P_{0a} / \left(1 + \frac{\gamma - 1}{2} M_a^2 \right)^{\gamma/(\gamma - 1)} = 11386 \text{ Pa}$$

$$\rho_1 = P_1 / R T_1 = 0.1722 \text{ kg/m}^3$$

$$\begin{aligned} \text{Therefore, area at the inlet entry, } A_1 &= \frac{\dot{m}}{u_1 \rho_1} = \frac{\dot{m}}{M_1 \sqrt{\gamma R T_1} \rho_1} \\ &= \frac{80}{0.6 \sqrt{1.4 \times 287 \times 230.4} \times 0.1722} \\ &= 2.54 \text{ m}^2 \end{aligned}$$

Now, $T_{02} = T_{0a}$

$$\text{Diffuser efficiency, } \eta_d = \frac{T_{02s} - T_a}{T_{0a} - T_a}$$

Substituting the values, $T_{02s} = 245.75 K$

$$\therefore \text{Pressure recovery, } \frac{P_{02}}{P_{01}} = \left(\frac{T_{02s}}{T_{01}} \right)^{\gamma/(\gamma-1)} = 0.982$$

The static pressure at the compressor face, T_2

$$T_2 = T_{02} \left[1 + \frac{\gamma-1}{2} M_2^2 \right] = 239.3 K$$

$$P_2 = P_1 (T_2 / T_1)^{\gamma/(\gamma-1)} = 13001 Pa$$

$$\rho_2 = P_2 / RT_2 = 0.1893 kg / m^3$$

$$\begin{aligned} \text{Velocity at the compressor face, } u_2 &= M_2 \sqrt{\gamma RT_2} \\ &= 124.03 m / s \end{aligned}$$

$$\begin{aligned} \text{Area of the compressor face, } A_2 &= \dot{m} / u_2 \rho_2 \\ &= 3.407 m^2 \end{aligned}$$

\therefore the diameter, $d = 2.08 m$

Problem 3: A turbojet engine operates at an altitude where the ambient temperature and pressure are 216.7 K and 24.444 kPa, respectively. The flight Mach number is 0.9 and the inlet conditions to the convergent nozzle are 1000 K and 60 kPa. If the nozzle efficiency is 0.98, the ratio of specific heat is 1.33, determine whether the nozzle is operating under choked condition or not. Determine the nozzle exit pressure.

The nozzle efficiency is defined as

$$\eta_n = \frac{h_{06} - h_7}{h_{06} - h_{7s}} = \frac{T_{06} - T_7}{T_{06} - T_{7s}} = \frac{1 - T_7 / T_{06}}{1 - T_{7s} / T_{06}} = \frac{1 - T_7 / T_{07}}{1 - T_{7s} / T_{06}}$$

Under choked condition, $M = 1$,

$$\therefore \eta_n = \frac{1 - (2/(\gamma + 1))}{1 - (P_c / P_{06})^{(\gamma-1)/\gamma}}$$

$$\text{or, } \frac{P_{06}}{P_c} = \frac{1}{(1 - (1/\eta_n)((\gamma-1)/(\gamma+1)))^{\gamma/(\gamma-1)}}$$

Substituting the values,

$$\frac{P_{06}}{P_c} = 1.878$$

$$\text{Also, } \frac{P_{06}}{P_a} = \frac{60}{24.444} = 2.45 Pa$$

We can see that $P_c > P_a$

Therefore, the nozzle is operating under choked condition.

The exit pressure would therefore be equal to

$$P_e = \frac{60}{1.878} = 31.95 kPa$$

UNIT -II

AIRCRAFT ENGINE INLETS, EXHAUST NOZZLES, COMBUSTORS AND AFTERBURNERS

Role of the air intakes

Any vehicle with air-breathing propulsion needs at least one air intake to feed its engine so that it can move. The role of the air intake is to capture the airflow which the propulsion (engines) and conditioning (radiators) systems need. They must do this in such a way as to yield the best possible propulsive balance, which is expressed in two objectives:

- provide maximum thrust,
- induce minimum drag.

Maximum thrust is obtained by designing the air intake to transform kinetic energy (i.e., the velocity of the flow as it arrives in front of the air intake) into potential energy (the pressure after the diffuser, at the engine input) with the best possible efficiency. Efficiency is a parameter that is calculated by taking the ratio of the total pressure in front of the engine to that of the upstream flow. This thrust is maximum if the air intake captures just what the engine needs for each flight configuration and provides the engine input with a flow of good homogeneity (low distortion) to ensure correct engine operation, which is essential for turbojets. Minimum drag is obtained with air intakes that are dimensioned to just what the engine needs (critical regime) and the design Mach number (Shock-on-lip Mach number). Careful attention is paid to the side walls and cowls in light of the small variations in angle of attack and yaw angle about the flight configurations.

Engine Inlet Ducts

The dynamic intake is the first component that meets the flow in its evolution through the engine. It is positioned to provide the minimum external resistance. The task of the air intake is to channel the flow at low velocity through the compressor (or to the combustor in the case of the ramjet) without causing the detachment of the boundary layer (because by the slowdown of the flow, the static pressure increases, and the flow is then submitted an adverse pressure gradient).

The air intake must be designed to provide the engine the required flow rate and also so that the output of the dynamic intake flow entering the compressor is uniform, stable, and with “good quality”. So the goals of the Inlet are:

- slow down the flow (up to $M = 0.4$ to 0.5);
- increase the pressure;
- Uniform flow at the upstream of the compressor;
- Minimal loss of total pressure;
- Minimum aerodynamic disorder;
- Minimum weight (ie minimum length).

The performance should not be prejudice in the presence of an incidence angle or yaw. It is useful to observe that the requirement that the flow is uniform before the compressor could be more important than to have small total pressure loss. The inlet is essentially a duct where the air flows in stationary conditions. it is designed according to rules of gas dynamics; since such laws have different implications depending on how the flow enters in the duct, if in supersonic or subsonic conditions, the main classification of distinguishes between:

1. Subsonic inlet;
2. Supersonic inlet

SUBSONIC INTAKES

Subsonic intakes are found in the turbojet or turbofan engines powering most of the present civil transports. The surface of the inlet is a continuous smooth curve where the very front (most upstream portion) is called the inlet lip. A subsonic aircraft has an inlet with a relatively thick lip. Concerning turboprop engines, the intakes are much complicated by the propeller and gearbox at the inlet to the engine. Subsonic inlets have fixed geometry, although inlets for some high bypass ratio turbofan engines are designed with blow-in-doors. These doors are spring-loaded parts installed in the perimeter of the inlet duct designed to deliver additional air to the aero engine during takeoff and climb conditions when the highest thrust is needed and the aircraft speed is low.

The most common type of subsonic intake is the pitot intake. This type of intakes makes the fullest use of ram due to forward speed, and suffers the minimum loss of ram pressure with changes of aircraft altitude. However, as sonic speed is approached, the efficiency of this type of air intake begins to fall because of the formation of a shock wave at the intake lip. It consists of a simple forward entry hole with a cowl lip.

The three major types of pitot intakes as shown in Fig 2.1 are as follows

1. Podded intakes
2. Integrated intake
3. Flush intakes.

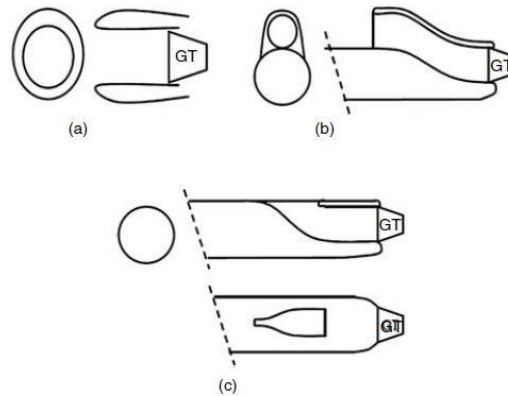


Fig. 2.2: Types of pitot intakes: (a) podded pitot, (b) integrated pitot, and (c) flush pitot.

Podded intake is common in transport aircraft. The integrated intake is used in combat (military) aircraft. The flush intake is usually used in missiles since they can be more readily accommodated into missile airframes.

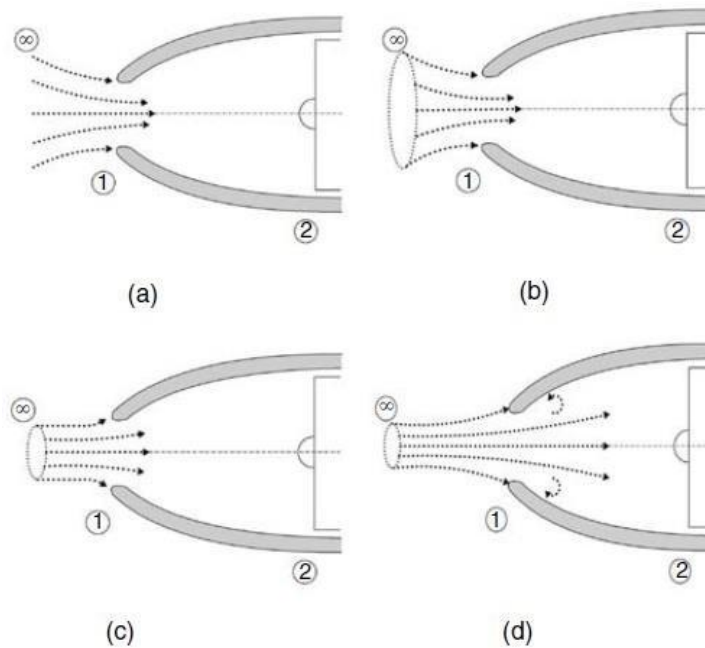


Fig. 2.2: Flow characteristics of podded intakes: (a) ground run, (b) climb, (c) high-speed cruise, and (d) top speed.

Subsonic inlet performance

Depending on the flight speed and the mass flow demanded by the engine, the inlet might have to operate with a wide range of incident stream conditions. Fig 2.3 a and b show the performances of subsonic intake during two typical subsonic conditions, takeoff and cruise, respectively. The first illustrates the stream tube, while the second depicts the pressure and speed variation and the third is a temperature–entropy diagram.

The flow in intake is identified by three states, namely far upstream that is denoted as (∞), at the duct entry denoted by (1) and at the engine face denoted by (2). The flow outside the engine (from state ∞ to 1) is an isentropic one, where no losses are associated with the total temperature and pressure. For high speed, or cruise condition (Figure 2.3b), the stream tube will have a divergent shape and following conditions can be stated:

$$u_1 < u_\infty, P_1 > P_\infty, P_{01} = P_{0\infty}, T_{01} = T_{0\infty}$$

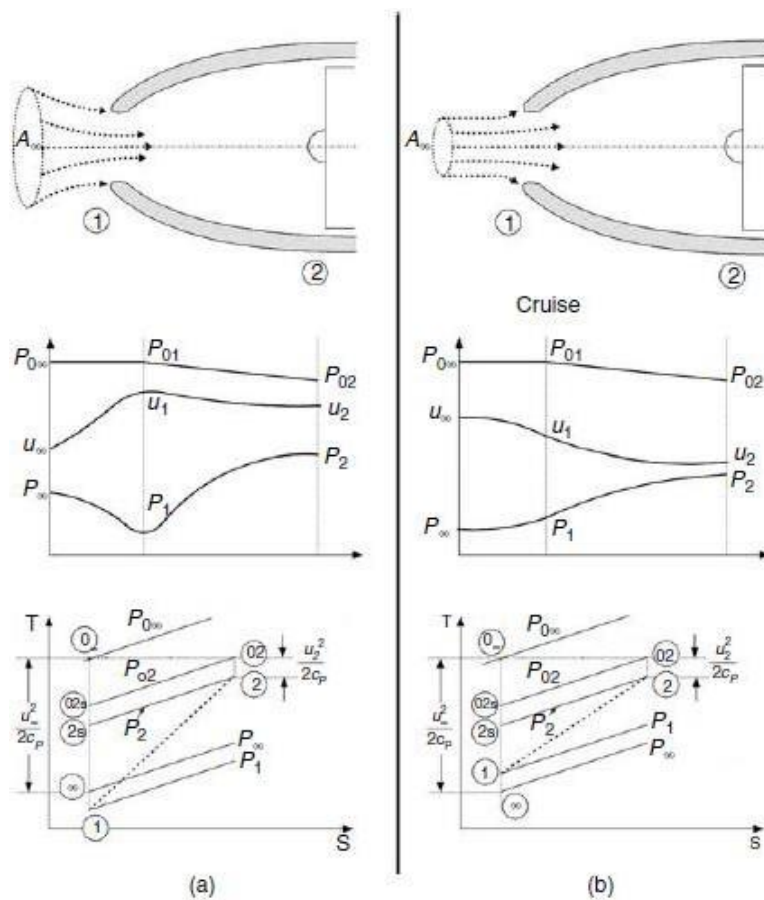


Fig. 2.2: Subsonic inlet during (a) takeoff and (b) cruise.

During low speed high-thrust operation (e.g., during takeoff and climb), as shown in Figure 2.3a, the same engine will demand more mass flow and the air stream upstream the intake will be accelerated. The stream tube will have a converging shape and the following conditions are satisfied:

$$u_1 > u_\infty, P_1 < P_\infty, P_{01} = P_{0\infty}, T_{01} = T_{0\infty}$$

For both cases of takeoff and cruise, there will be internal diffusion within the intake up to the engine face. The static pressure will rise and the air speed will be reduced. The total pressure will also decrease owing to skin friction while the total temperature remains unchanged, as the flow through diffuser is adiabatic. Thus, for both takeoff and cruise conditions

$$P_2 > P_1, P_{02} < P_{0\infty}, u_2 < u_1$$

Since the inlet speed to the engine (compressor/fan) should be nearly constant for different operating conditions, then

$$\left(\frac{P_2}{P_1}\right)_{\text{takeoff}} > \left(\frac{P_2}{P_1}\right)_{\text{cruise}}$$

If this pressure increase is too large, the diffuser may stall due to boundary layer separation.

Stalling usually reduces the stagnation pressure of the stream as a whole. Conversely, for cruise conditions (Fig. 2.3b) to avoid separation, or to have a less severe loading on the boundary layer, it is recommended to have a low velocity ratio (u_1/u_∞) and consequently less internal pressure rise. Therefore, the inlet area is often chosen so as to minimize external acceleration during takeoff with the result that external deceleration occurs during level-cruise operation. Under these conditions the “upstream capture area” A_∞ is less than the inlet area A_1 , and some flow is spilled over the inlet.

Supersonic intakes

The design of inlet systems for supersonic aircraft is a highly complex matter involving engineering trade-offs between efficiency, complexity, weight, and cost. A typical supersonic intake is made up of a supersonic diffuser, in which the flow is decelerated by a combination of

shocks and diffuse compression, and a subsonic diffuser, which reduces the Mach number from high subsonic value after the last shock to the value acceptable to the engine. Subsonic intakes that have thick lip are quite unsuitable for supersonic speeds.

The reason is that a normal shock wave ahead of the intake is generated, which will yield a very sharp static pressure rise without change of flow direction and correspondingly big velocity reduction. The adiabatic efficiency of compression through a normal shock wave is very low as compared with oblique shocks.

At Mach 2.0 in the stratosphere adiabatic efficiency would be about 80% or less for normal shock waves, whereas its value will be about 95% or even more for an intake designed for oblique shocks.

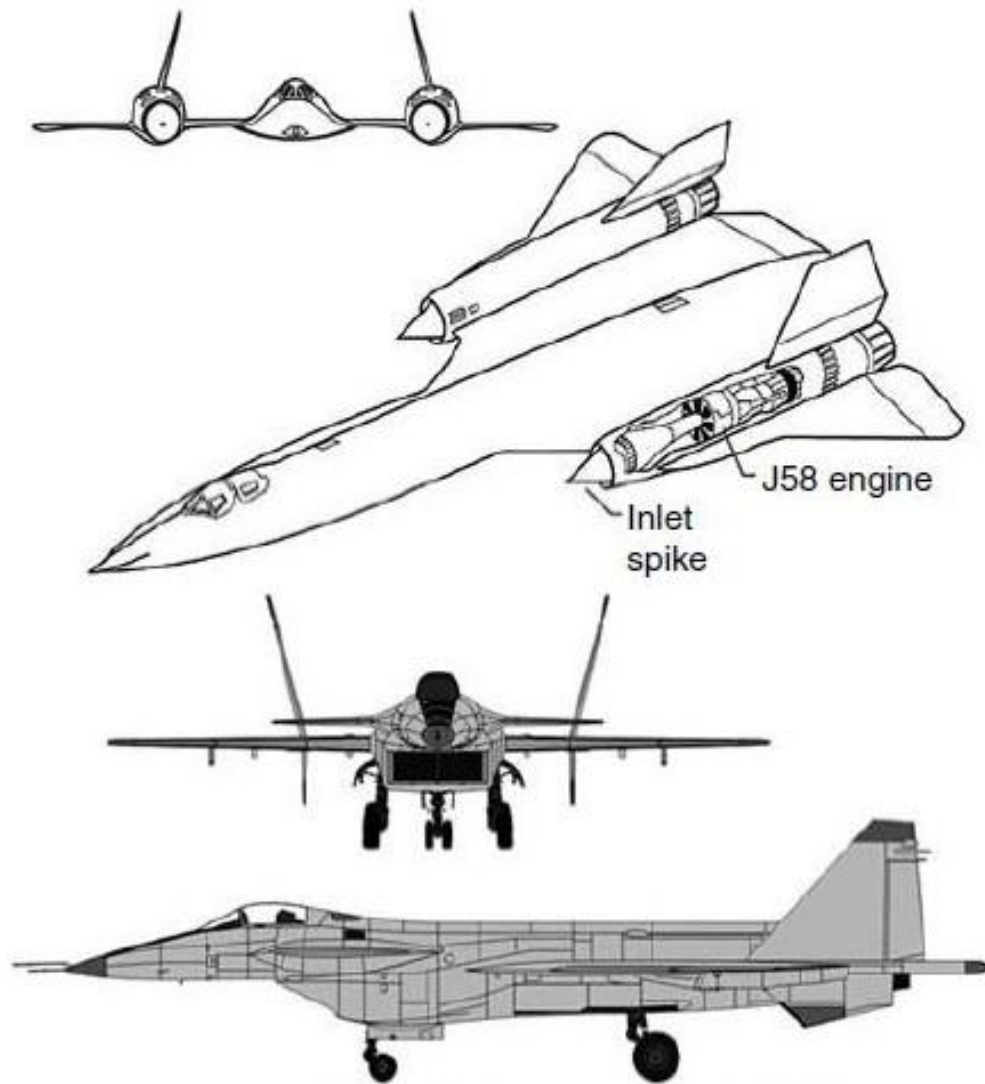
.Flight at supersonic speeds complicates the diffuser design for the following reasons

1. The existence of shock waves that lead to large decrease in stagnation pressure even in the absence of viscous effects.
2. The large variation in capture stream tube area between subsonic and supersonic flight for a given engine, as much as a factor of four between $M_\infty = 1$ and $M_\infty = 3$.
3. As M_∞ increases, the inlet compression ratio becomes a larger fraction of the overall cycle compression ratios and as a result, the specific thrust becomes more sensitive to diffuser pressure ratio.
4. It must operate efficiently both during the subsonic flight phases (takeoff, climb, and subsonic cruise) and at supersonic design speed.

Supersonic intake may be classified as follows

1. Axisymmetric or two-dimensional intakes

The axisymmetric intakes use axisymmetric central cone to decelerate the flow down to subsonic speeds. The two-dimensional inlets has rectangular cross sections as found in the F-14 and F-15 fighter aircraft.



SR-71-A & MIG-MFI Axisymmetric & 2-D Intakes

Fig. 2.2:Axisymmetric and two-dimensional supersonic intakes.

2. Variable or fixed geometry

For variable geometry axisymmetric intakes, the central cone may move fore-and-aft to adjust the intake area. Alternatively, the inlet area is adjusted in the case of rectangular section through hinged flaps (or ramps) that may change its angles. For flight at Mach numbers much beyond 1.6, variable geometry features must be incorporated in the inlet to achieve high inlet pressure recoveries together with low external drag.

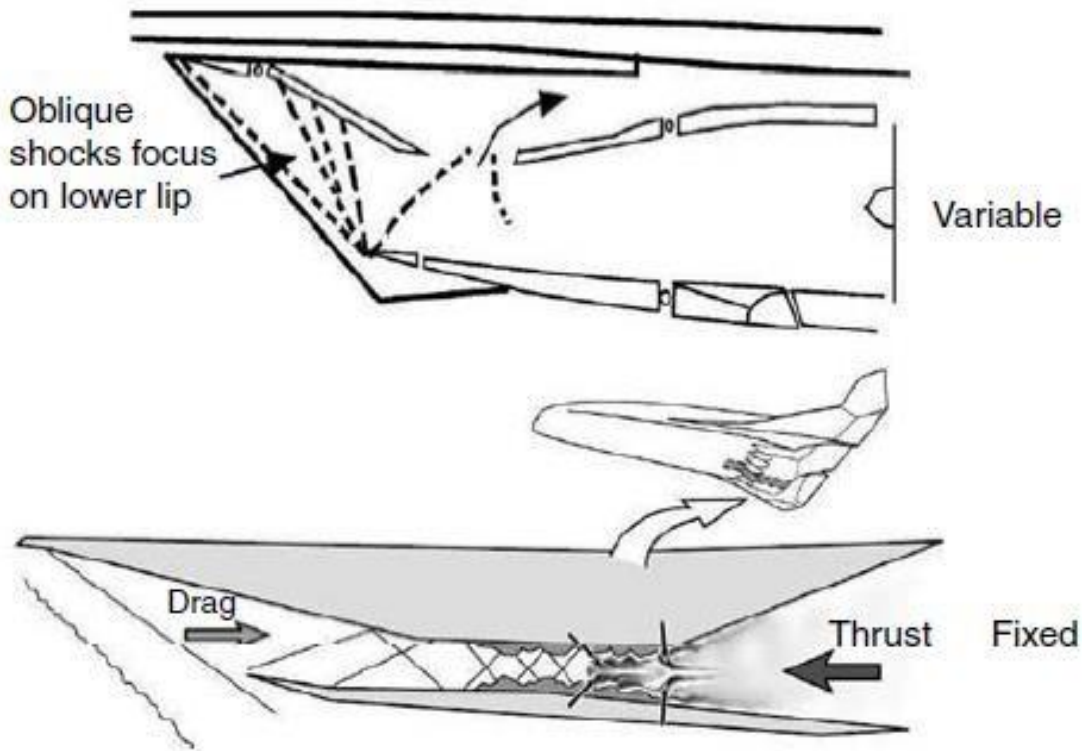


Fig. 2.3: Variable and fixed geometry supersonic intakes.

3. Internal, external or mixed compression

As shown in Fig 2.4. The set of shocks situated between the forebody and intake lip are identified as external shocks, while the shocks found between the nose lip and the intakes throat are called internal shocks. Some intakes have one type of shocks either external or internal and given the same name as the shocks, while others have both types and denoted as mixed compression intakes.

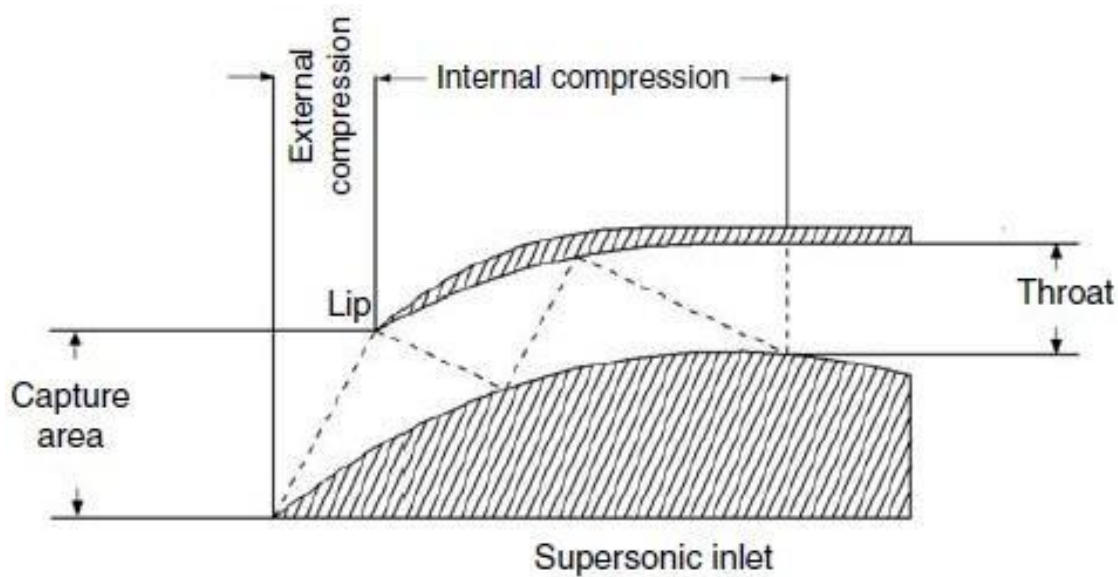


Fig. 2.4:External and internal compression supersonic intake.

External compression intake

External compression intakes complete the supersonic diffusion process outside the covered portion of the inlet where the flow is decelerated through a combination of oblique shocks (may be a single, double, triple, or multiple). These oblique shocks are followed by a normal shock wave that changes the flow from supersonic to subsonic flow. Both the normal shock wave and the throat are ideally located at the cowl lip. The supersonic diffuser is followed by a subsonic diffuser, which reduces the Mach number from high subsonic value after the last shock to the value acceptable to the engine.

The simplest form of staged compression is the single oblique shock, produced by a single-angled wedge or cone that projects forward of the duct, followed by a normal shock as illustrated in Fig 2.5. The intake in this case is referred to as a two-shock intake. With a wedge, the flow after the oblique shock wave is at constant Mach number and parallel to the wedge surface. With a cone the flow behind the conical shock is itself conical, and the Mach number is constant along rays from the apex and varies along streamline. Forebody intake is frequently used for “external compression intake of wedge or cone form”.

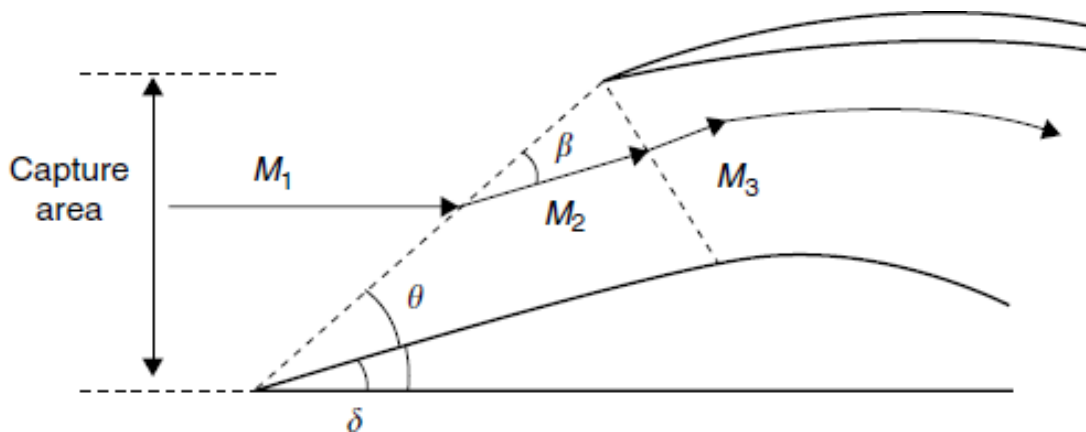


Fig. 2.5:Single oblique shock external compression intake.

Mode of operation

Critical condition

The capture area (A_c) for supersonic intakes is defined as the area enclosed by the leading edge, or “highlight,” of the intake cowl, including the cross-sectional area of the forebody in that plane. The maximum flow ratio is achieved when the boundary of the free stream tube (A_∞) arrives undisturbed at the lip. This means

$$\frac{A_\infty}{A_c} = 1.0$$

This condition is identified as the full flow [6] or the critical flow [5]. This condition depends on the Mach number, angle of the forebody and the position of the tip. In this case, the shock angle θ is equal to the angle subtended by lip at the apex of the body and corresponds to the maximum possible flow through the intake.

Subcritical operation

At Mach numbers (or speeds) below the value of the critical (design) value described above, the mass flow is less than that at the critical condition and the normal shock wave occurs in front of the cowl lip and this case is identified as subcritical. It is to be noted here that

$$\frac{A_\infty}{A_c} < 1.0$$

Supercritical operation

If the at air speeds is greater than the design value, then the oblique shock will impinge inside the cowl lip and the normal shock will move to the diverging section. This type of operation is referred to as the supercritical operation.

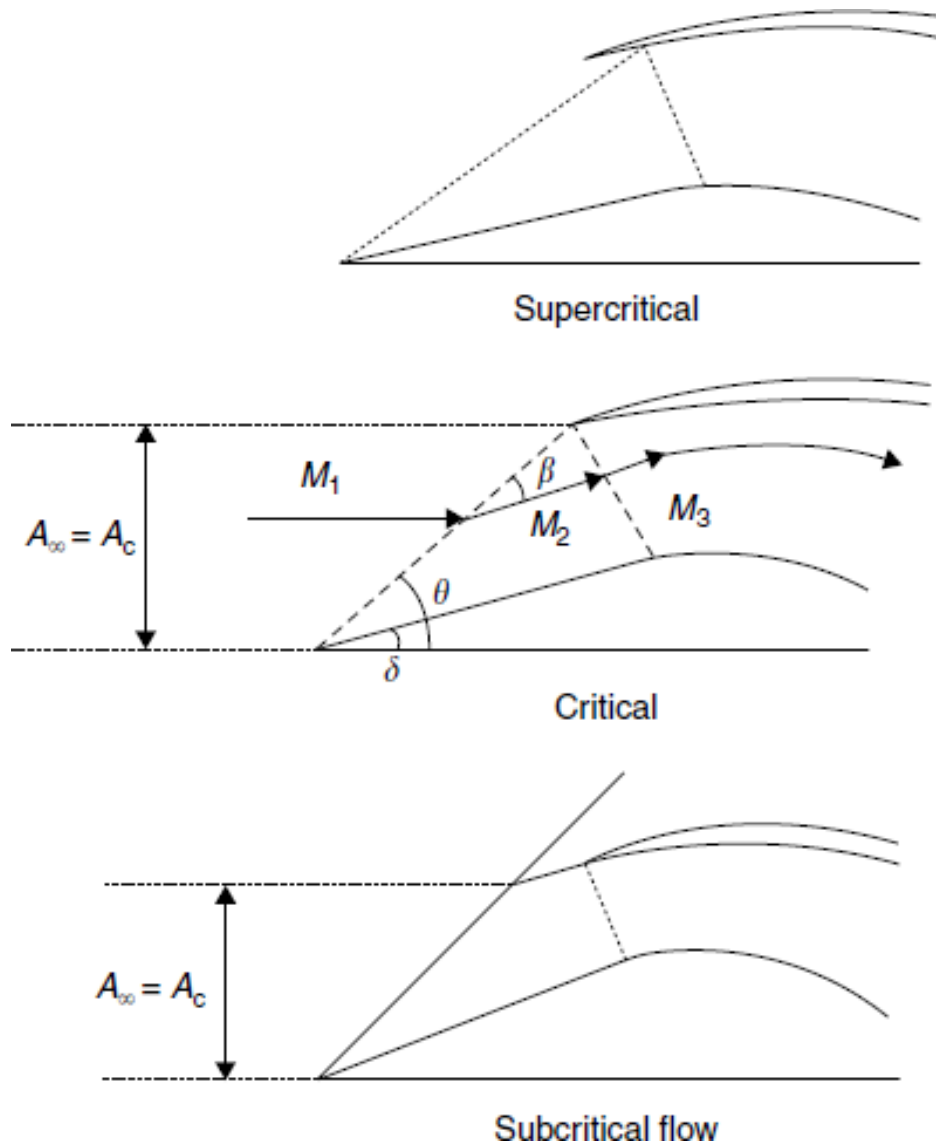


Fig. 2.5:Types of flow in an external compression intake.

Internal compression inlet

The internal compression inlet locates all the shocks within the covered passageway (Fig 2.6). The terminal shock wave is also a normal one, which is located near or at the throat. A principal difference between internal and external compression intakes is that with internal

compression, since the system is enclosed, oblique shocks are reflected from an opposite wall, which have to be considered. The simplest form is a three-shock system. The single-wedge turns the flow toward the opposite wall. The oblique shock is reflected from the opposite wall and the flow passing the reflected shock is restored to an axial direction. A normal shock terminates the supersonic as usual.

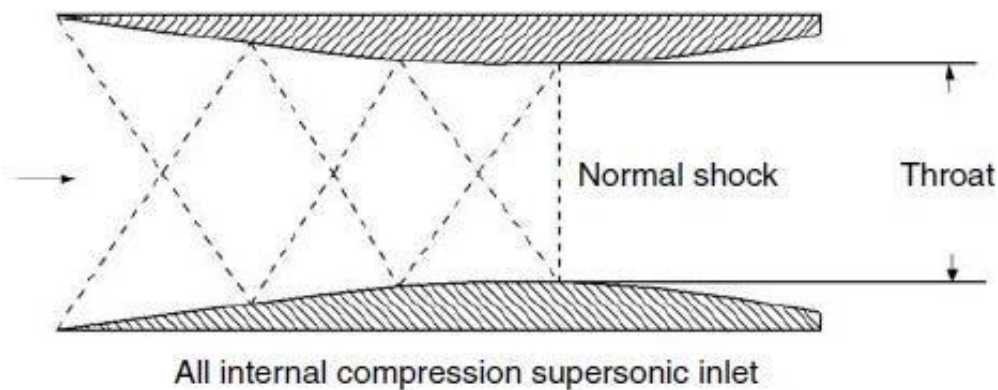


Fig. 2.5:Internal compression supersonic intake.

Methods for Starting an Intake

Some methods for overcoming the ‘starting’ problem have been discussed in the following section.

Over-speeding

Consider an intake designed for a Mach number of 1.7. The design point for this intake, represented by the point B in this plot, has been shown in Fig. 2.6.

One of the methods of starting the intake is by increasing the free-stream Mach number. Referring Fig. 2.6, conditions are modified so as to move the operating point from B to C. Once at C the intake starts and the expected shock system is developed. Then again the free-stream flow is decelerated to reach the design point B, while retaining the appropriate shock structure. This method of starting the intake is called ‘Over-speeding’.

It is the simplest method for starting the intake from the point of view of design complexity as it does not require any modifications to the intake aircraft.

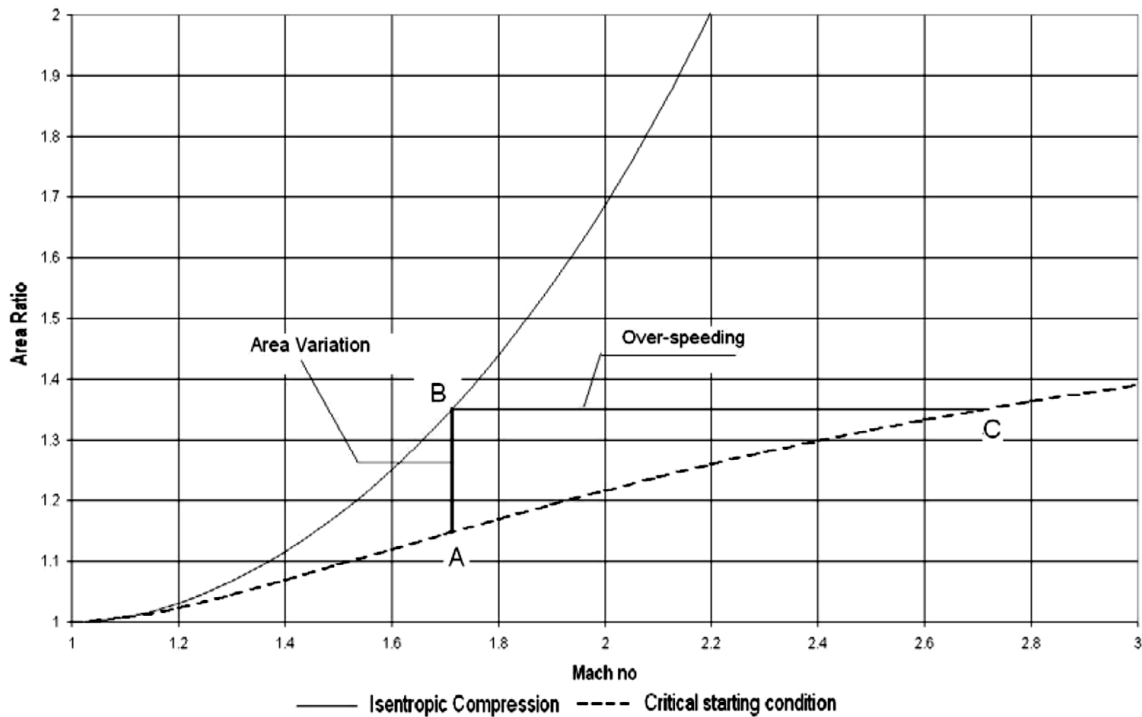


Fig 2.6: Method of Over-speeding and Area Variation for Starting an Intake

However, from Fig. 2.6, it can be seen that the amount of over-speeding required even for modest area ratios is very high. Hence, this method can best be employed for intakes aircrafts designed for a very low supersonic Mach number. Also, as has been discussed in Section 3.2, there exists a limiting area ratio (about 1.66) beyond which the intake cannot be started even if accelerated it to an infinitely high Mach number.

Hence the method of over-speeding cannot be used for intakes which are designed for Mach numbers beyond 2. Another problem with this method is that the intake remains in the 'non-started' condition for quite some time in the supersonic flight regime, which is not acceptable. Use of the method of 'over-speeding' has not been reported on any aircraft and its study is primarily of academic interest. As a result of its deficiencies, other methods need to be explored for overcoming the starting problem.

Variable area

Referring again to Fig. 2.6, we can see that another way of modifying the conditions at

point B so as to enable flow starting is by varying the area ratio, without over-speeding. The area ratio at B can be reduced so as to reach point A. Once the intake starts at point A, the area ratio can again be modified to operate at the design point. This method is referred to as 'Variation of Intake Geometry' and can be used for starting intakes designed even for high Mach numbers. However, it does require complex mechanisms for varying the area ratio. This adds to cost, weight and complexity. This method can further be categorized depending on the mechanism of modifying the intake geometry.

a) Rotation of a pivoted cowl

In this method, a cowl is pivoted to the main body and the position of the other end of the cowl is controlled, so as to vary the intake geometry. By this method, the entry area can be changed, thereby modifying the overall area ratio. This approach is relatively less complicated and has been employed in hypersonic intakes

b) Lateral movement of the ramp / cowl / centre-body

By moving the ramp or cowl or centre-body, a variation in the throat area as well as the inlet area can be achieved. Such a system has considerable flexibility and has been used in most military aircrafts. The centre-body system is for axisymmetric intakes. Although slightly more complex in design due to the requirement of moving a larger portion of the intake, this method gives better off-design performance in terms of matching the intake and hence enjoys widespread application.

Porous bleed

Another method employed for starting intakes is the use of porosity in the cowl. By doing this, the back-pressure at the throat is reduced so that, the normal shock can be positioned. Also, the use of bleed allows additional flow spillage without creating adverse conditions at the intake entry. The effective reduction in back pressure is dictated by the amount of mass removed using porous bleed and thus by the size and density of the holes used. Use of porosity in a 2D intake at the wedge has been experimentally studied.

The total pressure recovery as well as drag increase as a function of Mach number. These have been however found to be within limits, when compared with a solid wedge intake. Other factors that dictate the performance characteristics include the amount of bleed and its location. Cubbison, et al have experimentally studied the effects of variation in the location and bleed amount on the performance in axisymmetric intakes.

It has been reported that the best starting and stability characteristics were obtained when porosity was located just downstream of the terminal shock. Also, the intake performance in terms of pressure recovery has been reported to have improved with an increase in bleed percentage, though at the cost of increased inlet flow distortion.

Thus, it is seen that the use of porosity does enhance the overall performance of the intake, particularly under off-design conditions. Also, this method does not require any of the complicated and weight intensive equipment as needed in case of variable geometry. However, one of the major disadvantages associated with this method is the flow distortion, and this has been the major deterrent for most applications. Also, there are always losses related to mass flow even after the intake has started.

This leads to a lower critical performance. An improvement suggested is the use of variable bleed by controlling the bleed plenum exit area. This however comes at the cost of added complexity.

Other methods for Starting

Innovative methods for starting an intake designed for high supersonic and hypersonic speeds have been discussed in this section. The capture cross-section in hypersonic aircraft intakes employing the airframe-integrated-scamjet concept has been recommended to be rectangular. The initial compression is performed by the vehicle bow-shock.

The intake is then expected to start at ramjet speeds (around Mach 4) and operate over a large Mach number range. One of the proposed designs employs a rectangular capture area and elliptic throat (also known as REST; acronym for Rectangular to Elliptic Shape Transition). The combustor too is elliptic allowing better combustion characteristics. Three views of such a design are depicted in Fig. 3.5. Key features of this type of intake include

- Self-starting characteristics at Mach 4.
- Area ratio greater than the critical area ratio required for starting.

Starting is assisted by the use of spillage holes on the side walls and the peculiar shape of the cowl. Due to its simple construction which excludes any moving parts, this configuration seems to have a good scope for development in the future.

Combustion chamber

The combustion process in aircraft engines and gas turbines is a heat addition process to the compressed air in the combustor or burner. Thus, the combustion is a direct-fired air heater

in which fuel is burned. The combustor is situated between the compressor and turbine, where it accepts air from the compressor and delivers it at elevated temperature to the turbine.

Main requirements from gas turbine combustors

1. Its length and frontal area to remain within the limits set by other engine components, that is, size and shape compatible with engine envelop.
2. Its diffuser minimizes the pressure loss.
3. The presence of a liner to provide stable operation [i.e., the flame should stay alight over a wide range of air–fuel ratios (AFRs)].
4. Fulfills the pollutant emissions regulations (low emissions of smoke, unburned fuel, and gaseous pollutant species).
5. Ability to utilize much broader range of fuels.
6. Durability and relighting capability.
7. High combustion efficiency at different operating conditions: (1) altitude ranging from sea level to 11 km for civil transport and higher for some military aircraft and (2) Mach numbers ranging from zero during ground run to supersonic for military aircraft.
8. Design for minimum cost and ease of maintenance.
9. An outlet temperature distribution (pattern form) that is tailored to maximize the life of the turbine blades and nozzle guide vanes.
10. Freedom from pressure pulsations and other manifestations of combustion-induced instabilities.
11. Reliable and smooth ignition both on the ground (especially at very low ambient temperature) and in the case of aircraft engine flameout at high altitude.
12. The formation of carbon deposits (coking) must be avoided, particularly the hard brittle variety. Small particles carried into the turbine in the high velocity gas stream can erode the blades. Furthermore, aerodynamically excited vibration in the combustion chamber might cause sizeable pieces of carbon to break free, resulting in even worse damage to

the turbine.

Classification of combustion chambers

There are three main types of subsonic combustion chambers in use in gas turbine engines, namely, multiple chamber (tubular or can type), tubo-annular chamber, and the annular chamber.

Tubular (or can) combustion chambers

Tubular type is sometimes identified as multiple- or can-type combustion chamber. As shown in Fig 2.7 this type of combustor is composed of cylindrical chambers disposed around the shaft connecting the compressor and turbine. Compressor delivery air is split into a number of separate streams, each supplying a separate chamber. These chambers are interconnected to allow stabilization of any pressure fluctuations. Ignition starts sequentially with the use of two igniters.

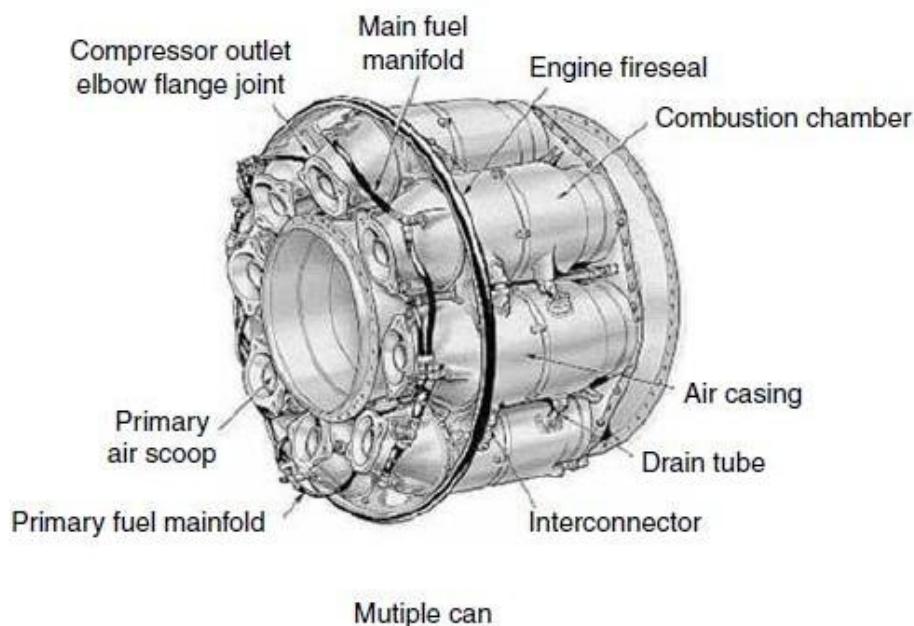


Fig 2.7:Multiple combustion chambers.

The number of combustion chambers varies from 7 to 16 per engine. The can-type combustion chamber is typical of the type used on both centrifugal and axial-flow engines. It is particularly well suited for the centrifugal compressor engine since the air leaving the compressor is already divided into equal portions as it leaves the diffuser vanes. It is then a simple matter to duct the air from the diffuser into the respective combustion chambers arranged radially around the axis of the engine.

The advantages of tubular type are as follows:

- Mechanically robust
- Fuel flow and airflow patterns are easily matched
- Rig testing necessitates only a small fraction of total engine air mass flow
- Easy replacement for maintenance.

The disadvantages are as follows:

- Bulky and heavy
- High pressure loss
- Requires interconnectors
- Incur problem of light-round
- Large frontal area and high drag

Turbo-annular combustion chambers

This type may also be identified as can-annular or cannular. It consists of a series of cylindrical burners arranged within common single annulus as is shown in Fig 2.8. Thus, it bridges the evolutionary gap between the tubular (multiple) and annular types. It combines the compactness of the annular chamber with the best features of the tubular type. The combustion chambers are enclosed in a removable shroud that covers the entire burner section. This feature makes the burners readily available for any required maintenance.

Cannular combustion chambers must have fuel drain valves in two or more of the bottom chambers. This ensures drainage of residual fuel to prevent its being burned at the next start. The flow of air through the holes and louvers of the can-annular system is almost identical to the flow through other types of burners. Reverse-flow combustors are mostly of the can-annular type. Reverse-flow combustors make the engine more compact.

Advantages of can-annular types are as follows:

- Mechanically robust.
- Fuel flow and airflow patterns are easily matched.
- Rig testing necessitates only a small fraction of total engine air mass flow.
- Shorter and lighter than tubular chambers.
- Low pressure loss.

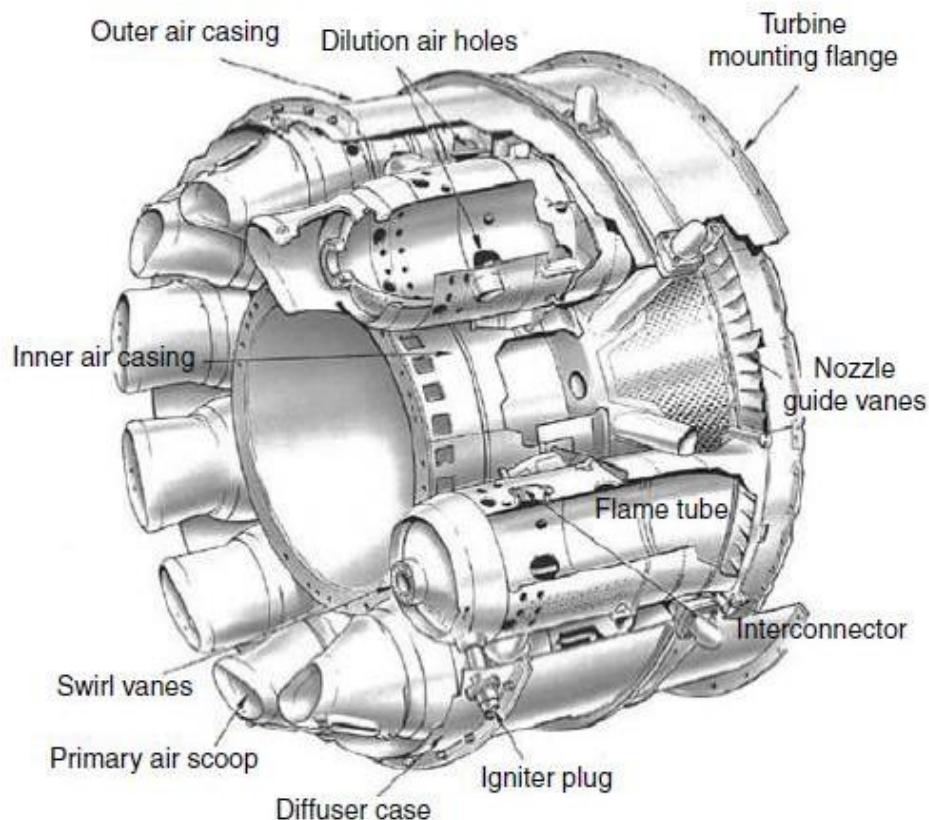


Fig2.8:Turbo-annular combustion chamber

Their disadvantages are as follows:

- Less compact than annular
- Requires connectors
- Incur a problem of light around.

Annular combustion chambers

In this type an annular liner is mounted concentrically inside an annular casing. This combustor represents the ideal configuration for combustors since its “clean” aerodynamic layout results in compact dimensions (and consequently an engine of small diameter) (Fig 2.9) and lower pressure loss than other designs.

Usually, enough space is left between the outer liner wall and the combustion chamber housing to permit the flow of cooling air from the compressor. Normally, this type is used in many engines using axial-flow compressor and also others incorporating dualtype compressors (combinations of axial flow and centrifugal flow). Currently, most aero engines use annular type combustors.

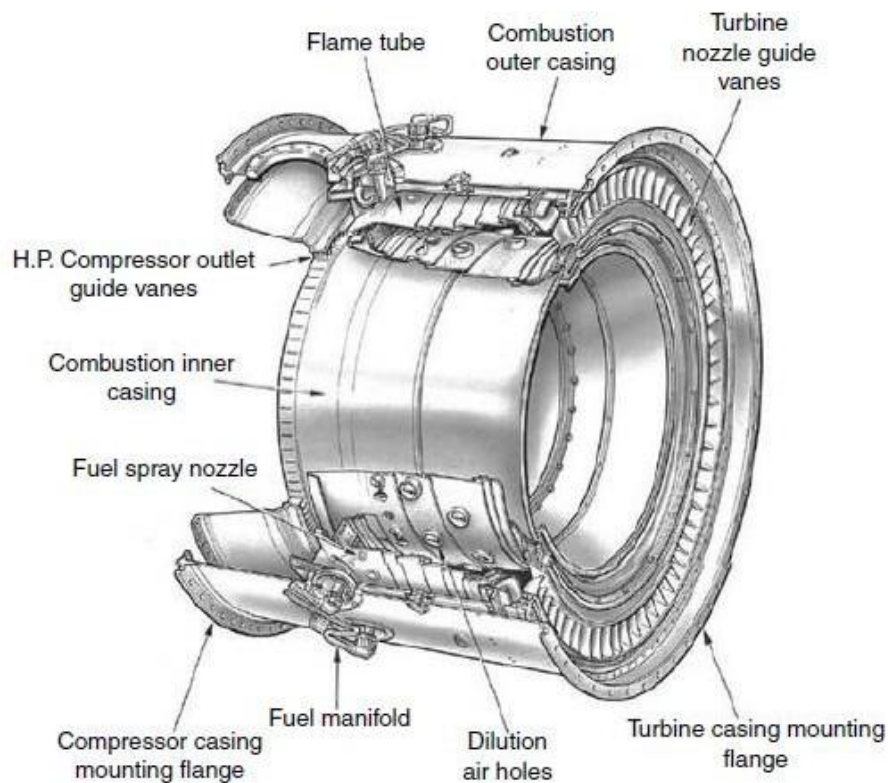


Fig 2.8:Annular type combustor.

The advantages of annular type may be summarized as follows:

- Minimum length and weight (its length is nearly 0.75 of cannular combustor length).
- Minimum pressure loss.
- Minimum engine frontal area.
- Less wall area than cannular and thus cooling air required is less; thus the combustion efficiency rises as the unburnt fuel is reduced.
- Easy light-round.
- Design simplicity.
- Combustion zone uniformity.
- Permits better mixing of the fuel and air.
- Simple structure compared to can burners.
- Increased durability.

Disadvantages

- Serious buckling problem on outer liner.
- Rig testing necessitates full engine air mass flow.

INLET PERFORMANCE

Depending on the flight speed and the mass flow demanded by the engine, the inlet might have to operate with a wide range of incident stream conditions. Figures 2.9(a) and (b) show the performances of subsonic intake during two typical subsonic conditions, take-off and cruise, respectively.

For each operating condition, three plots are given in Figure 2.9. The first illustrates the stream tube, while the second depicts the pressure and speed variation and the third is a temperature–entropy diagram. The flow in intake is identified by three states, namely far upstream that is denoted as (∞), at the duct entry denoted by (1) and at the engine face denoted by (2). The flow outside the engine (from state ∞ to 1) is an isentropic one, where no losses are associated with the total temperature and pressure. For high speed, or cruise condition, the stream tube will have a divergent shape and following conditions can be stated:

$$u_1 < u_\infty, \quad P_1 > P_\infty, \quad P_{01} = P_{0\infty}, \quad T_{01} = T_{0\infty}$$

During low speed high-thrust operation (e.g., during takeoff and climb), as shown in Figure , the same engine will demand more mass flow and the air stream upstream the intake will be accelerated. The stream tube will have a converging shape and the following conditions are satisfied:

$$u_1 > u_\infty, \quad P_1 < P_\infty, \quad P_{01} = P_{0\infty}, \quad T_{01} = T_{0\infty}$$

For both cases of takeoff and cruise, there will be internal diffusion within the intake up to the engine face. The static pressure will rise and the air speed will be reduced. The total pressure will also decrease owing to skin friction while the total temperature remains unchanged, as the flow through diffuser is adiabatic. Thus, for both take-off and cruise conditions

$$P_2 > P_1, \quad P_{02} < P_{0\infty}, \quad u_2 < u_1$$

Since the inlet speed to the engine (compressor/fan) should be nearly constant for different operating conditions, then

$$\left(\frac{P_2}{P_1}\right)_{\text{takeoff}} > \left(\frac{P_2}{P_1}\right)_{\text{cruise}}$$

If this pressure increase is too large, the diffuser may stall due to boundary layer separation. Stalling usually reduces the stagnation pressure of the stream as a whole. Conversely, for cruise conditions to avoid separation or to have a less severe loading on the boundary layer, it is

recommended to have a low velocity ratio (u_1/u_∞) and consequently less internal pressure rise. Therefore, the inlet area is often chosen so as to minimize external acceleration during take-off with the result that external deceleration occurs during level-cruise operation. Under these conditions the “upstream capture area” A_∞ is less than the inlet area A_1 , and some flow is spilled over the inlet.

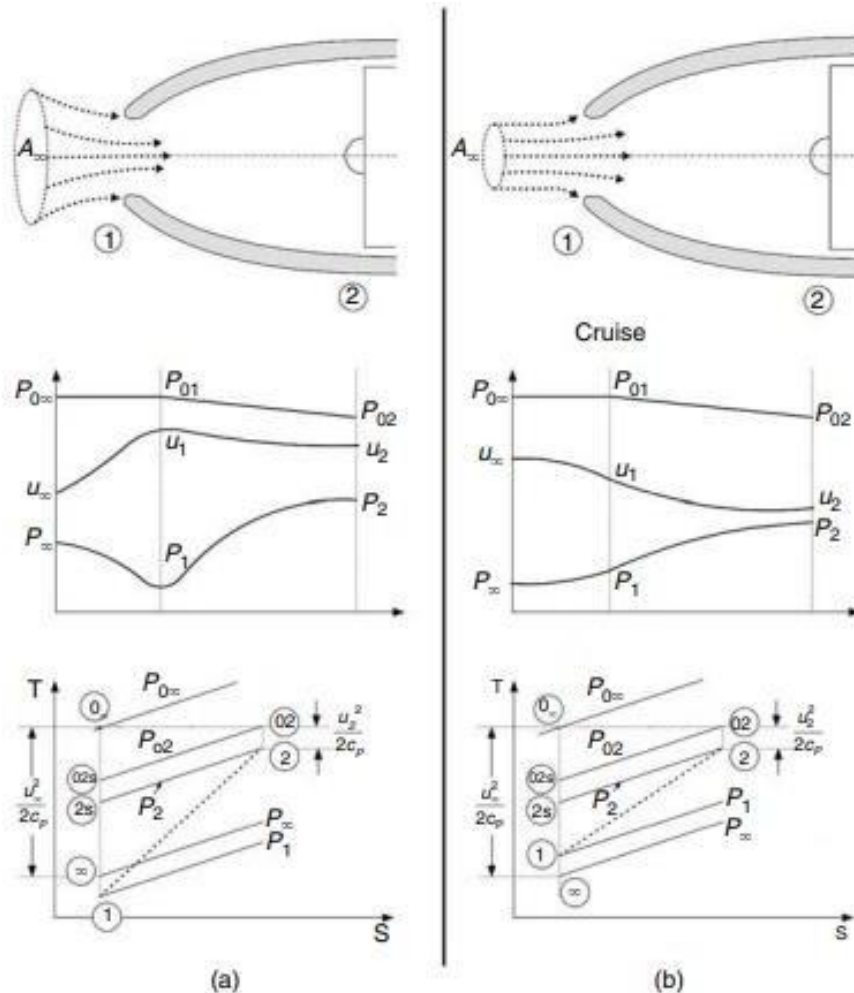


Fig 2.9: Subsonic inlet during (a) takeoff and (b) cruise

The serious problem is the change in M_∞ from zero at take-off to about 0.8 at cruise. If optimized for the $M_\infty = 0.8$ cruise, the inlet would have a thin lip to minimize the increase in Mach number as the flow is divided. However, this inlet would separate badly on the inside at take-off and low subsonic conditions because the turn around the sharp lip would impose severe pressure gradients. To compromise, the lip is rounded making it less sensitive to flow angle, but incurring some loss due to separation in the exterior flow. When fully developed a good inlet will produce a pressure recovery $P_{02}/P_{0a} = 0.95-0.97$ at its optimum condition.

Example 1 Prove that the capture area (A_∞) for a subsonic diffuser is related to the free stream Mach number (M_∞) by the relation:

$$A_{\infty} = \lambda / M_{\infty}$$

Where

$$\lambda = \frac{\dot{m}_{\infty}}{P_{\infty}} \sqrt{\frac{RT_{\infty}}{\gamma}}$$

A turbofan engine during ground ingests airflow at the rate of $\dot{m}_{\infty} = 500$ kg/s through an inlet area (A_1) of 3.0 m^2 . If the ambient conditions (T_{∞} , P_{∞}) are 288 K and 100 kPa, respectively, calculate the area ratio (A_{∞}/A_1) for different free stream Mach numbers. What is the value of the Mach number where the capture area is equal to the inlet area? Draw the air stream tube for different Mach numbers.

Solution: The mass flow rate is

$$\dot{m}_{\infty} = \rho_{\infty} V_{\infty} A_{\infty} = \frac{P_{\infty}}{RT_{\infty}} (M_{\infty} \sqrt{\gamma RT_{\infty}}) A_{\infty}$$

$$A_{\infty} = \frac{\dot{m}_{\infty}}{P_{\infty} M_{\infty}} \sqrt{\frac{RT_{\infty}}{\gamma}}$$

$$A_{\infty} = \frac{\lambda}{M_{\infty}}$$

$$\lambda = \frac{\dot{m}_{\infty}}{P_{\infty}} \sqrt{\frac{RT_{\infty}}{\gamma}}$$

From the given data, then

$$\lambda = \frac{\dot{m}_{\infty}}{P_{\infty}} \sqrt{\frac{RT_{\infty}}{\gamma}} = \frac{500}{100 \times 10^3} \sqrt{\frac{287 \times 288}{1.4}} = 1.215$$

From (b), the capture area is equal to the engine inlet area ($A_{\infty}/A_1 = 1$) when $M_{\infty} = 0.405$. From relation (b), the following table is constructed:

M_{∞}	0.05	0.1	0.2	0.3	0.4	0.5
A_{∞}/A_1	8.1	4.05	2.025	1.35	1.0125	0.81
D_{∞}/D_1	2.84	2.0125	1.42	1.162	1.006	0.9

PERFORMANCE PARAMETERS

Two parameters will be discussed here:

1. Isentropic efficiency (η_d)
2. Stagnation pressure ratio (r_d)

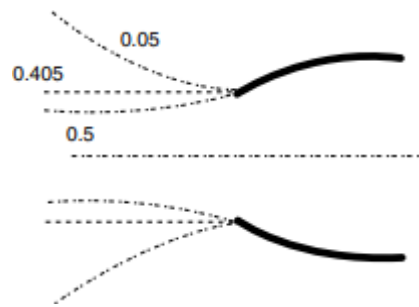


Fig 2.10: Stream tubes for different free stream Mach numbers

1. Isentropic efficiency (η_d)

The isentropic efficiency of the intake η_d is a static-to-total efficiency and as previously defined, it is a measure for the losses from the far upstream conditions to the engine face. The efficiency is then expressed by the following relation (refer to Figure 2.9a):

$$\eta_d = \frac{h_{02s} - h_\infty}{h_{02} - h_\infty} = \frac{T_{02s} - T_\infty}{T_{02} - T_\infty} = \frac{(T_{02s}/T_\infty) - 1}{(T_{02}/T_\infty) - 1}$$

$$\frac{T_{02}}{T_\infty} = \frac{T_{0\infty}}{T_\infty} = 1 + \frac{\gamma - 1}{2} M_\infty^2$$

$$\therefore \eta_d = \frac{(P_{02}/P_\infty)^{(\gamma-1)/\gamma} - 1}{[(\gamma - 1)/2] M_\infty^2}$$

$$\frac{P_{02}}{P_\infty} = \left(1 + \eta_d \frac{\gamma - 1}{2} M_\infty^2\right)^{\gamma/(\gamma-1)}$$

2. Stagnation pressure ratio (r_d)

Modern jet transports may cruise with values of the pressure recovery of 97%–98%. Supersonic aircraft with well-designed, practical inlet and internal flow systems may have pressure recoveries of 85% or more for Mach numbers in the 2.0–2.5 range.

Stagnation pressure ratio is defined as the ratio between the average total pressure of the air entering the engine to that of the free stream air, or

$$r_d = P_{02}/P_{0\infty}$$

$$\frac{P_{02}}{P_\infty} = \frac{P_{02}}{P_{0\infty}} \frac{P_{0\infty}}{P_\infty} = r_d \left[1 + \frac{\gamma - 1}{2} M_\infty^2\right]^{\gamma/(\gamma-1)}$$

From Equations 9.2 and 9.3

$$\therefore \eta_d = \frac{(r_d)^{(\gamma-1)/\gamma} \left[1 + \frac{\gamma-1}{2} M_\infty^2 \right] - 1}{\left(\frac{\gamma-1}{2} \right) M_\infty^2}$$

Moreover, the pressure recovery can be expressed as

$$r_d = P_{02}/P_{0\infty} = \left[\frac{1 + \eta_d \frac{\gamma-1}{2} M_\infty^2}{1 + \frac{\gamma-1}{2} M_\infty^2} \right]^{\gamma/(\gamma-1)}$$

Thus if the isentropic efficiency is known, the pressure recovery can be obtained from Equation, while if the pressure recovery is known, the diffuser efficiency can be determined from Equation 9.4. However, since the flow upstream of the intake is isentropic, then all the losses are encountered inside the intake, or from state (1) to state (2). In some cases, the efficiency is defined for the internal part of diffuser (η_d). In this case, the diffuser efficiency is defined as

$$\begin{aligned} \eta'_d &= \frac{h_{02s} - h_1}{h_{02} - h_1} = \frac{T_{02s} - T_1}{T_{02} - T_1} = \frac{(T_{02s}/T_1) - 1}{(T_{01}/T_1) - 1} \\ \eta'_d &= \frac{(P_{02}/P_1)^{(\gamma-1)/\gamma} - 1}{(P_{01}/P_1)^{(\gamma-1)/\gamma} - 1} = \frac{(P_{02}/P_1)^{(\gamma-1)/\gamma} - 1}{\frac{\gamma-1}{2} M_1^2} \\ (P_{02}/P_1) &= \left(1 + \eta'_d \frac{\gamma-1}{2} M_1^2 \right)^{\gamma/(\gamma-1)} \end{aligned}$$

Example 2 Consider the turbofan engine described in Example 1 during flight at a Mach number of 0.9 and altitude of 11 km where the ambient temperature and pressure are respectively -56.5°C and 22.632 kPa. The mass ingested into the engine is now 235 kg/s. If the diffuser efficiency is 0.9 and the Mach number at the fan face is 0.45, calculate the following:

1. The capture area
2. The static pressures at the inlet and fan face
3. The air speed at the same stations as above
4. The diffuser pressure recovery factor

Solution:

1. The ambient static temperature is $T_\infty = -56.5 + 273 = 216.5 \text{ K}$

The free stream speed is $u_\infty = M_\infty \sqrt{\gamma RT_\infty} = 271.6 \text{ m/s}$

The free stream density $\rho_\infty = P_\infty/RT_\infty = 0.3479 \text{ kg/m}^3$

The capture area is $A_\infty = \dot{m}/\rho_\infty u_\infty = 2.486 \text{ m}^2$

Which is smaller than the inlet area?

2. To calculate the static pressures at states (1) and (2) two methods may be used, namely,
- (a) Gas dynamics tables
 - (b) Isentropic relations

The first method

3. From gas dynamics tables, at Mach number equal to 0.9, the area ratio $A/A_* = 1.00886$

Then $A_* = 2.486/1.00886 = 2.465 \text{ m}^2$

$A_1/A_* = 3/2.465 = 1.217 \text{ m}^2$

From tables, $M_1 = 0.577$.

The corresponding temperature and pressure ratios are $P_1/P_{01} = 0.798$, $T_1/T_{01} = 0.93757$.

Since $T_{01} = T_{0\infty}$, $P_{01} = P_{0\infty}$, then $P_1 = 30.547 \text{ kPa}$, $T_1 = 246.9 \text{ K}$.

Moreover, $u_1 = M_1$

$\sqrt{\gamma} RT_1 = 181.7 \text{ m/s}$.

Since $M_2 = 0.45$, then $P_2/P_{02} = 0.87027$.

Now from the diffuser efficiency, from Equation 9.2, the pressure ratio

$$\frac{P_{02}}{P_{\infty}} = (1 + 0.9 \times 0.2 \times 0.9^2)^{3.5} = 1.6102$$

$$P_{02} = 36.442 \text{ kPa}$$

$$P_2 = \frac{P_{02}}{\left(1 + \frac{\gamma - 1}{2} M_2^2\right)^{\gamma/(\gamma - 1)}} = 31.714 \text{ kPa}$$

$$T_2 = \frac{T_{02}}{\left(1 + \frac{\gamma - 1}{2} M_2^2\right)} = 253.1 \text{ K}$$

Then $u_2 = M_2 \sqrt{\gamma RT_2} = 143.5 \text{ m/s}$.

The pressure recovery factor $r_d = P_{02}/P_{0\infty} = 36.442/38.278 = 0.952$.

The above results can be summarized in the following table:

State	∞	1	2
T (K)	226.65	246.9	253.1
T_0 (K)		263.36	
P (kPa)	22.632	30.547	31.71
P_0 (kPa)	38.278	38.278	36.442
u (m/s)	271.6	181.7	143.5
M	0.9	0.577	0.45

The second method

The continuity equation

$$\frac{\dot{m}}{A} = \rho u = \frac{P}{RT} M \sqrt{\gamma RT} = PM \sqrt{\frac{\gamma}{RT}}$$

$$\frac{\dot{m}}{A} = \frac{MP_0}{\left(1 + \frac{\gamma-1}{2} M^2\right)^{\gamma/(\gamma-1)}} \sqrt{\frac{\gamma}{R}} \sqrt{\frac{(1 + \frac{\gamma-1}{2} M^2)}{T_0}}$$

$$\frac{\dot{m}}{A} = \frac{MP_0}{\left(1 + \frac{\gamma-1}{2} M^2\right)^{(\gamma+1)/2(\gamma-1)}} \sqrt{\frac{\gamma}{RT_0}}$$

Applying the above equation at station (1), then

$$\frac{\dot{m}}{A_1 P_{01}} \sqrt{\frac{RT_{01}}{\gamma}} = \frac{M_1}{\left(1 + \frac{\gamma-1}{2} M_1^2\right)^{(\gamma+1)/2(\gamma-1)}}$$

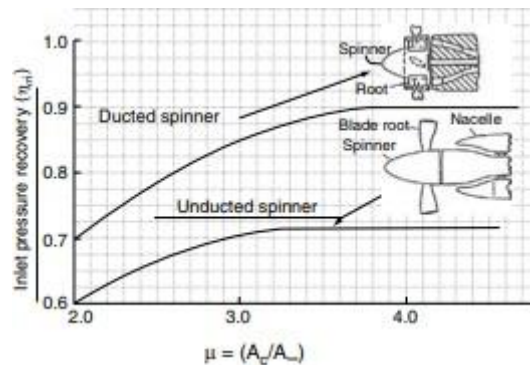


Fig 2.11: Efficiency of inlets of turboprop engine. (Courtesy of John Seddon [6].)

The left-hand side is known, and the Mach number M_1 is unknown, which can be determined iteratively. From M_1 determine T_1

$$T_1 = \frac{T_{0\infty}}{\left(1 + \frac{\gamma-1}{2} M_1^2\right)}$$

Determine $P_1 = P_{0\infty} / \left(1 + \frac{\gamma-1}{2} M_1^2\right)^{\gamma/(\gamma-1)}$ and u_1 as above.

Determine P_{02} from Equation 9.2, thus determine the recovery pressure ratio.

Determine $P_2 = P_{02} / \left(1 + \frac{\gamma-1}{2} M_2^2\right)^{\gamma/(\gamma-1)}$ and $T_2 = T_{0\infty} / \left(1 + \frac{\gamma-1}{2} M_2^2\right)$.

Next, determine the air speed at the fan face from the relation $u_2 = M_2 \sqrt{\gamma R T_2}$.

TURBOPROP INLETS

The intake for turboprop engines is much complicated due to the bulk gearbox. However, an aerodynamically efficient turboprop intake can be achieved by use of a ducted spinner. Improvement of intake performance is achieved by choosing large entry area. In addition, minimum cylindrical roots are encased in fairings of low thickness/chord, which form the structural members supporting the spinner cowl. The efficiency of the intake, defined as the ratio between the difference between the static pressure at the engine face and the free stream value to the dynamic pressure is plotted versus the ratio between the capture area and the duct entry.

SUPERSONIC INTAKES

The design of inlet systems for supersonic aircraft is a highly complex matter involving engineering trade-offs between efficiency, complexity, weight, and cost. A typical supersonic intake is made up of a supersonic diffuser, in which the flow is decelerated by a combination of shocks and diffuse compression, and a subsonic diffuser, which reduces the Mach number from high subsonic value after the last shock to the value acceptable to the engine. Subsonic intakes that have thick lip are quite unsuitable for supersonic speeds. The reason is that a normal shock wave ahead of the intake is generated, which will yield a very sharp static pressure rise without change of flow direction and correspondingly big velocity reduction. The adiabatic efficiency of compression through a normal shock wave is very low as compared with oblique shocks. At Mach 2.0 in the stratosphere adiabatic efficiency would be about 80% or less for normal shock waves, whereas its value will be about 95% or even more for an intake designed for oblique shocks.

Flight at supersonic speeds complicates the diffuser design for the following reasons:

1. The existence of shock waves that lead to large decrease in stagnation pressure even in the absence of viscous effects.
2. The large variation in capture stream tube area between subsonic and supersonic flight for a given engine, as much as a factor of four between $M_\infty = 1$ and $M_\infty = 3$.

3. As M_∞ increases, the inlet compression ratio becomes a larger fraction of the overall cycle compression ratios and as a result, the specific thrust becomes more sensitive to diffuser pressure ratio.
4. It must operate efficiently both during the subsonic flight phases (takeoff, climb, and subsonic cruise) and at supersonic design speed.

Generally, supersonic intake may be classified as follows.

I. Axisymmetric or two-dimensional intakes

The axisymmetric intakes use axisymmetric central cone to shock the flow down to subsonic speeds. The two-dimensional inlets have rectangular cross sections as found in the F-14 and F-15 fighter aircraft.

II. Variable or fixed geometry

For variable geometry axisymmetric intakes, the central cone may move fore-and-aft to adjust the intake area. Alternatively, the inlet area is adjusted in the case of rectangular section through hinged flaps (or ramps) that may change its angles. For flight at Mach numbers much beyond 1.6, variable geometry features must be incorporated in the inlet to achieve high inlet pressure recoveries together with low external drag. The General Dynamics F-111 airplane has a quarter-round inlet equipped with a translating center body or spike. The inlet is bounded on the top by the wing and on one side by the fuselage. An installation of this type is often referred to as an “armpit” inlet. The spike automatically translates fore and aft as the Mach number changes. The throat area of the inlet also varies with Mach number. This is accomplished by expansion and contraction of the rear part of the spike.

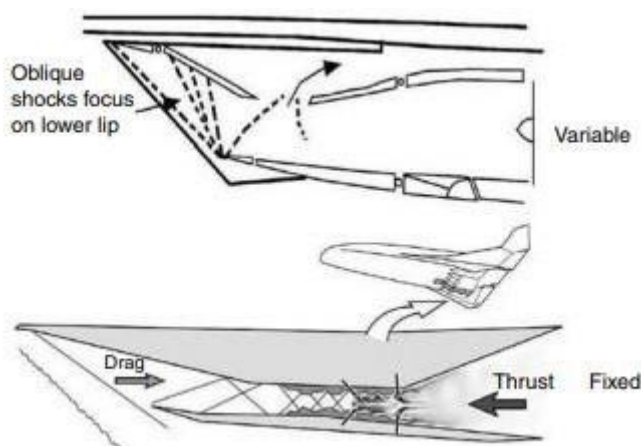


Fig 2.12: Variable and fixed geometry supersonic intakes.

III. Internal, external or mixed compression

As shown in Figure 2.13 the set of shocks situated between the forebody and intake lip are

identified as external shocks, while the shocks found between the nose lip and the intakes throat are called internal shocks. Some intakes have one type of shocks either external or internal and given the same name as the shocks, while others have both types and denoted as mixed compression intakes. A constant area (or fixed geometry) intake may be either axisymmetric or two-dimensional. The supersonic pitot intake is a constant cross-sectional area intake similar to the subsonic pitot intake but it will require a sharp lip for shock wave attachment. This will substantially reduce intake drag compared with that of the subsonic round-edged lip operating at the same Mach number. Sharp edges unfortunately result in poor pressure recovery at low Mach numbers. However, this design presents a very simple solution for supersonic intakes. Variable geometry intakes may involve the use of translating center body, variable geometry center body, and the use of a cowl with a variable lip angle, variable ramp angles, and/or variable throat area. Using variable geometry inlets requires the use of sensors, which add complexity and weight to the inlet.

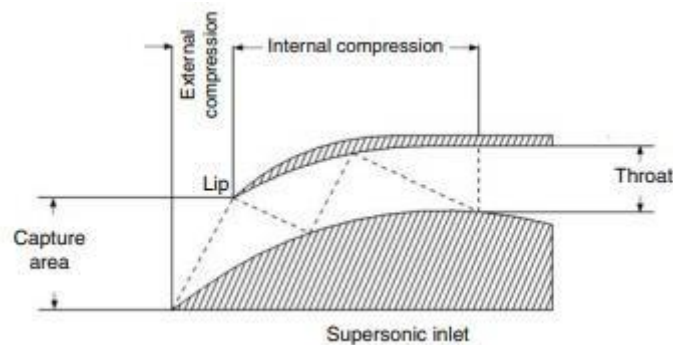


Fig 2.13: External and internal compression supersonic intake.

The use of axisymmetric or two-dimensional inlets is dependent on the method of engine installation on the aircraft, the cruise Mach number, and the type of the aircraft (i.e., military or civil) as clearly illustrated in Figures 2.14 and 2.15.

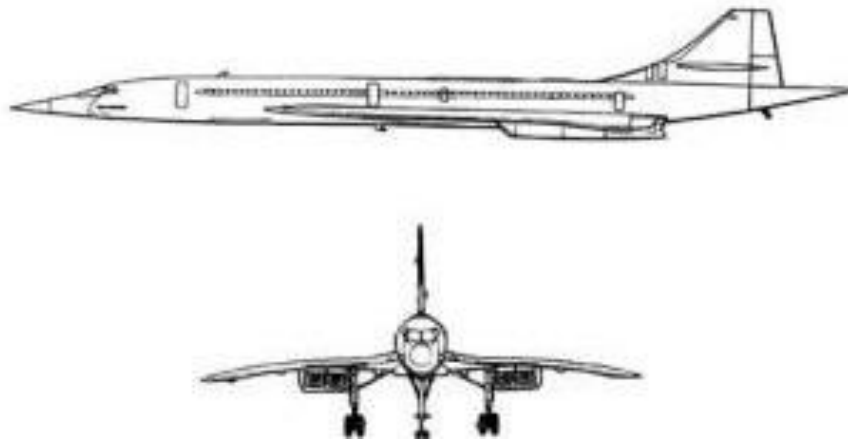


Fig 2.14: Concorde Aircraft

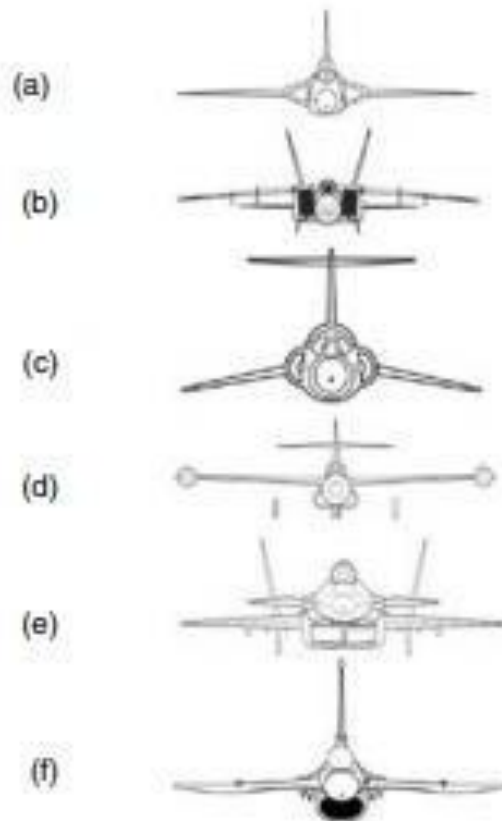


Fig 2.15: Intakes for military aircrafts: (a) F5D-1 Skylancer, (b) MIG-25, (c) F-104, (d) F-89, (e) MIG-FMI, and (f) F-16-A.

Review Of Gas Dynamic Relations For Normal And Oblique Shocks

Normal Shock Waves

For a normal shock wave, denoting the conditions upstream and downstream the shock by

subscripts 1 and 2, respectively, the following relations give the downstream Mach number, static temperature and pressure ratios, density ratio, and total pressure ratio across the shock:

$$M_2^2 = \frac{(\gamma - 1)M_1^2 + 2}{2\gamma M_1^2 - (\gamma - 1)}$$

$$\frac{T_2}{T_1} = \left[\frac{2}{(\gamma + 1)M_1^2} + \left(\frac{\gamma - 1}{\gamma + 1} \right) \right] \left[\left(\frac{2\gamma}{\gamma + 1} \right) M_1^2 - \left(\frac{\gamma - 1}{\gamma + 1} \right) \right]$$

$$\frac{P_2}{P_1} = \left[1 + \left(\frac{2\gamma}{\gamma + 1} \right) (M_1^2 - 1) \right]$$

$$\frac{\rho_2}{\rho_1} = \left[\frac{(\gamma + 1)M_1^2}{2 + (\gamma - 1)M_1^2} \right]$$

$$\frac{P_{02}}{P_{01}} = \left[\frac{(\gamma + 1)M_1^2}{2 + (\gamma - 1)M_1^2} \right]^{\gamma/(\gamma-1)} \left[\left(\frac{2\gamma}{\gamma + 1} \right) M_1^2 - \left(\frac{\gamma - 1}{\gamma + 1} \right) \right]^{-1/(\gamma-1)}$$

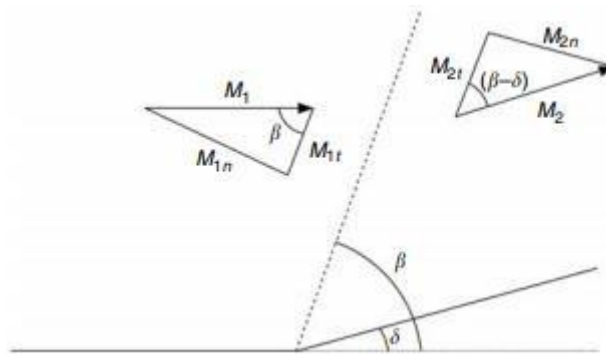


Fig 2.16 Nomenclature of oblique shock wave

Oblique Shock Waves

The shown oblique shock (Figure 2.16) has a shock angle β and a deflection angle δ . Oblique shock can be treated as a normal shock having an upstream Mach number $M_{1n} = M_1 \sin \beta$ and a tangential component $M_{1t} = M_1 \cos \beta$. The tangential velocity components upstream and downstream the shocks are equal. From References 11 and 12, the following relations are given:

$$\tan \delta = \frac{2 \cot \beta (M_1^2 \sin^2 \beta - 1)}{(\gamma + 1)M_1^2 - 2(M_1^2 \sin^2 \beta - 1)} \quad (9.12a)$$

For $\gamma = 7/4$, then

$$\tan \delta = 5 \frac{M_1^2 \sin 2\beta - 2 \cot \beta}{10 + M_1^2(7 + 5 \cos 2\beta)} \quad (9.12b)$$

$$M_2^2 \sin^2(\beta - \delta) = \frac{(\gamma - 1)M_1^2 \sin^2 \beta + 2}{2\gamma M_1^2 \sin^2 \beta - (\gamma - 1)} \quad (9.13a)$$

For $\gamma = 7/4$, then

$$M_2^2 = \frac{36M_1^4 \sin^2 \beta - 5(M_1^2 \sin^2 \beta - 1)(7M_1^2 \sin^2 \beta + 5)}{(7M_1^2 \sin^2 \beta - 1)(M_1^2 \sin^2 \beta + 5)} \quad (9.13b)$$

$$\frac{P_2}{P_1} = \left[1 + \left(\frac{2\gamma}{\gamma + 1} \right) (M_1^2 \sin^2 \beta - 1) \right] \quad (9.14a)$$

For $\gamma = 7/4$, then

$$\frac{P_2}{P_1} = \left(\frac{7M_1^2 \sin^2 \beta - 1}{6} \right) \quad (9.14b)$$

$$\frac{T_2}{T_1} = \left[\frac{2}{(\gamma + 1)M_1^2 \sin^2 \beta} + \left(\frac{\gamma - 1}{\gamma + 1} \right) \right] \left[\left(\frac{2\gamma}{\gamma + 1} \right) M_1^2 \sin^2 \beta - \left(\frac{\gamma - 1}{\gamma + 1} \right) \right] \quad (9.15a)$$

For $\gamma = 7/4$, then

$$\frac{T_2}{T_1} = \frac{(7M_1^2 \sin^2 \beta - 1)(M_1^2 \sin^2 \beta + 5)}{36M_1^2 \sin^2 \beta}$$

$$\frac{\rho_2}{\rho_1} = \left[\frac{(\gamma + 1)M_1^2 \sin^2 \beta}{2 + (\gamma - 1)M_1^2 \sin^2 \beta} \right]$$

For $\gamma = 7/4$, then

$$\frac{\rho_2}{\rho_1} = \left[\frac{6M_1^2 \sin^2 \beta}{M_1^2 \sin^2 \beta + 5} \right]$$

$$\frac{P_{02}}{P_{01}} = \left[\frac{(\gamma + 1)M_1^2 \sin^2 \beta}{2 + (\gamma - 1)M_1^2 \sin^2 \beta} \right]^{\gamma/(\gamma-1)} \left[\left(\frac{2\gamma}{\gamma + 1} \right) M_1^2 \sin^2 \beta - \left(\frac{\gamma - 1}{\gamma + 1} \right) \right]^{-(1/(\gamma-1))}$$

For $\gamma = 7/4$, then the relation for total pressure ratio will be

$$\frac{P_{02}}{P_{01}} = \left[\frac{6M_1^2 \sin^2 \beta}{M_1^2 \sin^2 \beta + 5} \right]^{7/2} \left[\frac{6}{7M_1^2 \sin^2 \beta - 1} \right]^{5/2}$$

EXTERNAL COMPRESSION INTAKE (INLET)

External compression intakes complete the supersonic diffusion process outside the covered portion of the inlet where the flow is decelerated through a combination of oblique shocks (may be a single, double, triple, or multiple). These oblique shocks are followed by a normal shock wave that changes the flow from supersonic to subsonic flow. Both the normal shock wave and the throat are ideally located at the cowl lip. The supersonic diffuser is followed by a subsonic diffuser, which reduces the Mach number from high subsonic value after the last shock to the value acceptable to the engine. The simplest form of staged compression is the single oblique shock, produced by a single-angled wedge or cone that projects forward of the duct, followed by a normal shock as illustrated in Figure 2.17.

The intake in this case is referred to as a two-shock intake. With a wedge, the flow after the oblique shock wave is at constant Mach number and parallel to the wedge surface. With a cone the flow behind the conical shock is itself conical, and the Mach number is constant along rays from the apex and varies along streamline. Forebody intake is frequently used for “external compression intake of wedge or cone form”.

The capture area (A_c) for supersonic intakes is defined as the area enclosed by the leading edge, or “highlight,” of the intake cowl, including the cross-sectional area of the forebody in that plane. The maximum flow ratio is achieved when the boundary of the free stream tube (A_∞) arrives undisturbed at the lip. This means

$$\frac{A_\infty}{A_c} = 1.0$$

This condition is identified as the full flow or the critical flow. This condition depends on the Mach number, angle of the forebody and the position of the tip. In this case, the shock angle θ is equal to the angle subtended by lip at the apex of the body and corresponds to the maximum possible

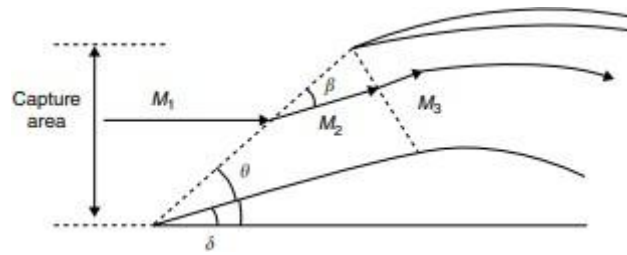


Fig 2.17: Single oblique shock external compression intake

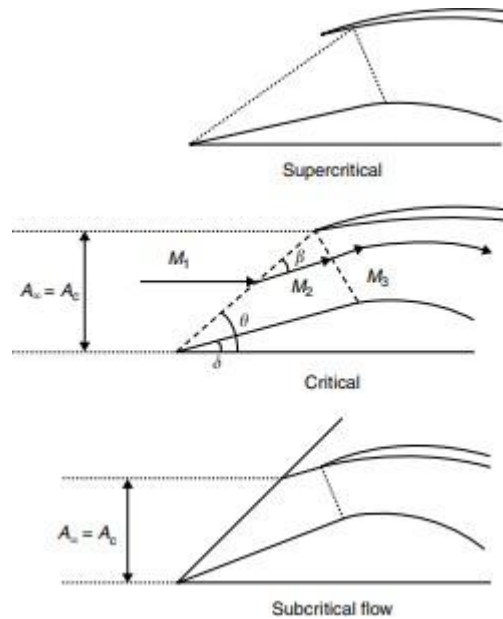


Fig 2.18: Types of flow in an external compression intake

flow through the intake (Figure 2.18). This is the design point for constant area intake and the goal of the variable area intake as to stay at that condition over the flight operating range. At Mach numbers (or speeds) below the value of the critical (design) value described above, the mass flow is less than that at the critical condition and the normal shock wave occurs in front of the cowl lip and this case is identified as subcritical. It is to be noted here that

$$\frac{A_{\infty}}{A_c} < 1.0$$

Moreover, the outer drag of the intake becomes very large and smaller pressure recovery is obtained. If the air speed is greater than the design value, then the oblique shock will impinge inside the cowl lip and the normal shock will move to the diverging section. This type of operation is referred to as the supercritical operation. The two-shock intake is only moderately good at Mach 2.0 and unlikely to be adequate at higher Mach numbers. The principle of breaking down an external shock system can be extended to any desired number of

stages. The next step is the three-shock intake where two oblique shocks are followed by a normal shock, where the double-wedge and double-cone are the archetypal forms (Figure 2.19).

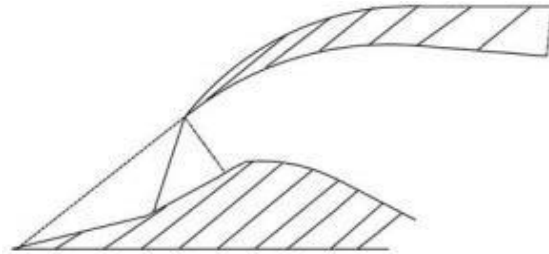


Fig 2.19: Three shocks for double-cone (or double-wedge) geometry.

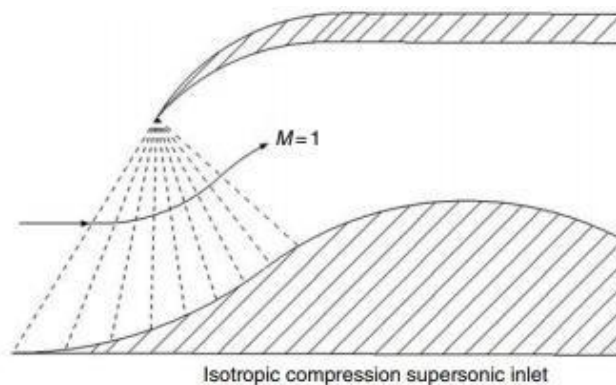


Fig 2.20: Isotropic compression supersonic inlet.

Continuing the process of breaking down the external shock system, three or more oblique shocks may be used ahead of the normal shock. For a system of (n-1) oblique shocks, the pressure recovery factor will be

$$r_d \frac{P_{02}}{P_{0\infty}} = \frac{P_{02}}{P_{01}} \frac{P_{03}}{P_{02}} \frac{P_{04}}{P_{03}} \dots \frac{P_{0n}}{P_{0n-1}} \left(\frac{P_{0n}}{P_{0n-1}} \right)_{\text{normal shock}}$$

Two remarks are to be mentioned here:

1. As the number of oblique shocks increases, the pressure recovery factor increases.
2. Up to Mach 2, equal deflections of the successive wedge angles give the best results, while for higher Mach numbers the first deflection angle needs to be the smallest and the last the largest.

Extending the principle of multi-shock compression to its limit leads to the concept of isentropic compression, in which a smoothly contoured fore-body produces an infinitely large number of infinitely weak oblique shocks, Figure 2.20. In this case, the supersonic stream is compressed with no losses in the total pressure.

NOZZLES

A nozzle (from nose, meaning 'small spout') is a tube of varying cross-sectional area (usually axisymmetric) aiming at increasing the speed of an outflow, and controlling its direction and shape. Nozzle flow always generates forces associated to the change in flow momentum, as we can feel by hand-holding a hose and opening the tap. In the simplest case of a rocket nozzle, relative motion is created by ejecting mass from a chamber backwards through the nozzle, with the reaction forces acting mainly on the opposite chamber wall, with a small contribution from nozzle walls. As important as the propeller is to shaft-engine propulsions, so it is the nozzle to jet propulsion, since it is in the nozzle that thermal energy (or any other kind of high-pressure energy source) transforms into kinetic energy of the exhaust, and its associated linear momentum producing thrust.

The flow in a nozzle is very rapid (and thus adiabatic to a first approximation), and with very little frictional losses (because the flow is nearly one-dimensional, with a favourable pressure gradient except if shock waves form, and nozzles are relatively short), so that the isentropic model all along the nozzle is good enough for preliminary design. The nozzle is said to begin where the chamber diameter begins to decrease (by the way, we assume the nozzle is axisymmetric, i.e. with circular cross-sections, in spite that rectangular cross-sections, said two-dimensional nozzles, are sometimes used, particularly for their ease of direction ability). The meridian nozzle shape is irrelevant with the 1D isentropic models; the flow is only dependent on cross-section area ratios.

Real nozzle flow departs from ideal (isentropic) flow on two aspects:

- Non-adiabatic effects. There is a kind of heat addition by non-equilibrium radical-species recombination and a heat removal by cooling the walls to keep the strength of materials in long-duration rockets (e.g. operating temperature of cryogenic SR-25 rockets used in Space Shuttle is 3250 K, above steel vaporization temperature of 3100 K, not just melting, at 1700 K). Short-duration rockets (e.g. solid rockets) are not actively cooled but rely on ablation; however, the nozzle-throat diameter cannot let widen too much, and reinforced materials (e.g. carbon, silica) are used in the throat region.

- There is viscous dissipation within the boundary layer, and erosion of the walls, what can be critical if the erosion widens the throat cross-section, greatly reducing exit-area ratio and consequently thrust.
- Axial exit speed is lower than calculated with the one-dimensional exit speed, when radial outflow is accounted for.

We do not consider too small nozzles, say with chamber size <10 mm and neck size <1 mm, where the effect of boundary layers become predominant.

Restricting the analysis to isentropic flows, the minimum set of input parameters to define the propulsive properties of a nozzle (the thrust is the mass-flow-rate times the exit speed $F = \dot{m}v_e$) are:

- Nozzle size, given by the exit area, A_e ; the actual area law, provided the entry area is large enough that the entry speed can be neglected, only modifies the flow inside the nozzle, but not the exit conditions.
- Type of gas, defined with two independent properties for a perfect-gas model, that we take as the thermal capacity ratio $\gamma = c_p/c_v$, and the gas constant, $R = R_u/M$, and with $R_u = 8.314$ J/(mol·K) and M being the molar mass, which we avoid using, to reserve the symbol M for the Mach number. If c_p is given instead of γ , then we compute it from $\gamma = c_p/c_v = c_p/(c_p - R)$, having used Mayer's relation, $c_p - c_v = R$.
- Chamber (or entry) conditions: p_c and T_c (a relatively large chamber cross-section, and negligible speed, is assumed at the nozzle entry: $A_c \rightarrow \infty$, $M_c \rightarrow 0$). Instead of subscript 'c' for chamber conditions, we will use 't' for total values because the energy conservation implies that total temperature is invariant along the nozzle flow, and the non-dissipative assumption implies that total pressure is also invariant, i.e. $T_t = T_c$ and $p_t = p_c$.
- Discharge conditions: p_0 , i.e. the environmental pressure (or back pressure), is the only variable of importance (because pressure waves propagate at the local speed of sound and quickly tend to force mechanical equilibrium, whereas the environmental temperature T_0 propagates by much slower heat-transfer physical mechanisms). Do not confuse discharge pressure, p_0 , with exit pressure, p_e , explained below.

Variable geometry nozzles

Variable area nozzle, which is sometimes identified as adjustable nozzle, is necessary for engines fitted with afterburners. Generally, as the nozzle is reduced in area, the turbine inlet temperature increases and the exhaust velocity and thrust increase. Three methods are available, namely:

1. Central plug at nozzle outlet
2. Ejector type nozzle
3. IRIS nozzle

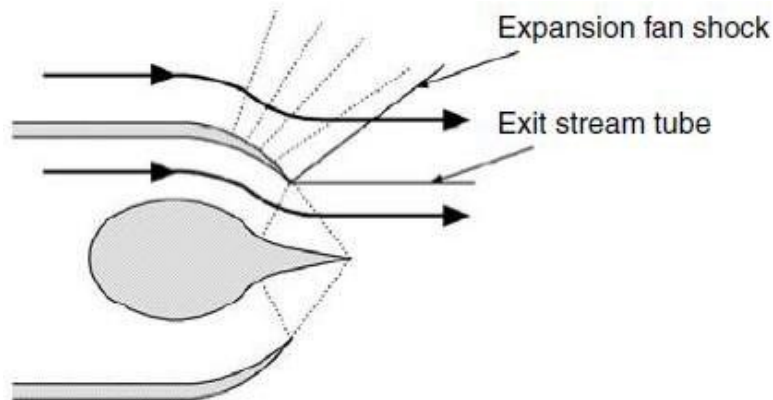


Fig 3.1: Plug nozzle at design point.

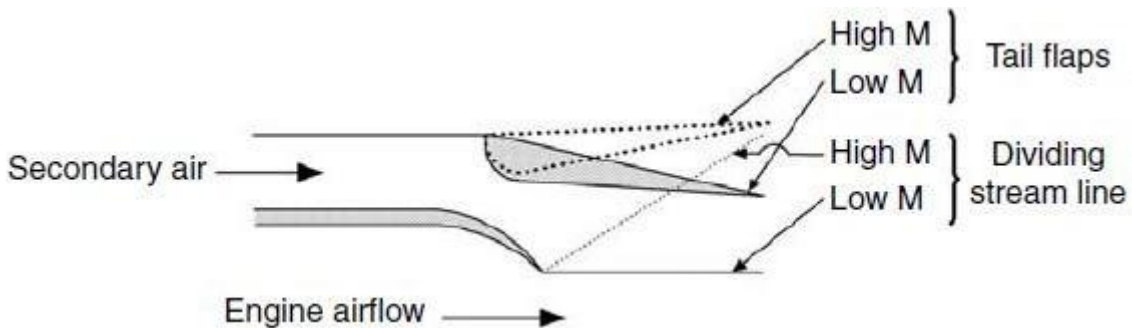


Fig 3.2: Variable geometry ejector nozzle.

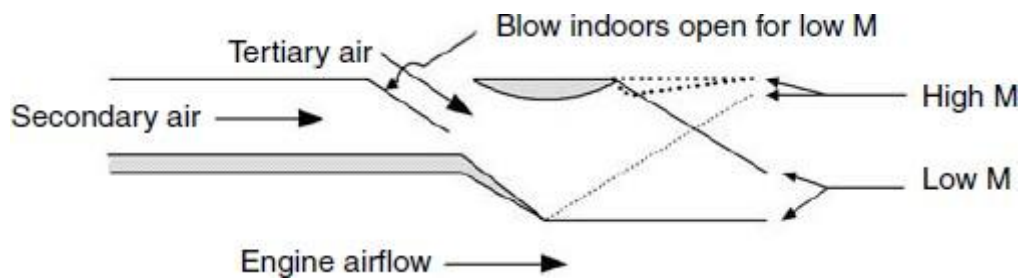


Fig 3.3:Ejector nozzle with blow-in doors for tertiary air.

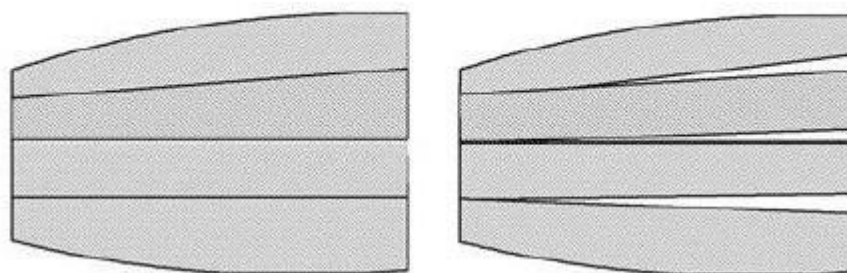


Fig 3.3:Iris variable nozzle.

Thrust reversal

Stopping an aircraft after landing is not an easy problem due to the increases in its gross weight, wing loadings and landing speeds . The amount of force required for stopping an aircraft at a given distance after touchdown increases with the gross weight of the aircraft and the square of the landing speed. The size of modern transport aircraft, which results in higher wing loadings and increased landing speeds, makes the use of wheel brakes alone unsatisfactory for routine operations. Moreover, in the cases of wet, icy, or snow-covered runways, the efficiency of aircraft brakes may be reduced by the loss of adhesion between aircraft tire and the runway.

On turbojet engines, low-bypass turbofan engines, whether fitted with afterburner or not, and mixed turbofan engines, the thrust reverser is achieved by reversing the exhaust gas flow (hot stream). On high-bypass ratio turbofan engines, reverse thrust is achieved by reversing the fan (cold stream) airflow. Mostly, in this case it is not necessary to reverse the hot stream as the majority of the engine thrust is derived from the fan, although some engines use both systems.

A good thrust reverser must fulfill the following conditions

1. Must not affect the engine operation whether the thrust reverser is applied or stowed
2. Withstand high temperature if it is used in the turbine exhaust
3. Mechanically strong
4. Relatively light in weight
5. When stowed should be streamlined into the engine nacelle and should not add appreciably to the frontal area of the engine
6. Reliable and fail safe
7. Cause few increased maintenance problems
8. Provide at least 50% of the full forward thrust.

Classification of thrust reverser systems

The most commonly used reversers are clamshell-type, external-bucket type doors and blocker doors, as shown in Fig 3.4.

Clamshell door system—sometimes identified as pre-exist thrust reverser [9]—is a pneumatically operated system. When reverse thrust is applied, the doors rotate to uncover the ducts and close the normal gas stream. Sometimes clamshell doors are employed together with cascade vanes; type (A) in Figure 3.4. Clamshell type is normally used for non-afterburning engines.

The bucket target system; type (B) in Fig3.4 , is hydraulically actuated and uses bucket-type doors to reverse the hot gas stream. Sometimes it is identified as post-exit or target thrust reverser. In the forward (stowed) thrust mode, the thrust reverser doors form the convergent–divergent final nozzle for the engine. When the thrust reverser is applied, the reverser automatically opens to form a “clamshell” approximately three-fourth to one nozzle diameter to the rear of the engine exhaust nozzle. When the thrust reverser is applied, the reverser automatically opens to form a “clamshell” approximately three-fourth to one nozzle diameter to the rear of the engine exhaust nozzle. The thrust reverser in Boeing 737-200 aircraft is an example for this type of thrust reverser.

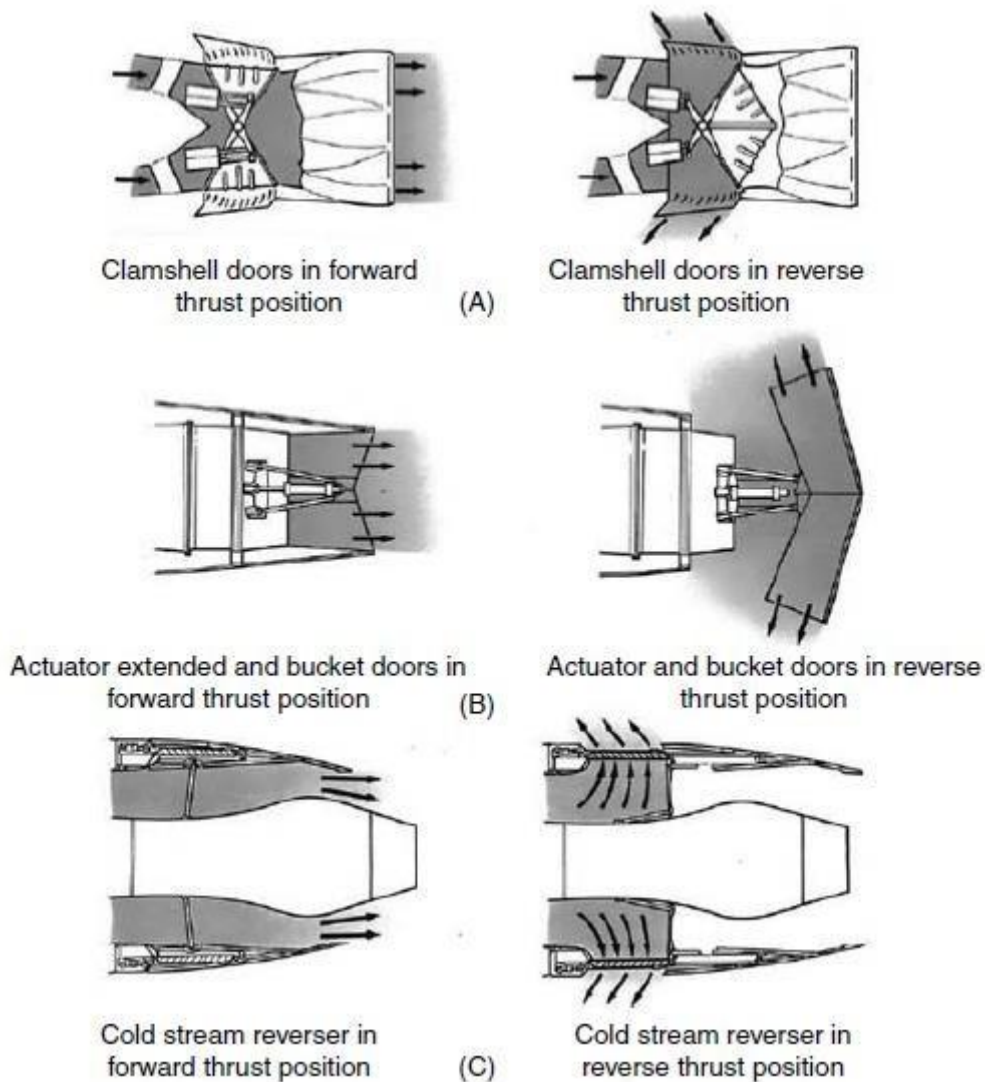


Fig 3.4: Methods of thrust reversal

High by-pass turbofan engines normally use blocker doors to reverse the cold stream airflow; type (C) in Figure 3.4. Cascade-type reverser uses numerous turning vanes in gas path to direct the gas flow outward and forward during operation. Some types utilize a sleeve to cover the fan cascade during forward thrust. Aft movement of the reverse sleeves causes blocker doors to blank off the cold stream final nozzle and deflect fan discharge air forward through fixed cascade vanes, producing reverse thrust. In some installations, cascade turning vanes are used in conjunction with clamshell to reverse the turbine exhaust gases. Both the cascade and the clamshell are located forward of the turbine exhaust nozzle. For reverse thrust, the clamshell blocks the flow of exhaust gases and exposes the cascade vanes, which act as an exhaust nozzle. Some installations in low-bypass turbofan unmixed engines use two sets of cascade: forward and rearward. For the forward cascade, the impinging exhaust is turned by the

blades in the cascade into the forward direction. Concerning the rearward cascade, the exhaust from the hot gas generator strikes the closed clamshell doors and is diverted forward and outward through a cascade installed in these circumferential openings in the engine nacelle.

Isentropic flow through varying area duct

Let us consider the varying area duct as shown in Fig. 3.5. Areas at different stations are mentioned in the same figure. The minimum cross-sectional area of this duct is called as throat if local Mach number of the same cross-section is 1. We can find out the area of throat under this constraint for known inlet or outlet area of the duct. We know that mass flow rate at the throat is,

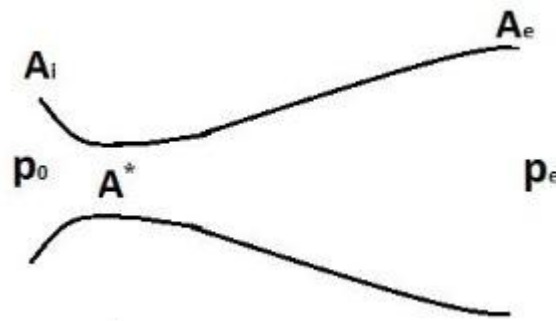


Fig 3.5: Flow through convergent divergent duct

$$\dot{m} = \rho^* u^* A^*$$

$$\frac{\rho_0}{\rho} = \left[1 + \frac{(\gamma - 1)}{2} M^2 \right]^{\frac{1}{(\gamma - 1)}}$$

$$\frac{\rho_0}{\rho^*} = \left[\frac{(\gamma + 1)}{2} \right]^{\frac{1}{(\gamma - 1)}}$$

$$\left[\frac{u}{a^*} \right]^2 = M^{*2} = \frac{\frac{(\gamma + 1)}{2} M^2}{1 + \frac{(\gamma - 1)}{2} M^2}$$

Hence the area relation can be written as,

$$\left[\frac{A}{A^*} \right]^2 = \frac{1}{M^2} \left[\frac{2}{(\gamma + 1)} \left(1 + \frac{(\gamma - 1)}{2} M^2 \right) \right]^{\frac{(\gamma + 1)}{(\gamma - 1)}}$$

Hence, if we know Mach number M at any cross section and corresponding area A then we can

calculate the area of the throat for the duct. From this expression it is also clear that the Mach number at any cross-section upstream or downstream of the throat is not dependent on the nature of variation of cross-sectional area of the duct in the streamwise direction.

Nozzle flow

Consider the convergent divergent duct shown in Fig 3.5. Left end of the duct corresponds to the stagnation or total conditions (T_0 , P_0 and ρ_0) due to its connection to the reservoir while right end of the duct is open to the atmospheric pressure P_a . If initially exit pressure (P_e) is same as the reservoir pressure (P_0) then there will not be any flow through the duct. If we decrease the exit pressure by small amount then flow takes place through the duct. Here convergent portion acts as nozzle where pressure decreases and Mach number increases in the streamwise direction while divergent portion acts as diffuser which leads to increase in pressure and Mach number along the length of the nozzle. Variation of pressure and Mach number for this condition is shown in Fig 3.6 and Fig 3.7 respectively by tag 1.

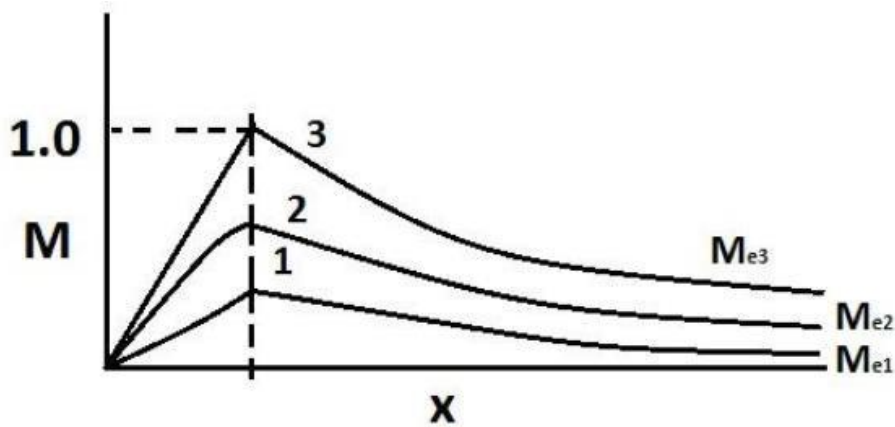


Fig. 3.6: Mach number variation along the length of the duct for various exit pressure conditions

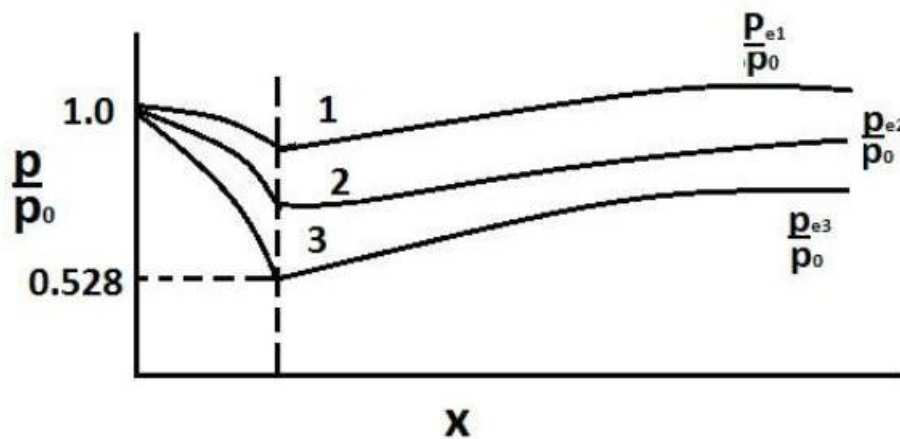


Fig 3.7: Pressure variation along the length of the duct for various exit pressure conditions

Further decrease in pressure at the exit of the duct shifts the pressure and Mach number curves as shown in Fig 3.7 tagged by 2. Mass flow continues to increase with decreasing the exit pressure from conditions from 1 to 2. Condition 3 in this figure represents first critical condition or a particular value of exit pressure at which Mach number at the minimum cross-section of the duct becomes 1 or sonic. From Fig. 3.6 it is clear that convergent portion continues to act as nozzle while divergent portion acts as diffuser. Pressure at the throat where Mach number has reached 1 attains the reference star value which is equal to 0.528 times the reservoir pressure for isentropic air flow. Further decrease in exit pressure beyond the first critical pressure (corresponding to situation 3), does not change the role of convergent portion as the nozzle. The pressure and Mach number in the convergent portion also remain unchanged with further decrease in exit pressure. Once the sonic state is achieved at the minimum cross section, mass flow rate through the duct attains saturation. Hence duct or the nozzle is said to be choked for any pressure value lower than the first critical condition. Typical mass flow rate variation for air flow with change in exit pressure is shown in Fig. 3.8.

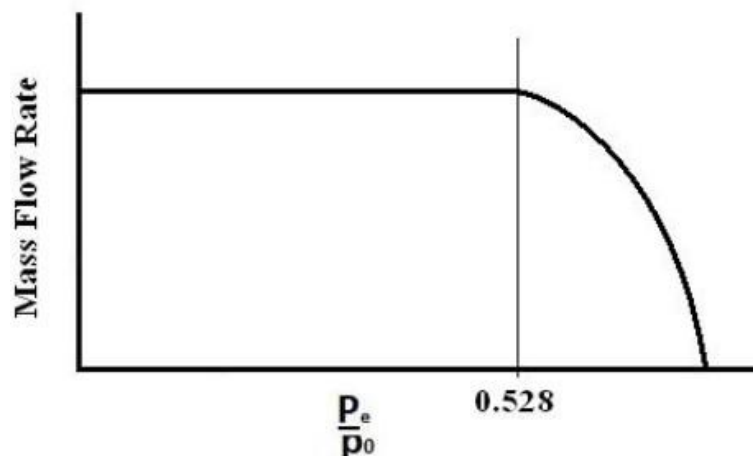


Fig 3.8: Variation of mass flow rate for air with change in exit pressure

Variation of pressure and Mach number for a typical exit pressure just below first critical conditions is shown in Fig 3.9 (a & b) respectively. As discussed earlier, for this situation also pressure decreases and Mach number increases in the convergent portion of the duct. Thus Mach number attains value 1 at the end of convergent section or at the throat. Fluid continues to expand in the initial part of the divergent portion which corresponds to decrease in pressure and increase in Mach number in the supersonic regime in that part of the duct. However, if fluid continues to expand in the rest part of the duct then pressure of the fluid is expected to reach a value at the exit which is much lower than the exit pressure (as shown by isentropic expansion in Fig 3.9(a &b). Therefore, a normal shock gets created after initial expansion in the

divergent portion to increase the pressure and decrease the Mach number to subsonic value (Fig3.10). Hence rest of the portion of divergent duct acts as diffuser to increase the pressure in the direction of flow to reach the exit pressure value smoothly.

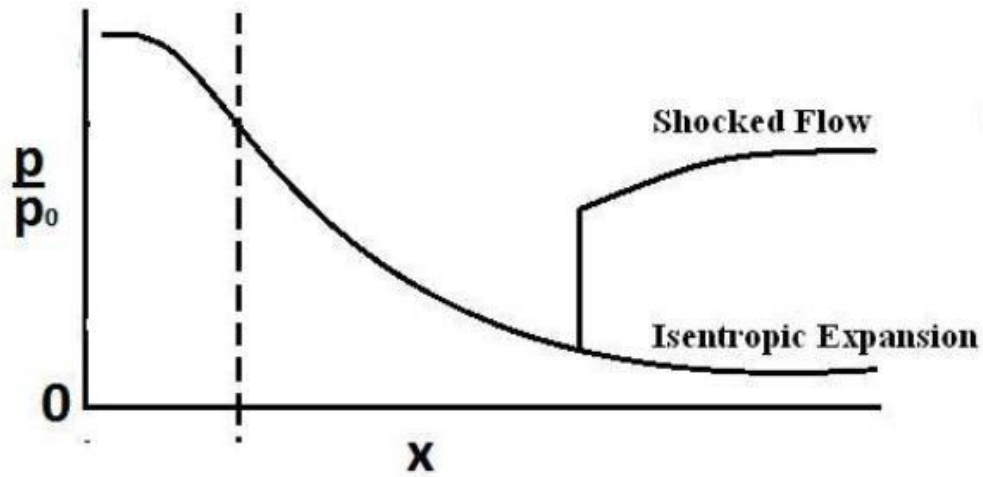


Fig 3.9a: Pressure variation along the length of the nozzle.

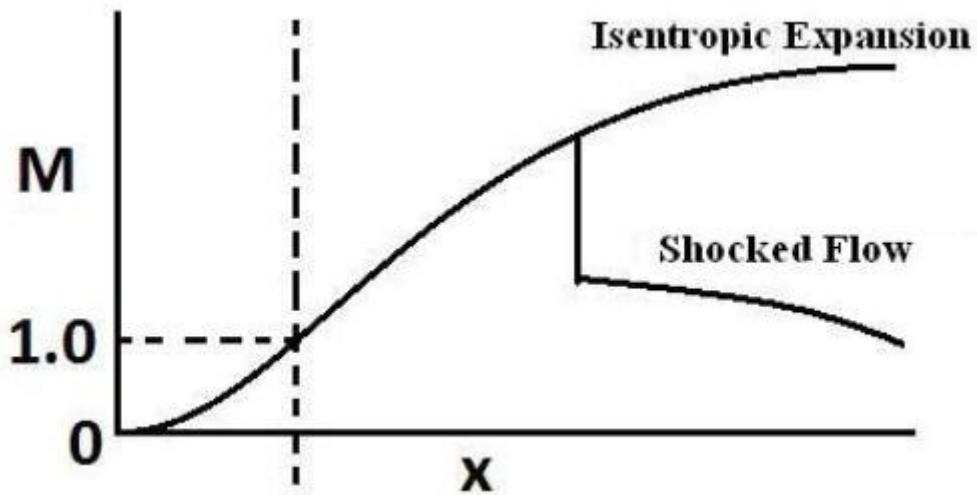


Fig 3.9b: Mach number variation along the length of the nozzle.

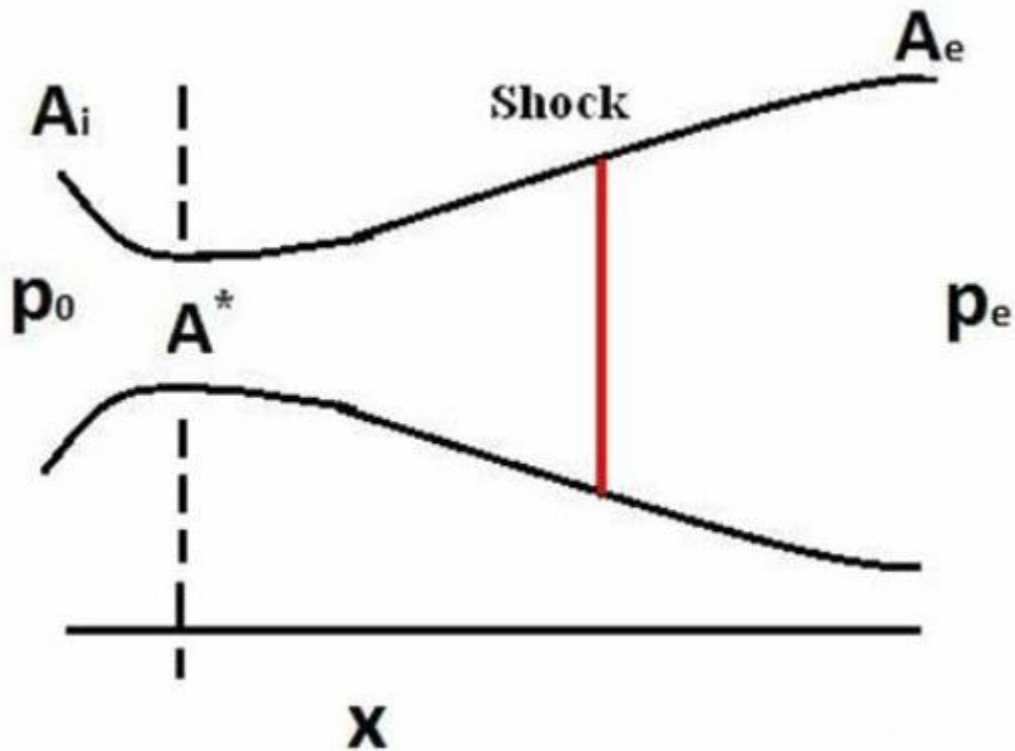


Fig 3.10: Presence of normal shock in the nozzle flow

For the further decrease in exit pressure for the same reservoir condition, the portion of divergent part acting as nozzle, internally the normal shock moves towards exit of the duct. For a particular value of exit pressure normal shock stands at the exit of the convergent-divergent duct. Decrease in the exit pressure beyond this condition provides an oblique shock pattern originating from the edge of the duct to raise the pressure in order to attain the exit pressure conditions. Corresponding condition is shown in Fig 3.1.

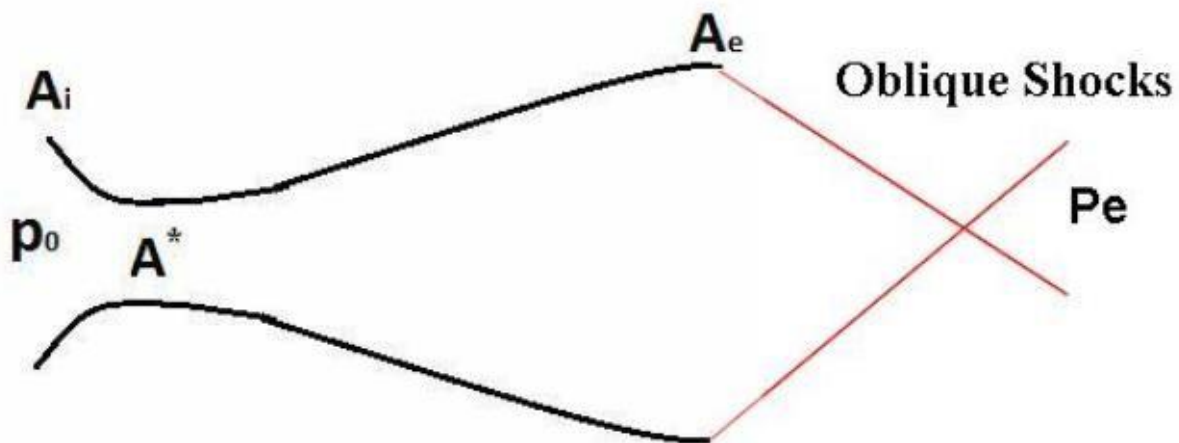


Fig 3.11: Oblique shock pattern for over expanded condition

For this exit pressure condition, the flow inside the duct is isentropic. However, fluid attains the

pressure at the exit of the duct which is lower than the exit pressure, hence it has to pass through the oblique shock and attain the pressure as that of exit pressure by the non-isentropic process. Hence such condition of the duct is called as 'over expanded nozzle' and it is shown in Fig 3.11. Decrease in exit pressure beyond this over expanded condition, decreases the strength of oblique shock and hence the amount of pressure rise. Hence at a particular value of exit pressure fluid pressure at the exit of the duct becomes exactly equal to the exit pressure and flow becomes completely isentropic for the duct. In this condition both convergent and divergent portions of the duct act as nozzle to expand the flow smoothly, hence duct is called as convergent divergent nozzle. Expansion of the flow in the convergent divergent nozzle is mentioned as 'isentropic expansion' in Fig3.9(a & b). Further decrease in exit pressure beyond the isentropic condition corresponds to more fluid pressure at the exit in comparison with the ambient pressure. Hence expansion fan gets originated from the edge of the nozzle to decrease the pressure smoothly to reach the ambient condition isentropically. Nozzle flow for such a situation is termed as 'under-expanded nozzle flow'. Corresponding flow pattern is shown in Fig3.12.

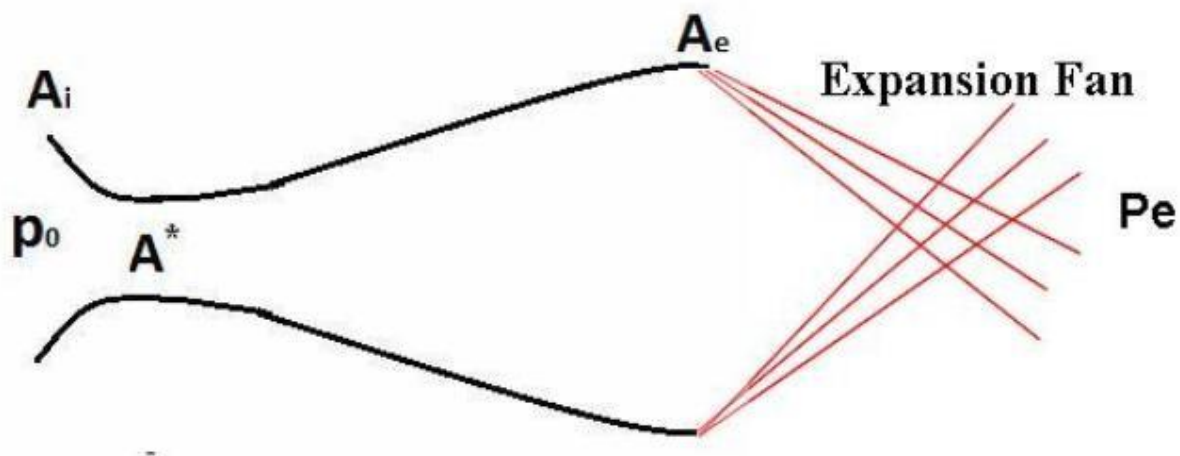


Fig 3.12: Expansion fan pattern for under expanded condition

Chocked mass flow rate of the nozzle

We have already seen that mass flow rate of the nozzle remains unaltered after flow gets chocked. This chocked mass flow rate can be calculated as,

$$\dot{m} = \rho^* u^* A^*$$

But we know that,

$$\frac{\rho_0}{\rho^*} = \left[\frac{(\gamma + 1)}{2} \right]^{\frac{1}{(\gamma-1)}}$$

$$u^* = a^* = \sqrt{\gamma RT^*}$$

Hence

$$\dot{m} = \rho_0 \left[\frac{(\gamma + 1)}{2} \right]^{\frac{-1}{(\gamma-1)}} \sqrt{\gamma RT^*} A^*$$

$$\dot{m} = \rho_0 \left[\frac{(\gamma + 1)}{2} \right]^{\frac{-1}{(\gamma-1)}} \sqrt{\gamma R \frac{T^*}{T_0} T_0} A^*$$

However,

$$\rho_0 = \frac{p_0}{RT_0}$$

$$\frac{T^*}{T_0} = \left[1 + \frac{(\gamma - 1)}{2} \right]^{-1}$$

Hence

$$\dot{m} = \frac{p_0}{RT_0} \left[\frac{(\gamma + 1)}{2} \right]^{\frac{-1}{(\gamma-1)}} \sqrt{\gamma R \frac{T^*}{T_0} T_0} A^*$$

$$\dot{m} = p_0 \left[\frac{(\gamma + 1)}{2} \right]^{\frac{-(\gamma+1)}{2(\gamma-1)}} \sqrt{\frac{\gamma}{RT_0}} A^*$$

From this expression it is clear that for a convergent divergent nozzle, for given throat area, choked mass flow rate remains constant for the fixed reservoir (P_0 and T_0) conditions. Therefore choked mass flow rate can be increased by increasing the reservoir pressure P_0 or decreasing reservoir temperature T_0 .

UNIT – III

AXIAL FLOW COMPRESSORS AND TURBINES

Centrifugal compressor Principle of operation

The centrifugal compressor consists essentially of a stationary casing containing a rotating impeller which imparts a high velocity to the air, and a number of fixed diverging passages in which the air is decelerated with a consequent rise in static pressure. The latter process is one of diffusion, and consequently the part of the compressor containing the diverging passages is known as the diffuser.

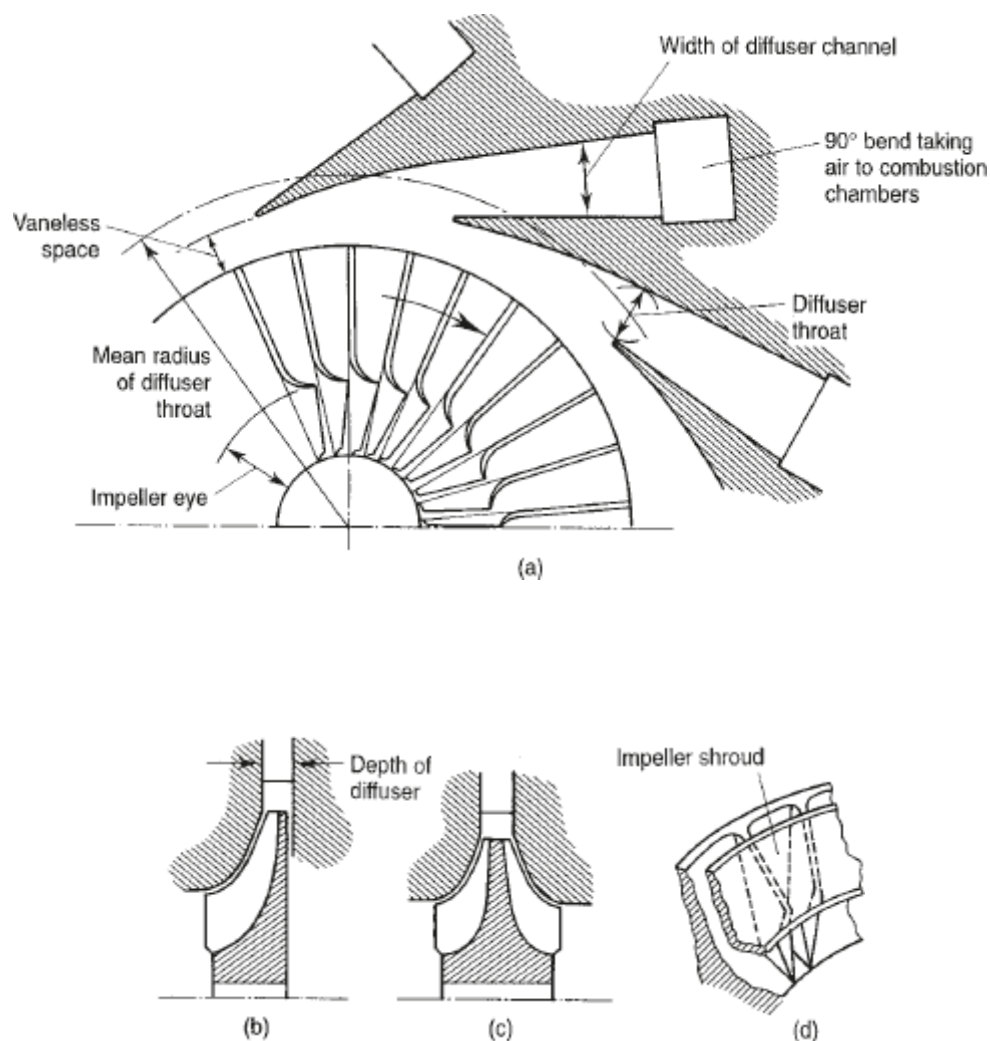


Fig. 4.1 Diagrammatic sketches of centrifugal compressors

Figure 4.1(a) is a diagrammatic sketch of a centrifugal compressor. The impeller may be single- or double-sided as in Fig. 4.1(b) or (c), but the fundamental theory is the same for both. The double-sided impeller was required in early aero engines because of the relatively small flow capacity of the centrifugal compressor for a given overall diameter.

Air is sucked into the impeller eye and whirled round at high speed by the vanes on the impeller disc. At any point in the flow of air through the impeller, the centripetal acceleration is obtained by a pressure head, so that the static pressure of the air increases from the eye to the tip of the impeller. The remainder of the static pressure rise is obtained in the diffuser, where the very high velocity of the air leaving the impeller tip is reduced to somewhere in the region of the velocity with which the air enters the impeller eye; it should be appreciated that friction in the diffuser will cause some loss in *stagnation* pressure. The normal practice is to design the compressor so that about half the pressure rise occurs in the impeller and half in the diffuser.

It will be appreciated that owing to the action of the vanes in carrying the air around with the impeller, there will be a slightly higher static pressure on the forward face of a vane than on the trailing face. The air will thus tend to flow round the edges of the vanes in the clearance space between the impeller and the casing. This naturally results in a loss of efficiency, and the clearance must be kept as small as possible.

A shroud attached to the vanes, Fig. 4.1(d), would eliminate such a loss, but the manufacturing difficulties are vastly increased and there would be a disc friction or 'windage' loss associated with the shroud. Although shrouds have been used on superchargers and process compressors, they are not used on impellers for gas turbines.

Work done and pressure rise

Since no work is done on the air in the diffuser, the energy absorbed by the compressor will be determined by the conditions of the air at the inlet and outlet of the impeller. Figure 4.2 shows the nomenclature employed. In the first instance it will be assumed that the air enters the impeller eye in the axial direction, so that the initial angular momentum of the air is zero. The axial portion of the vanes must be curved so that the air can pass smoothly into the eye. The angle which the leading edge of a vane makes with the tangential direction will be given by the direction of the relative velocity of the air at inlet, V_1 , as shown in Fig. 4.2.

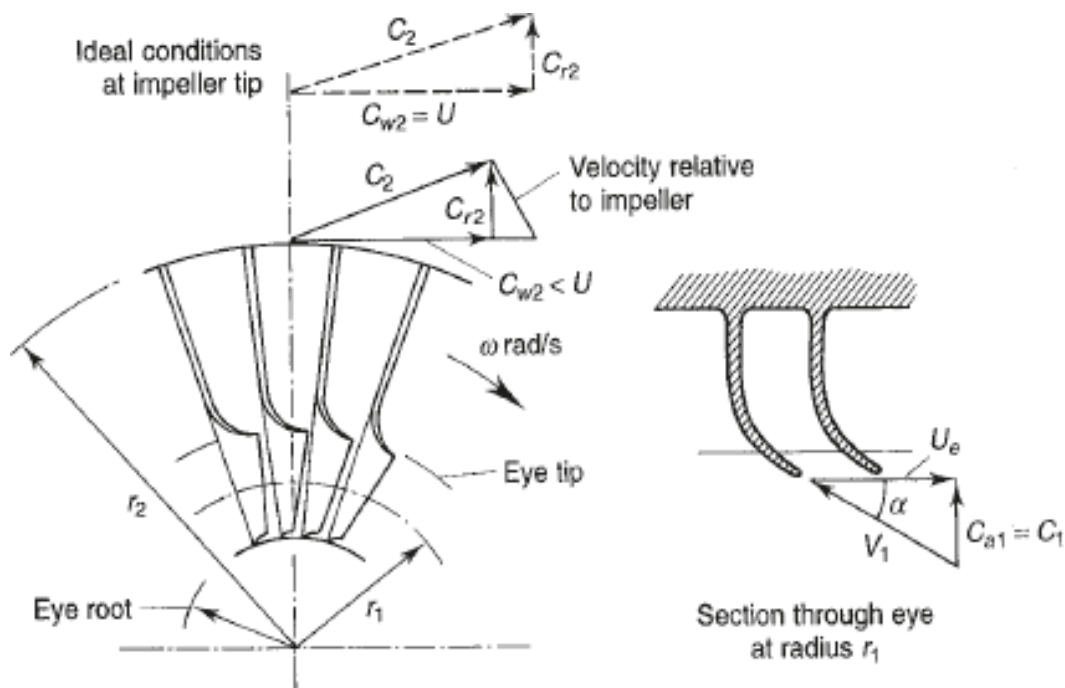


Fig. 4.2 Nomenclature

If the air leaves the impeller tip with an absolute velocity C_2 , it will have a tangential or whirl component C_{w2} and a comparatively small radial component C_{r2} . Under ideal conditions C_2 would be such that the whirl component is equal to the impeller tip speed U , as shown by the velocity triangle at the top of Fig. 4.2. Owing to its inertia, the air trapped between the impeller vanes is reluctant to move round with the impeller, and we have already noted that this results in a higher static pressure on the leading face of a vane than on the trailing face. It also prevents the air from acquiring a whirl velocity equal to the impeller speed.

This effect is known as slip. How far the whirl velocity at the impeller tip falls short of the tip speed depends largely upon the number of vanes on the impeller. The greater the number of vanes, the smaller the slip, i.e. the more nearly C_{w2} approaches U . It is necessary in design to assume a value for the slip factor s , where s is defined as the ratio C_{w2}/U .

Various approximate analyses of the flow in an impeller channel have led to formulae for s : the one appropriate to radial vaned impellers which seems to agree best with experiment is that due to Stanitz

$$s = 1 - 0.63p/n$$

where n is the number of vanes

Considering unit mass flow of air, this torque is given by

$$\text{Theoretical torque} = C_w 2r^2 \quad (4.1)$$

If ω is the angular velocity, the work done on the air will be

$$\text{Theoretical work done} = C_w 2r^2 \omega = C_w 2U$$

Or, introducing the slip factor,

$$\text{Theoretical work done} = sU^2 \quad (4.2)$$

Owing to friction between the casing and the air carried round by the vanes, and other losses which have a braking effect such as disc friction or 'windage', the applied torque and therefore the actual work input is greater than this theoretical value. A power input factor c can be introduced to take account of this, so that the actual work done on the air becomes

$$\text{Work done} = \psi \sigma U^2 \quad (4.3)$$

If $(T_{03} - T_{01})$ is the stagnation temperature rise across the whole compressor then, since no energy is added in the diffuser, this must be equal to the stagnation temperature rise $(T_{02} - T_{01})$ across the impeller alone. It will therefore be equal to the temperature equivalent of the work done on the air given by equation (4.3), namely where C_p is the mean specific heat over this temperature range. Typical values for the power input factor lie in the region of 1.03591.04.

$$T_{03} - T_{01} = \psi \sigma U^2 / C_p \quad (4.4)$$

So far we have merely considered the work which must be put into the compressor. If a value for the *overall* isentropic efficiency η_c is assumed, then it is known how much of the work is usefully employed in raising the pressure of the air. The overall stagnation pressure ratio follows as

$$\frac{P_{03}}{P_{01}} = \left(\frac{T'_{03}}{T_{01}} \right)^{\gamma/(\gamma-1)} = \left[1 + \frac{\eta_c (T_{03} - T_{01})}{T_{01}} \right]^{\gamma/(\gamma-1)} = \left[1 + \frac{\eta_c \psi \sigma U^2}{c_p T_{01}} \right]^{\gamma/(\gamma-1)} \quad (4.5)$$

Axial Flow Compressors

The basic components of an axial flow compressor are a rotor and stator, the former carrying the moving blades and the latter the stationary rows of blades. The stationary blades convert the kinetic energy of the fluid into pressure energy, and also redirect the flow into an angle suitable for entry to the next row of moving blades. Each stage will consist of one rotor row followed by a stator row, but it is usual to provide a row of so called inlet guide vanes. This is an additional stator row upstream of the first stage in the compressor and serves to direct the axially approaching flow correctly into the first row of rotating blades.

For a compressor, a row of rotor blades followed by a row of stator blades is called a stage. Two forms of rotor have been taken up, namely drum type and disk type. A disk type rotor illustrated in Figure 4.3 The disk type is used where consideration of low weight is most important. There is a contraction of the flow annulus from the low to the high pressure end of the compressor. This is necessary to maintain the axial velocity at a reasonably constant level throughout the length of the compressor despite the increase in density of air. Figure 4.4 illustrate flow through compressor stages. In an axial compressor, the flow rate tends to be high and pressure rise per stage is low. It also maintains fairly high efficiency.

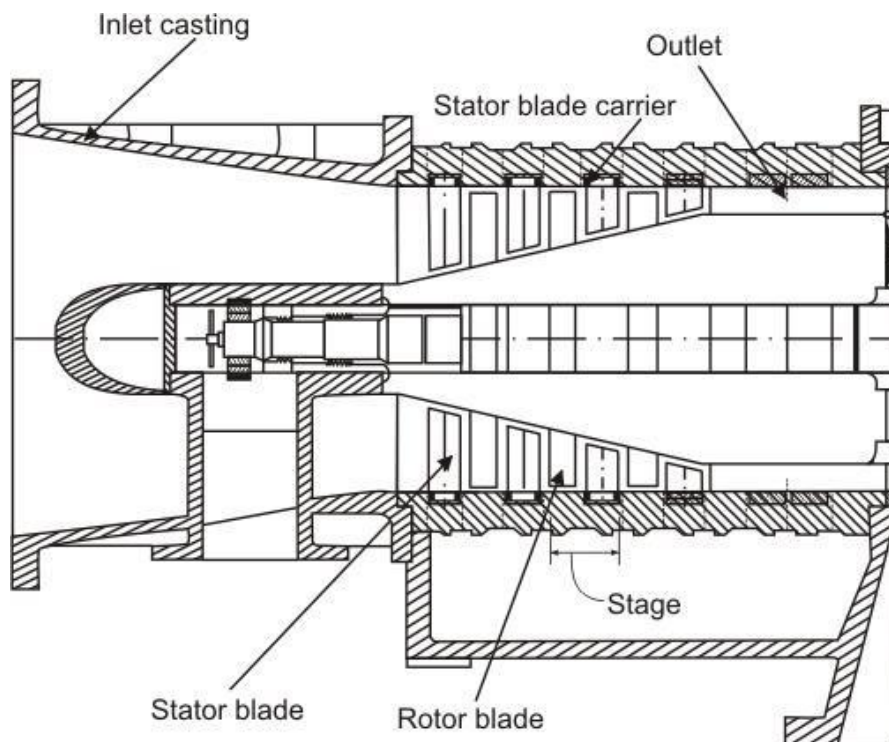


Figure 4.3 Disk type axial flow compressor

The basic principle of acceleration of the working fluid, followed by diffusion to convert acquired kinetic energy into a pressure rise, is applied in the axial compressor. The flow is considered as occurring in a tangential plane at the mean blade height where the blade peripheral velocity is U . This two dimensional approach means that in general the flow velocity will have two components, one axial and one peripheral denoted by subscript w , implying a whirl velocity. It is first assumed that the air approaches the rotor blades with an absolute velocity, V_1 , at an angle α_1 to the axial direction. In combination with the peripheral velocity U of the blades, its relative velocity will be V_{r1} at an angle β_1 as shown in the upper velocity triangle.

After passing through the diverging passages formed between the rotor blades which do work on the air and increase its absolute velocity, the air will emerge with the relative velocity of V_{r2} at angle β_2 which is less than β_1 . This turning of air towards the axial direction is, as previously mentioned, necessary to provide an increase in the effective flow area and is brought about by the camber of the blades. Since V_{r2} is less than V_{r1} due to diffusion, some pressure rise has been accomplished in the rotor. The velocity V_{r2} in combination with U gives the absolute velocity V_2 at the exit from the rotor at an angle α_2 to the axial direction. The air then passes through the passages formed by the stator blades where it is further diffused to velocity V_3 at an angle α_3 which in most designs equals to α_1 so that it is prepared for entry to next stage. Here again, the turning of the air towards the axial direction is brought about by the camber of the blades.

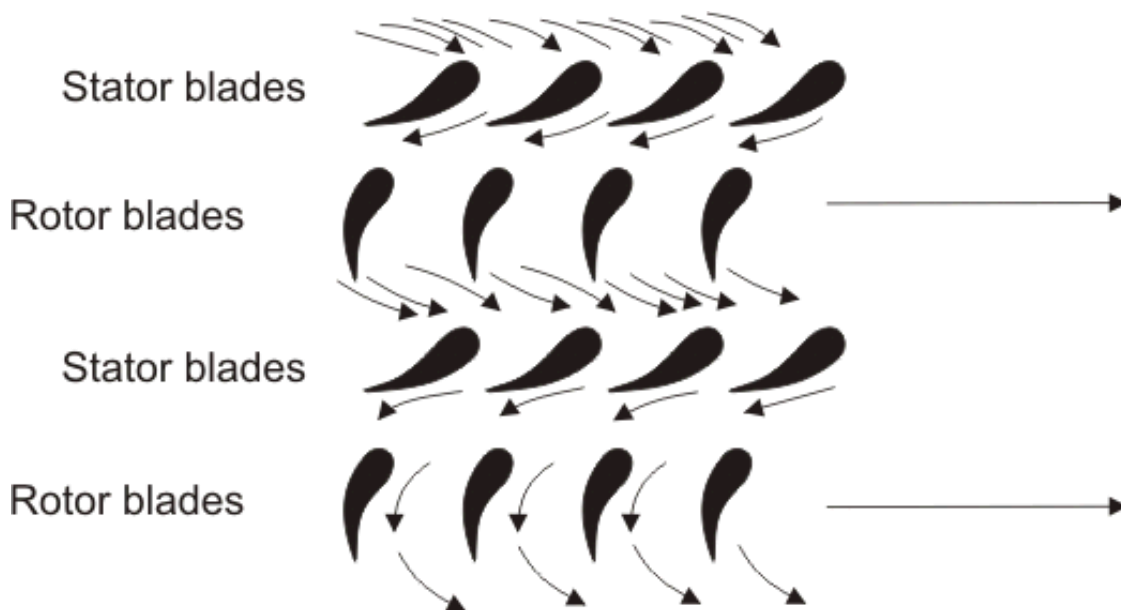


Figure 4.4 Flow through stages

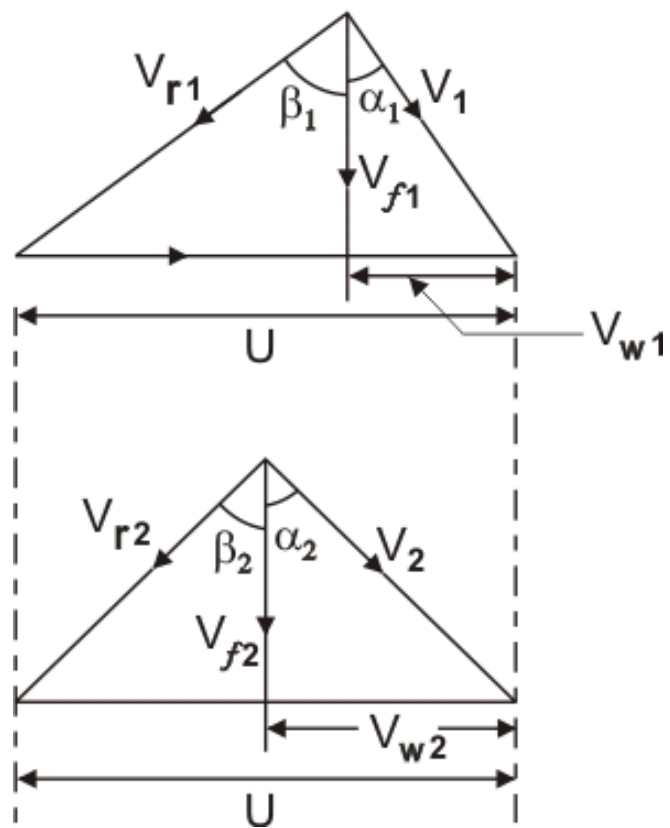
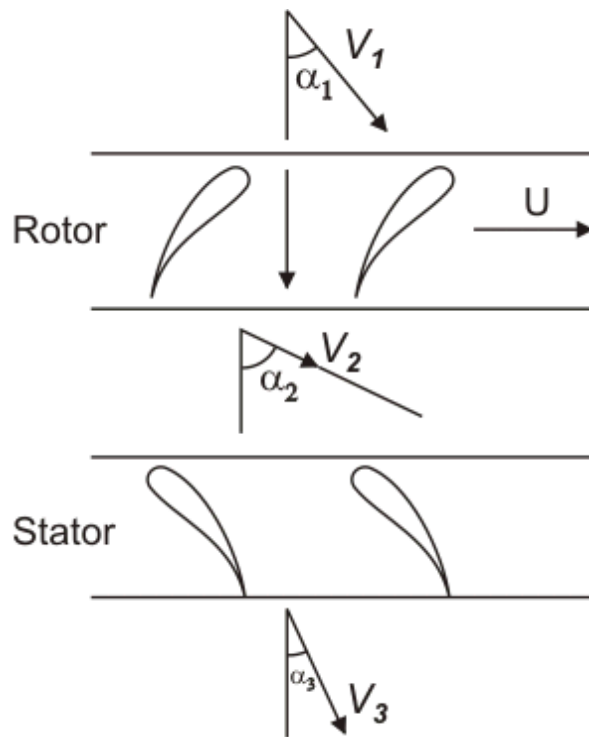


Figure 4.5 Velocity triangles

Two basic equations follow immediately from the geometry of the velocity triangles. These are:

$$\frac{U}{V_f} = \tan \alpha_1 + \tan \beta_1 \quad (4.6)$$

$$\frac{U}{V_f} = \tan \alpha_2 + \tan \beta_2 \quad (4.7)$$

In which $V_f = V_{f1} = V_{f2}$ is the axial velocity, assumed constant through the stage. The work done per unit mass or specific work input, w being given by

$$w = U(V_{w2} - V_{w1}) \quad (4.8)$$

This expression can be put in terms of the axial velocity and air angles to give

$$w = UV_f(\tan \alpha_2 - \tan \alpha_1) \quad (4.9)$$

or by using Eqs. (4.6) and (4.7)

$$w = UV_f(\tan \beta_1 - \tan \beta_2) \quad (4.10)$$

This input energy will be absorbed usefully in raising the pressure and velocity of the air. A part of it will be spent in overcoming various frictional losses. Regardless of the losses, the input will reveal itself as a rise in the stagnation temperature of the air ΔT_0 . If the absolute velocity of the air leaving the stage V_3 is made equal to that at the entry V_1 , the stagnation temperature rise ΔT_0 will also be the static temperature rise of the stage, ΔT_s , so that

$$\Delta T_0 = \Delta T_s = \frac{UV_f}{c_p} (\tan \beta_1 - \tan \beta_2) \quad (4.11)$$

In fact, the stage temperature rise will be less than that given in Eq. (4.11) owing to three dimensional effects in the compressor annulus. Experiments show that it is necessary to multiply the right hand side of Eq. (4.11) by a work-done factor λ which is a number less than unity. This is a measure of the ratio of actual work-absorbing capacity of the stage to its ideal value.

The radial distribution of axial velocity is not constant across the annulus but becomes increasingly peaky (Figure. 4.9) as the flow proceeds, settling down to a fixed profile at about the fourth stage. Equation (4.10) can be written with the help of Eq. (4.6) as

$$\begin{aligned}
 w &= U[(U - V_f \tan \alpha_1) - V_f \tan \beta_2] \\
 &= U(U - V_f (\tan \alpha_1 + \tan \beta_2)) \quad (4.12)
 \end{aligned}$$

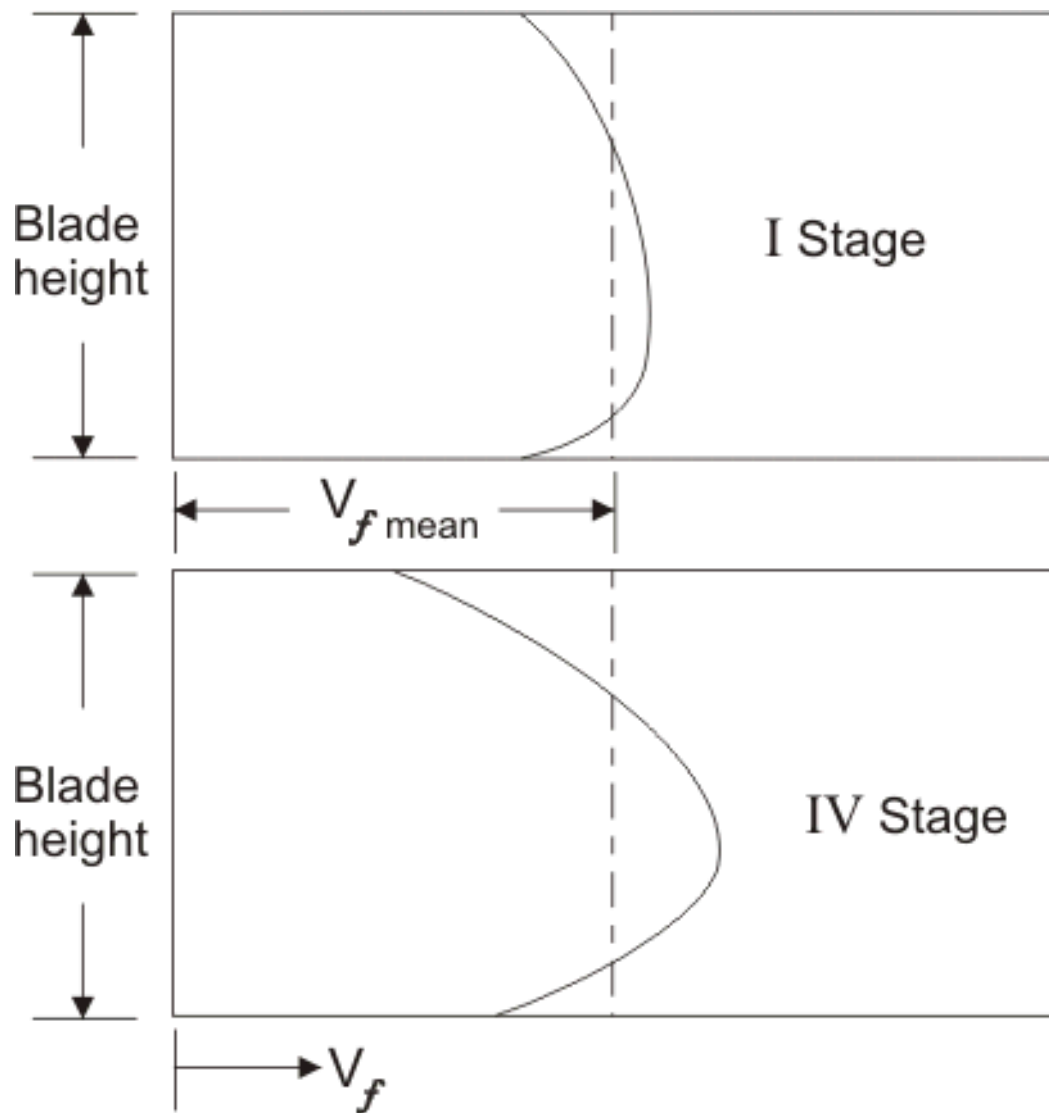


Figure 4.6 Axial velocity distributions

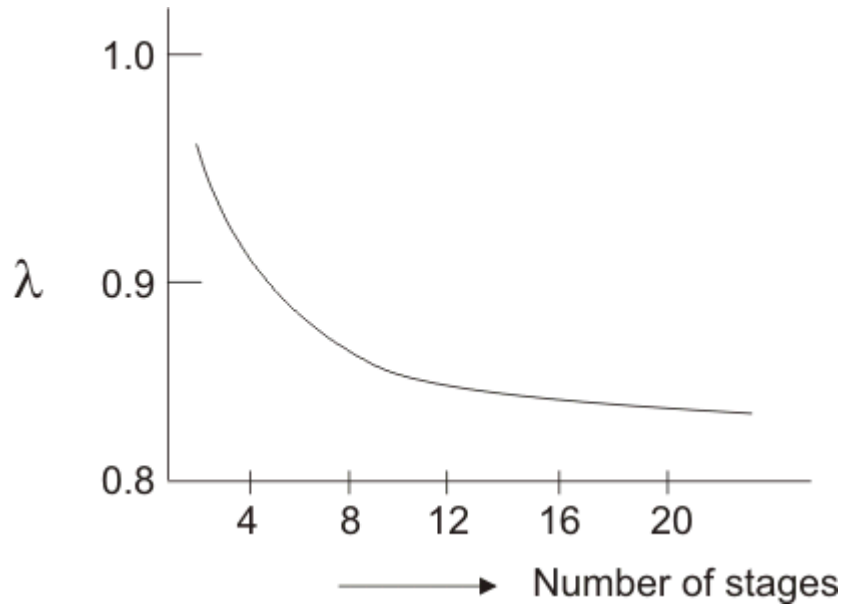


Figure 4.7: Variation of work-done factor with number of stages

Since the outlet angles of the stator and the rotor blades fix the value of α_1 and β_2 and hence the value of $(\tan \alpha_1 + \tan \beta_2)$. Any increase in V_f will result in a decrease in ∞ and vice-versa. If the compressor is designed for constant radial distribution of V_f as shown by the dotted line in Figure (4.6), the effect of an increase in V_f in the central region of the annulus will be to reduce the work capacity of blading in that area. However this reduction is somewhat compensated by an increase in ∞ in the regions of the root and tip of the blading because of the reduction of V_f at these parts of the annulus.

The net result is a loss in total work capacity because of the adverse effects of blade tip clearance and boundary layers on the annulus walls. This effect becomes more pronounced as the number of stages is increased and the way in which the mean value varies with the number of stages. The variation of λ with the number of stages is shown in Figure. 4.7. Care should be taken to avoid confusion of the work done factor with the idea of an efficiency. If ∞ is the expression for the specific work input (Equation. 4.8), then $\lambda \infty$ is the actual amount of work which can be supplied to the stage. The application of an isentropic efficiency to the resulting temperature rise will yield the equivalent isentropic temperature rise from which the stage pressure ratio may be calculated. Thus, the actual stage temperature rise is given by

$$\Delta T_0 = \frac{\lambda U V_f}{c_p} (\tan \beta_1 - \tan \beta_2) \quad (4.13)$$

and the pressure ratio R_s by

$$R_s = \left[1 + \frac{n_s \Delta T_0}{T_{01}} \right]^{\frac{\gamma}{\gamma-1}} \quad (4.14)$$

where, T_{01} is the inlet stagnation temperature and η_{s1} is the stage isentropic efficiency.

Degree of Reaction

A certain amount of distribution of pressure (a rise in static pressure) takes place as the air passes through the rotor as well as the stator; the rise in pressure through the stage is in general, attributed to both the blade rows. The term degree of reaction is a measure of the extent to which the rotor itself contributes to the increase in the static head of fluid. It is defined as the ratio of the static enthalpy rise in the rotor to that in the whole stage. Variation of C_p over the relevant temperature range will be negligibly small and hence this ratio of enthalpy rise will be equal to the corresponding temperature rise.

It is useful to obtain a formula for the degree of reaction in terms of the various velocities and air angles associated with the stage. This will be done for the most common case in which it is assumed that the air leaves the stage with the same velocity (absolute) with which it enters ($V_1 = V_3$).

This leads to $\Delta T_s = \Delta T_0$. If ΔT_A and ΔT_B are the static temperature rises in the rotor and the stator respectively, then from Eqs (4.9),(4.10),(4.11),

$$\begin{aligned} w &= c_p(\Delta T_A + \Delta T_B) = c_p \Delta T_s \\ &= UV_f (\tan \beta_1 - \tan \beta_2) \\ &= UV_f (\tan \alpha_2 - \tan \alpha_1) \end{aligned} \quad (4.15)$$

Since all the work input to the stage is transferred to air by means of the rotor, the steady flow energy equation yields,

$$w = c_p \Delta T_A + \frac{1}{2}(V_2^2 - V_1^2)$$

With the help of Eq. (4.15), it becomes

$$c_p \Delta T_A = UV_f (\tan \alpha_2 - \tan \alpha_1) - \frac{1}{2}(V_2^2 - V_1^2)$$

But $V_2 = V_f \sec \alpha_2$ and $V_1 = V_f \sec \alpha_1$, and hence

$$\begin{aligned} c_p \Delta T_A &= UV_f (\tan \alpha_2 - \tan \alpha_1) - \frac{1}{2} V_f^2 (\sec^2 \alpha_2 - \sec^2 \alpha_1) \\ &= UV_f (\tan \alpha_2 - \tan \alpha_1) - \frac{1}{2} V_f^2 (\tan^2 \alpha_2 - \tan^2 \alpha_1) \end{aligned} \quad (4.16)$$

The degree of reaction

$$\Lambda = \frac{\Delta T_A}{\Delta T_A + \Delta T_B} \quad (4.17)$$

With the help of Eq. (10.2), it becomes

$$\Lambda = \frac{UV_f(\tan \alpha_2 - \tan \alpha_1) - \frac{1}{2}V_f^2(\tan^2 \alpha_2 - \tan^2 \alpha_1)}{UV_f(\tan \alpha_2 - \tan \alpha_1)}$$

and

$$\Lambda = 1 - \frac{V_f}{2U}(\tan \alpha_2 + \tan \alpha_1)$$

By adding up Eq. (4.6) and Eq. (4.7) we get

$$\frac{2U}{V_f} = \tan \alpha_1 + \tan \beta_1 + \tan \alpha_2 + \tan \beta_2$$

Replacing α_1 and α_2 in the expression for Λ with β_1 and β_2 ,

$$\Lambda = \frac{V_f}{2U}(\tan \beta_1 + \tan \beta_2) \quad (4.18)$$

As the case of 50% reaction blading is important in design, it is of interest to see the result for $\Lambda = 0.5$,

$$\tan \beta_1 + \tan \beta_2 = \frac{U}{V_f}$$

and it follows from Eqs. (4.6) and (4.7) that

$$\tan \alpha_1 = \tan \beta_2, \text{ i.e. } \alpha_1 = \beta_2 \quad (4.19a)$$

$$\tan \beta_1 = \tan \alpha_2, \text{ i.e. } \beta_1 = \alpha_2 \quad (4.20b)$$

Furthermore since V_f is constant through the stage.

$$V_f = V_1 \cos \alpha_1 = V_3 \cos \alpha_3$$

And since we have initially assumed that ($V_3 = V_1$), it follows that $\alpha_1 = \alpha_3$. Because of this equality of angles, namely, $\alpha_1 = \beta_2 = \alpha_3$ and $\beta_1 = \alpha_2$ blading designed on this basis is sometimes referred to as *symmetrical blading*. The 50% reaction stage is called a repeating stage.

It is to be remembered that in deriving Eq. (4.18) for λ , we have implicitly assumed a work done factor λ of unity in making use of Eq. (4.16). A stage designed with symmetrical

blading is referred to as 50% reaction stage, although λ will differ slightly for λ .

Types of Whirl Distribution

The whirl (vortex) distributions normally used in compressor design practice are:

- Free vortex $r C_{\theta} = \text{constant}$
- Forced vortex $C_{\theta} / r = \text{constant}$
- Constant reaction $R = \text{constant}$
- Exponential $C_{\theta 1} = a - b/r$ (after stator)
- Free vortex whirl distribution results in highly twisted blades and is not advisable for blades of small height.
- The current design practice for transonic compressors is to use constant pressure ratio across the span.

Elementary Cascade Theory

The previous module dealt with the axial flow compressors, where all the analyses were based on the flow conditions at inlet to and exit from the impeller following kinematics of flow expressed in terms of velocity triangles. However, nothing has been mentioned about layout and design of blades, which are aerofoil sections. In the development of the highly efficient modern axial flow compressor or turbine, the study of the two-dimensional flow through a cascade of aerofoils has played an important part. An array of blades representing the blade ring of actual turbo machinery is called the cascade.

Figure 4.8 shows a compressor blade cascade tunnel. As the air stream is passed through the cascade, the direction of air is turned. Pressure and velocity measurements are made at up and downstream of cascade as shown. The cascade is mounted on a turn-table so that its angular direction relative to the direction of inflow can be changed, which enables tests to be made for a range of incidence angle. As the flow passes through the cascade, it is

deflected and there will be a circulation Γ and thus the lift generated will be $\rho V_m \Gamma$ (Fig 4.9 & 4.10). V_m is the mean velocity that makes an angle α_m with the axial direction

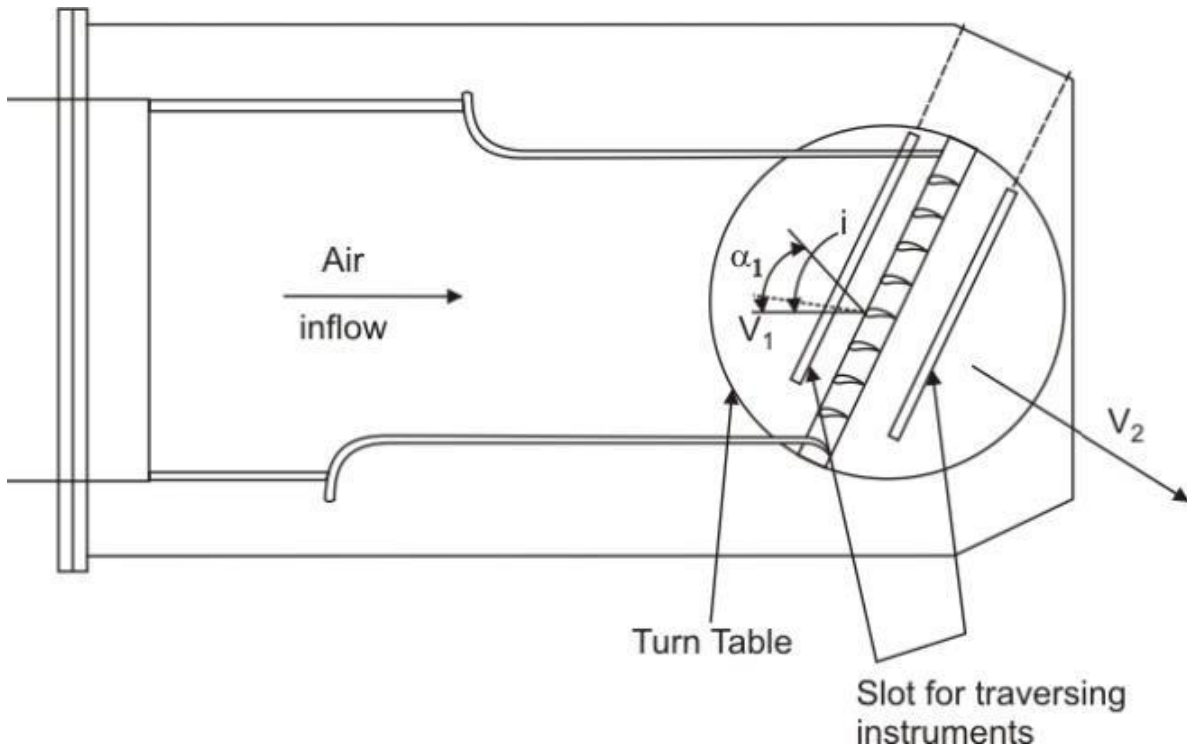


Figure 4.8: A Cascade Tunnel

Compressor cascade:

For a compressor cascade, the static pressure will rise across the cascade, i.e. $P_2 > P_1$

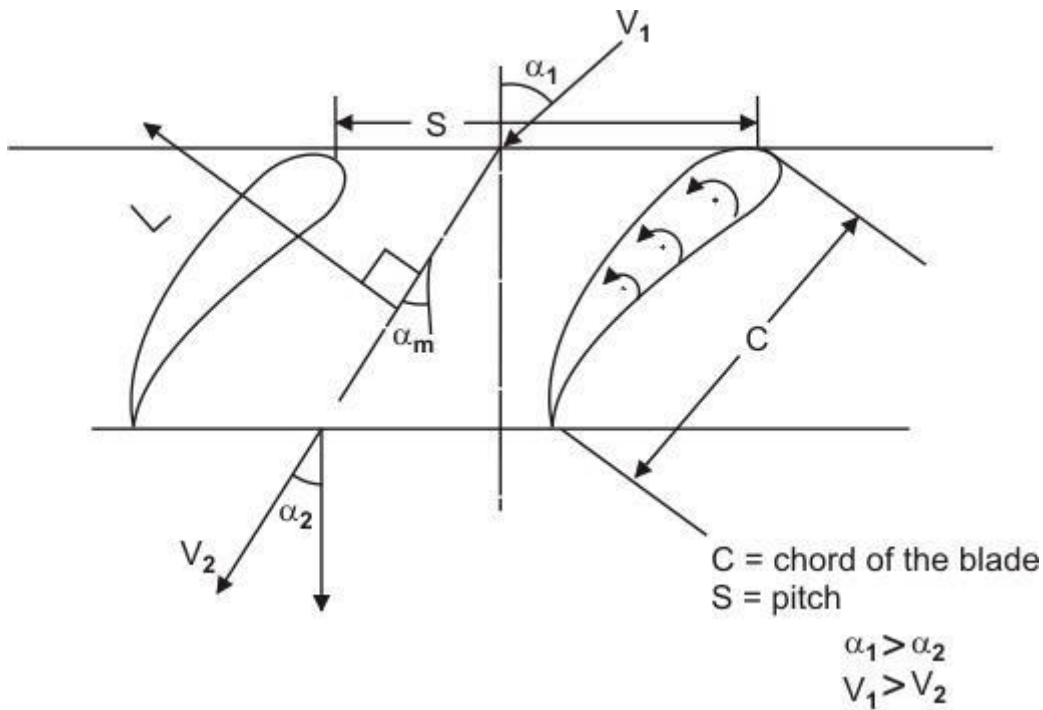


Figure 4.9 Compressor Cascade

C = chord of the blade

S = pitch

$\alpha_1 > \alpha_2$

$V_1 > V_2$

$$\tan \alpha_m = \frac{1}{2}(\tan \alpha_1 + \tan \alpha_2)$$

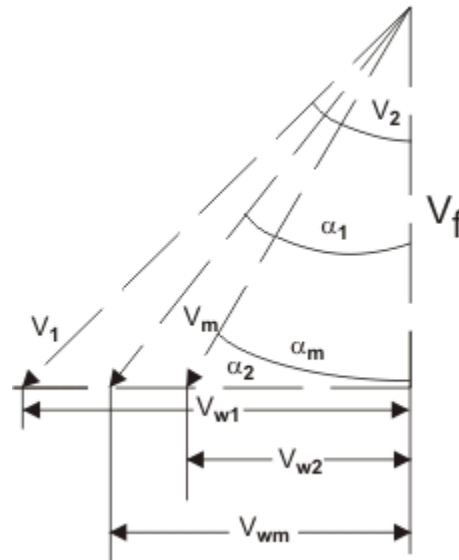


Figure 4.10 Velocity triangle

Circulation:

$$\Gamma = S(V_{w1} - V_{w2})$$

$$\text{Lift} = \rho V_m \Gamma = \rho V_m S(V_{w1} - V_{w2})$$

$$C_L = \frac{L}{\frac{1}{2} \rho V_m^2 C} = \frac{\rho V_m S(V_{w1} - V_{w2})}{\frac{1}{2} \rho V_m^2 C}$$

Lift coefficient,

$$= \frac{2S}{C} * \frac{1}{V_m} (V_{w1} - V_{w2})$$

from velocity triangles,

$$V_{w1} = V_f \tan \alpha_1, \quad V_{w2} = V_f \tan \alpha_2$$

$$C_L = 2 \frac{S}{C} \left(\frac{V_f}{V_m} \right) (\tan \alpha_1 - \tan \alpha_2)$$

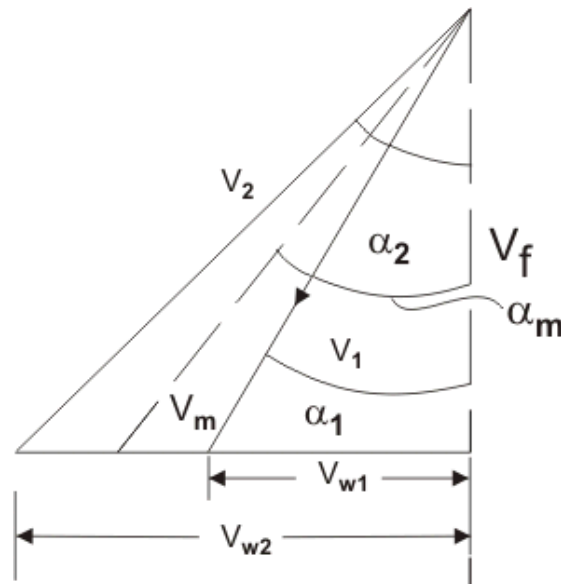
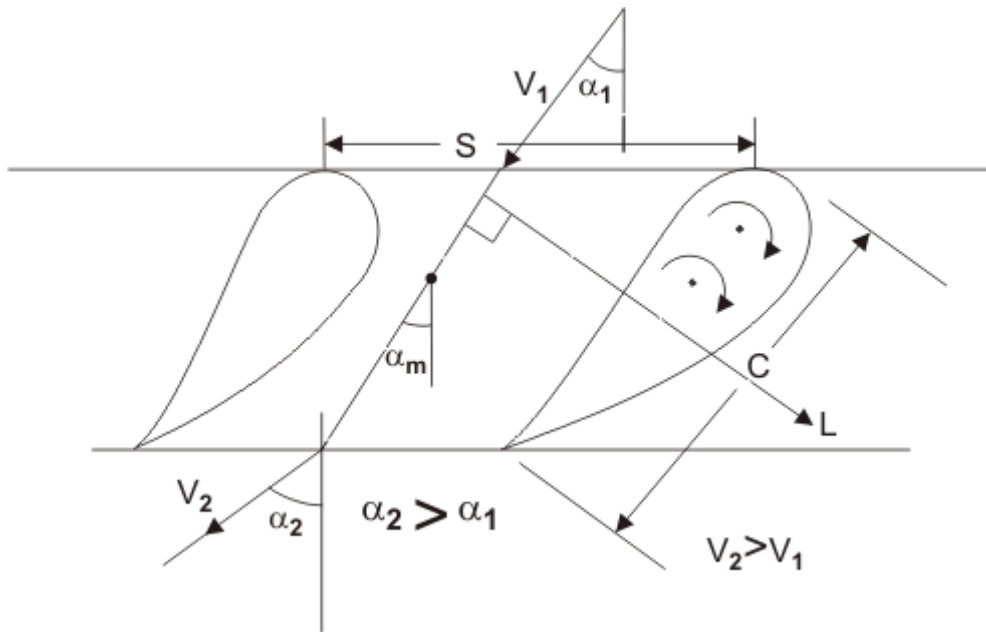
$$= 2 \frac{S}{C} (\tan \alpha_1 - \tan \alpha_2) \cos \alpha_m, \quad \tan \alpha_m = \frac{\tan \alpha_1 + \tan \alpha_2}{2}$$

S, C - depend on the design of the cascade

α_1, α_2 - flow angles at the inlet and outlet

Lift is perpendicular to α_m line

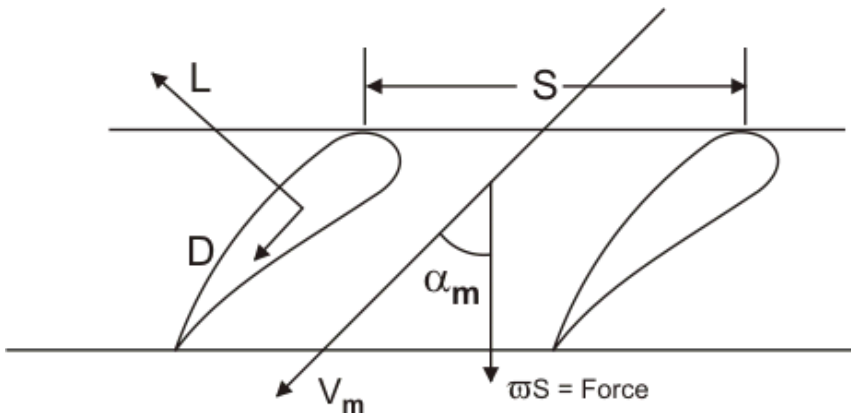
Turbine Cascade: Static pressure will drop across the turbine cascade, i.e. $p_2 < p_1$



Compressor Cascade (Viscous Case)

In compressor cascade, due to losses in total pressure ($\bar{\omega}$), there will be an axial force $S\bar{\omega}$ as shown in figure below. Thus the drag, which is perpendicular to the lift, is defined as

$$D = \bar{\omega} S \cos \alpha_m$$



The lift will be reduced due to the effect of drag which can be expressed as:

$$\text{Effective lift} = \bar{L} = L - \rho S \sin \alpha_m = \rho V_m \Gamma - \rho S \sin \alpha_m$$

The lift has decreased due to viscosity, $\bar{L} = \rho V_m \Gamma - D \tan \alpha_m$

Actual lift coefficient

$$C_L = 2 \frac{S}{C} (\tan \alpha_1 - \tan \alpha_2) \cos \alpha_m - C_D \tan \alpha_m$$

$$C_D = \frac{D}{\frac{1}{2} \rho V_m^2 C}$$

where, C_D = drag coefficient,

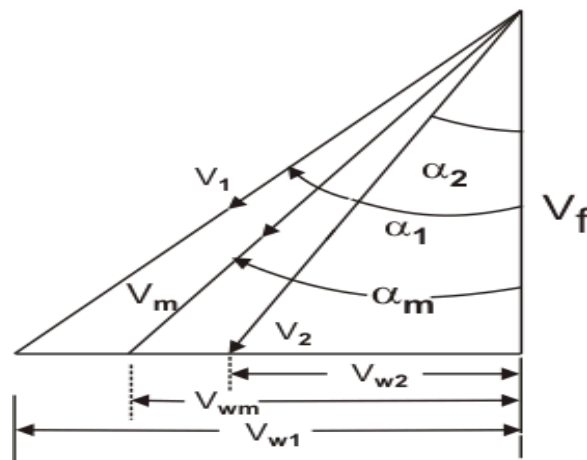
In the case of turbine, drag will contribute to work (and is considered as useful).

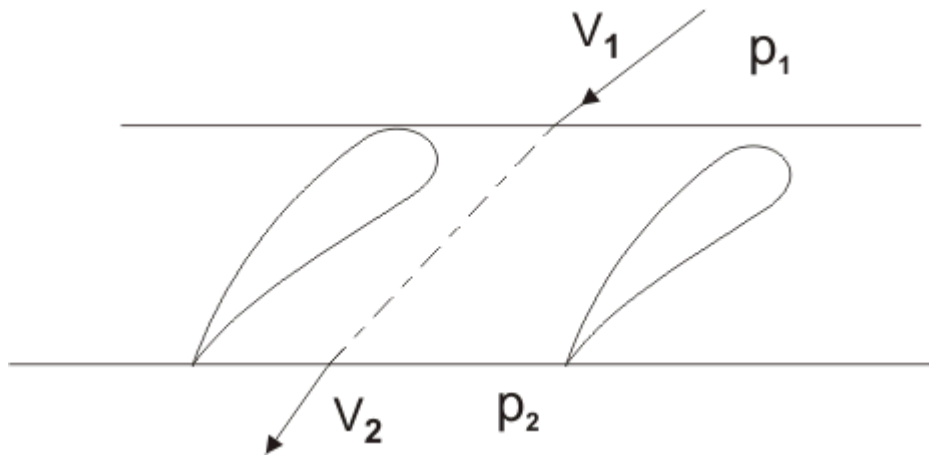
Blade efficiency (or diffusion efficiency)

For a compressor cascade, the blade efficiency is defined as:

$$\eta_b = \frac{\text{Actual rise in static pressure}}{\text{Ideal static pressure rise}}$$

Due to viscous effect, static pressure rise is reduced





$$\eta_b = \frac{(P_2 - P_1)_{\text{ideal}} - \text{loss}}{(P_2 - P_1)_{\text{ideal}}}$$

$$\eta_b = \frac{\frac{\rho}{2}(V_1^2 - V_2^2) - \bar{\omega}}{\frac{\rho}{2}(V_1^2 - V_2^2)} = 1 - \frac{\bar{\omega}}{\frac{\rho}{2}(V_1^2 - V_2^2)}$$

from velocity triangle:

$$V_1^2 = V_{w1}^2 + V_f^2, V_2^2 = V_{w2}^2 + V_f^2$$

$$V_1^2 - V_2^2 = (V_{w1} + V_{w2})(V_{w1} - V_{w2})$$

$$\eta_b = 1 - \frac{\bar{\omega}}{\frac{\rho}{2}(V_{w1} + V_{w2})(V_{w1} - V_{w2})}$$

$$\begin{aligned} \frac{V_{w1} + V_{w2}}{2} &= V_{wm} \\ &= V_m \sin \alpha_m \end{aligned}$$

Also we get

$$L \simeq \rho \Gamma V_m$$

$$(\eta_b)_{\text{comp cascade}} = 1 - \frac{2C_D}{C_L \sin 2\alpha_m}$$

η -maximum,

η if

$$\alpha_m = 45^\circ$$

$$\frac{d\eta_b}{d\alpha_m} = 0 \Rightarrow \cos 2\alpha_m = 0$$

The value of α_m for which efficiency is maximum, $\alpha_m = 45^\circ$

The blade efficiency for a turbine cascade is defined as:

$$\eta_b = \frac{\text{Ideal static pressure drop } (\Delta p)_s \text{ to obtain a certain change in kinetic energy}}{\text{Actual static pressure drop to produce the same change in kinetic energy}}$$

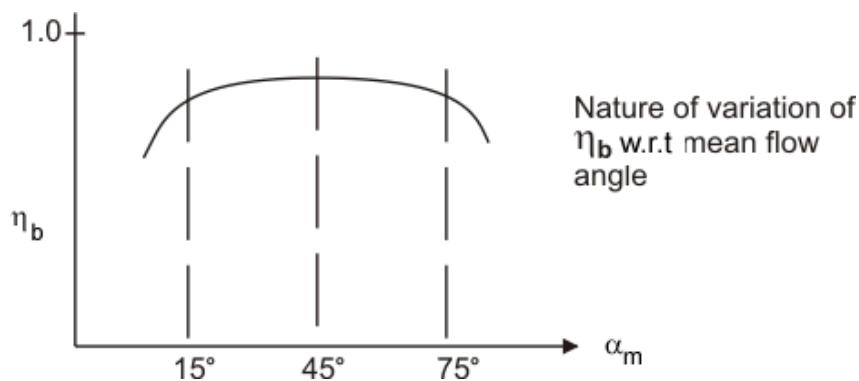
$$= \frac{\frac{\rho}{2}(V_2^2 - V_1^2)}{\frac{\rho}{2}(V_2^2 - V_1^2) + \bar{\phi}} = \frac{1}{1 + \frac{\bar{\phi}}{\frac{\rho}{2}(V_{w2} + V_{w1})(V_{w2} - V_{w1})}}$$

$$(\eta_b)_{\text{turbine}} = \frac{1}{1 + \frac{2C_D}{C_L \sin 2\alpha_m}}$$

For very small ratio of C_D / C_L

$$(\eta_b)_{\text{turbine}} = \left(1 + 2 \frac{C_D}{C_L} \cdot \frac{1}{\sin 2\alpha_m} \right)^{-1}$$

$$(\eta_b)_{\text{turbine}} = 1 - 2 \frac{C_D}{C_L \sin 2\alpha_m} \text{ which is same as the compressor cascade}$$



Nature of variation of η_b wrt mean flow angle

In the above derivation for blade efficiency of both the compressor and turbine cascade, the lift is assumed as $\rho\Gamma V_m$, neglecting the effect of drag. With the corrected expression of lift, actual blade efficiencies are as follows:

$$(\eta_b)_{\text{comp cascade}} = \frac{1 - \frac{C_D}{C_L} \cot \alpha_m}{1 + \frac{C_D}{C_L} \tan \alpha_m}$$

$$(\eta_b)_{\text{turb cascade}} = \frac{1 - \frac{C_D}{C_L} \tan \alpha_m}{1 + \frac{C_D}{C_L} \cot \alpha_m}$$

Axial Flow Turbine

A gas turbine unit for power generation or a turbojet engine for production of thrust primarily consists of a compressor, combustion chamber and a turbine. The air as it passes through the compressor, experiences an increase in pressure. There after the air is fed to the combustion chamber leading to an increase in temperature. This high pressure and temperature gas is then passed through the turbine, where it is expanded and the required power is obtained.

Turbines, like compressors, can be classified into radial, axial and mixed flow machines. In the axial machine the fluid moves essentially in the axial direction through the rotor. In the radial type, the fluid motion is mostly radial. The mixed-flow machine is characterized by a combination of axial and radial motion of the fluid relative to the rotor. The choice of turbine type depends on the application, though it is not always clear that any one type is superior.

Comparing axial and radial turbines of the same overall diameter, we may say that the axial machine, just as in the case of compressors, is capable of handling considerably greater mass flow. On the other hand, for small mass flows the radial machine can be made more efficient than the axial one. The radial turbine is capable of a higher pressure ratio per stage than the axial one. However, multi-staging is very much easier to arrange with the axial turbine, so that large overall pressure ratios are not difficult to obtain with axial turbines. In this chapter, we will focus on the axial flow turbine.

Generally the efficiency of a well-designed turbine is higher than the efficiency of a compressor. Moreover, the design process is somewhat simpler. The principal reason for this fact is that the fluid undergoes a pressure drop in the turbine and a pressure rise in the compressor. The pressure drop in the turbine is sufficient to keep the boundary layer generally well behaved, and the boundary layer separation which often occurs in compressors because of an adverse pressure gradient, can be avoided in turbines. Offsetting this advantage is the much more critical stress problem, since turbine rotors must operate in very high temperature gas. Actual blade shape is often more dependent on stress and cooling considerations than on aerodynamic considerations, beyond the satisfaction of the velocity-triangle requirements.

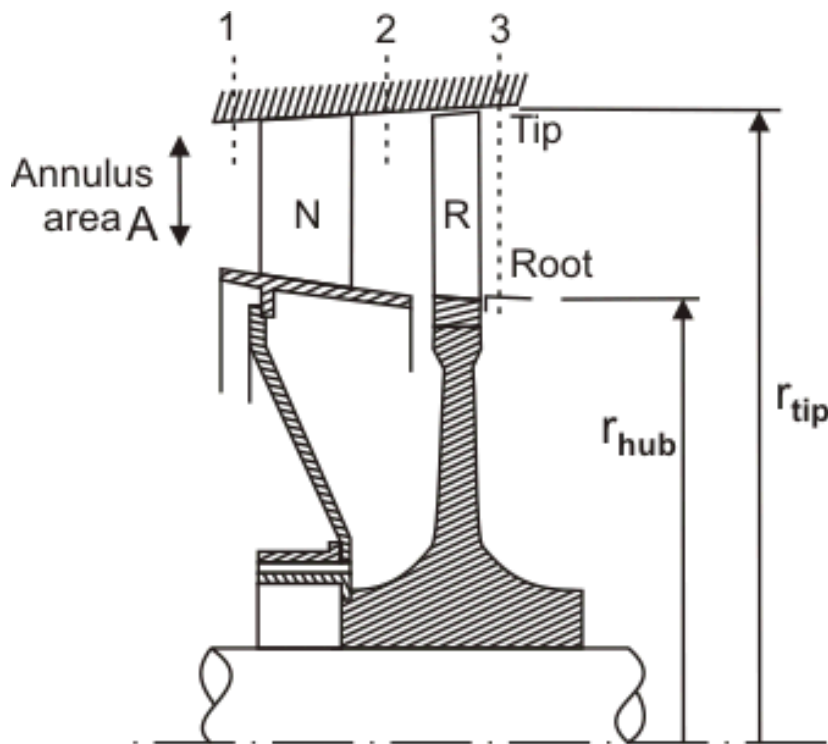
Because of the generally falling pressure in turbine flow passages, much more turning in a given blade row is possible without danger of flow separation than in an axial compressor blade row. This means much more work, and considerably higher pressure ratio, per stage. In recent years advances have been made in turbine blade cooling and in the metallurgy of turbine blade materials. This means that turbines are able to operate successfully at increasingly high inlet gas temperatures and that substantial improvements are being made in turbine engine thrust, weight, and fuel consumption.

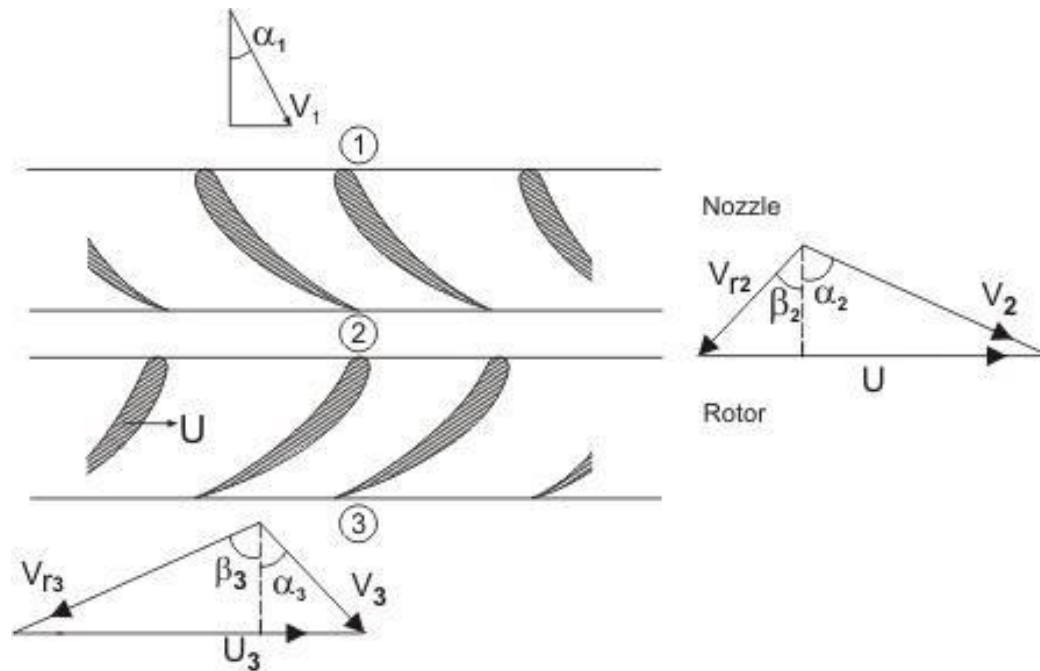
Two-dimensional theory of axial flow turbine.

An axial turbine stage consists of a row of stationary blades, called nozzles or stators, followed by the rotor, as Figure 13.1 illustrates. Because of the large pressure drop per stage, the nozzle and rotor blades may be of increasing length, as shown, to accommodate the rapidly expanding gases, while holding the axial velocity to something like a uniform value through the stage.

It should be noted that the hub-tip ratio for a high pressure gas turbine is quite high, that is, it is having blades of short lengths. Thus, the radial variation in velocity and pressure may be neglected and the performance of a turbine stage is calculated from the performance of the blading at the mean radial section, which is a two-dimensional "pitch-line design analysis". A low-pressure turbine will typically have a much lower hub-tip ratio and a larger blade twist. A two dimensional design is not valid in this case.

In two dimensional approach the flow velocity will have two components, one axial and the other peripheral, denoted by subscripts 'f' and ∞ respectively. The absolute velocity is denoted by V and the relative velocity with respect to the impeller by V_r . The flow conditions '1' indicates inlet to the nozzle or stator vane, '2' exit from the nozzle or inlet to the rotor and '3' exit from the rotor. Absolute angle is represented by α and relative angle by β as before.





Axial Turbine Stage

A section through the mean radius would appear as in Figure.13.1. One can see that the nozzles accelerate the flow imparting an increased tangential velocity component. The velocity diagram of the turbine differs from that of the compressor in that the change in tangential velocity in the rotor, ΔV_{sw} in the direction opposite to the blade speed U . The reaction to this change in the tangential momentum of the fluid is a torque on the rotor in the direction of motion. Hence the fluid does work on the rotor.

Again applying the angular momentum relation-ship, we may show that the power output as,

$$P = \dot{m}(U_2 V_{w_2} - U_3 V_{w_3}) \quad (13.1)$$

In an axial turbine,

$$U_2 \approx U_3 = U \text{ (say)}$$

The work output per unit mass flow rate is

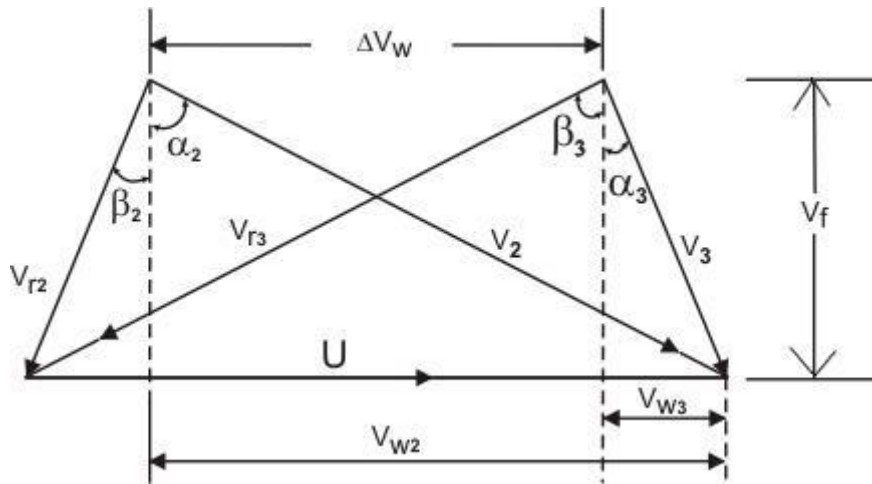
$$W_T = U(V_{w_2} - V_{w_3})$$

Again,
$$W_T = C_p(T_{01} - T_{03})$$

Defining
$$\Delta T_o = T_{o1} - T_{o3} = T_{o2} - T_{o3}$$

We find that the stage work ratio is

$$\frac{\Delta T_o}{T_{o1}} = \frac{W_T}{C_p T_{o1}} = \frac{U(V_{w_2} - V_{w_3})}{C_p T_{o1}} \quad (13.2)$$



Combined velocity diagram

The velocity diagram gives the following relation:

$$\begin{aligned} \frac{U}{V_f} &= \tan \alpha_2 - \tan \beta_2 \\ &= \tan \alpha_3 - \tan \beta_3 \end{aligned}$$

Thus,

$$\begin{aligned} W_T &= U(V_{w2} - V_{w3}) \\ &= UV_f[\tan \alpha_2 - \tan \alpha_3] \end{aligned}$$

i.e.,

$$W_T = UV_f[\tan \alpha_2 - \tan \alpha_3] \quad (13.3)$$

The Eq.(13.3) gives the expression for W_T in terms of gas angles associated with the rotor blade.

Note that the "work-done factor" required in the case of the axial compressor is unnecessary here. This is because in an accelerating flow the effect of the growth of boundary layer along the annulus passage is much less than when there is a decelerating flow with an average pressure gradient.

Instead of temperature drop ratio [defined in Eq. (13.2)], turbine designers generally refer to the work capacity of a turbine stage as,

$$\begin{aligned} \Psi &= \frac{c_p \Delta T_o}{U^2} = \frac{V_{w2} - V_{w3}}{U} \\ &= \frac{V_f}{U}[\tan \beta_2 - \tan \beta_3] \end{aligned} \quad (13.4)$$

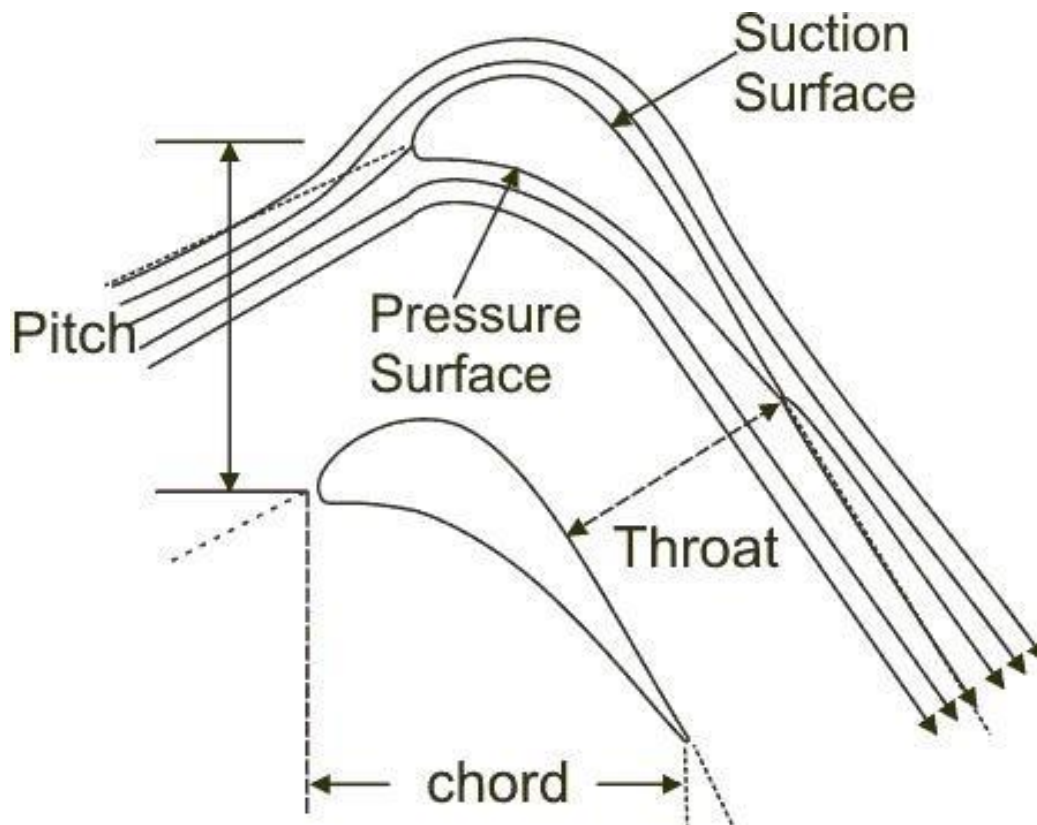
Ψ is a dimensionless parameter, which is called the "blade loading capacity" or "temperature drop coefficient". In gas turbine design, V_f is kept generally constant across a stage and the ratio V_f/U is called "the flow coefficient" ϕ .

Thus, Eq. (13.4) can be written as,

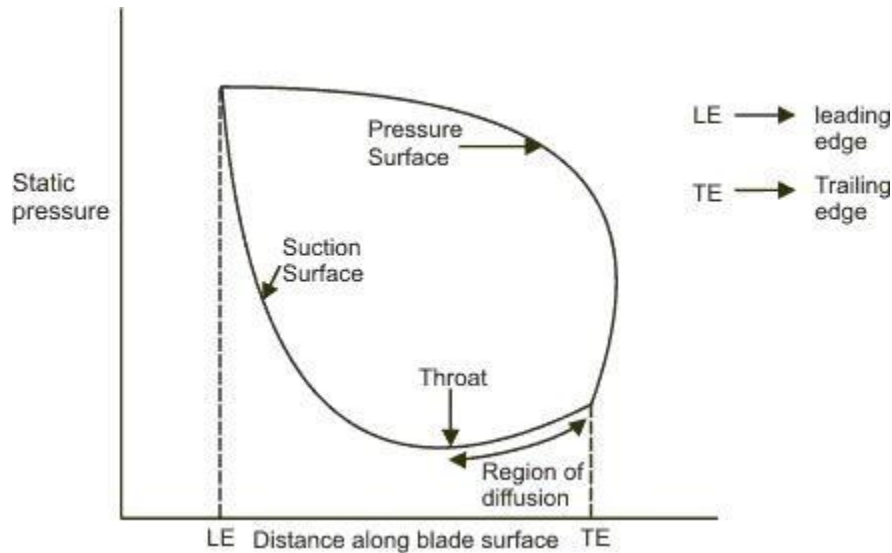
$$\psi = \phi[\tan \beta_2 - \tan \beta_3] \quad (13.5)$$

As the boundary layer over the blade surface is not very sensitive in the case of a turbine, the turbine designer has considerably more freedom to distribute the total stage pressure drop between the rotor and the stator. However, locally on the suction surface of the blade there could be a zone of an adverse pressure gradient depending on the turning and on the pitch of the blades. Thus, the boundary layer could grow rapidly or even separate in such a region affecting adversely the turbine efficiency.

Figure 13.3 illustrates the schematic of flow within the blade passage and the pressure distribution over the section surface depicting a zone of diffusion. Different design groups have their own rules, learned from experience of blade testing, for the amount of diffusion which is permissible particularly for highly loaded blades.



Schematic diagram of flow through a turbine blade passage



Pressure distribution around a turbine blade

Radial flow turbine

Figure 7.44 illustrates a rotor having the back-to-back configuration mentioned in the introduction to this chapter, and [Ref. (29)] discusses the development of a successful family of radial industrial gas turbines. In a radial flow turbine, gas flow with a high tangential velocity is directed inwards and leaves the rotor with as small a whirl velocity as practicable near the axis of rotation. The result is that the turbine looks very similar to the centrifugal compressor, but with a ring of nozzle vanes replacing the diffuser vanes as in Fig. 7.45 Degree of reaction

Another useful dimensionless parameter is the "degree for reaction" or simply the "reaction" R . It may be defined for a turbine as the fraction of overall enthalpy drop (or pressure drop) occurring in the rotor Also, as shown there would normally be a diffuser at the outlet to reduce the exhaust velocity to a negligible value.

The velocity triangles are drawn for the normal design condition in which the relative velocity at the rotor tip is radial (i.e. the incidence is zero) and the absolute velocity at exit is axial. Because C_{w3} is zero, the specific work output W becomes simply

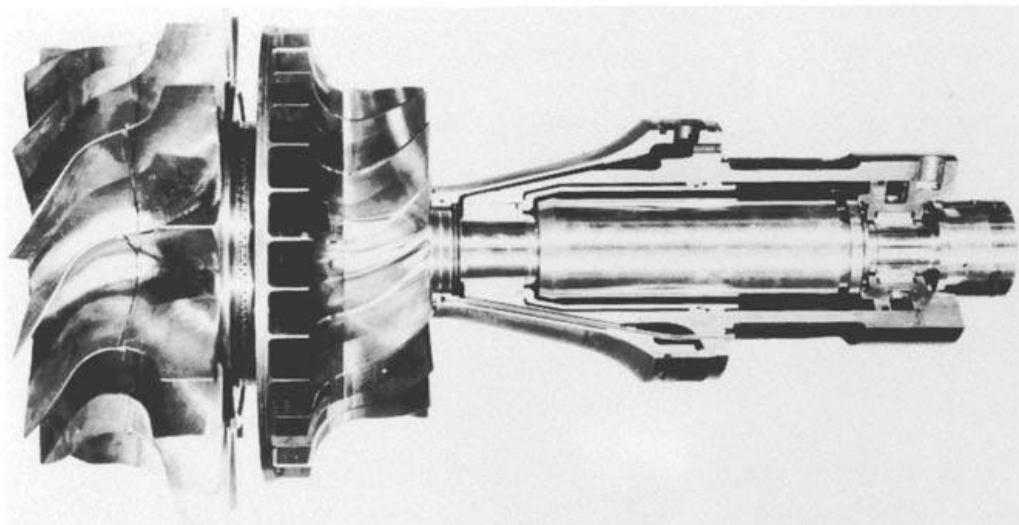


Fig. 7.45 :Radial turbine with Back-to-back rotor [courtesy Kongsberg Ltd]

$$W = c_p(T_{01} - T_{03}) = C_{w2}U_2 = U_2^2 \quad (7.45)$$

In the ideal isentropic turbine with perfect diffuser the specific work output would be

$$W' = c_p(T_{01} - T_4') = C_0^2/2$$

where the velocity equivalent of the isentropic enthalpy drop, C_0 , is sometimes called the 'spouting velocity' by analogy with hydraulic turbine practice. For this ideal case it follows that $U_2^2 = C_0^2 > 2$ or $U_2 > C_0 = 0.707$. In practice, it is found that a good overall efficiency is obtained if this velocity ratio lies between 0.68 and 0.71. In terms of the turbine pressure ratio, C_0 is given by

$$\frac{C_0^2}{2} = c_p T_{01} \left[1 - \left(\frac{1}{p_{01}/p_a} \right)^{(\gamma-1)/\gamma} \right]$$

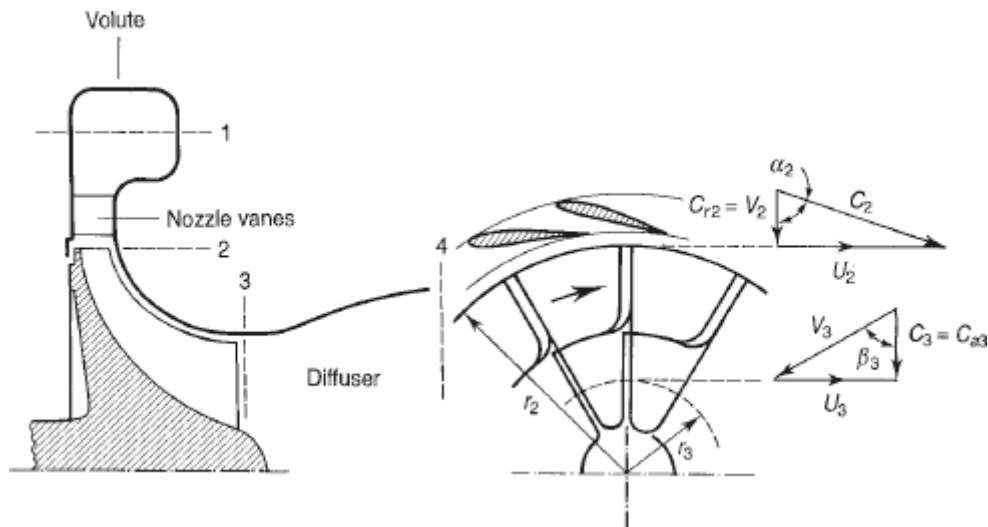


FIG. 7.46 Radial inflow turbine

Figure 7.46 depicts the processes in the turbine and exhaust diffuser on the T-s diagram. The overall isentropic efficiency of the turbine and diffuser may be expressed by

$$\eta_0 = \frac{T_{01} - T_{03}}{T_{01} - T_4'}$$

because $(T_{01} - T_4')$ is the temperature equivalent of the maximum work that could be produced by an isentropic expansion from the inlet state (p_{01}, T_{01}) to p_a . Considering the turbine alone, however, the efficiency is more suitably expressed by

$$\eta_t = \frac{T_{01} - T_{03}}{T_{01} - T_3'}$$

which is the 'total-to-static' isentropic efficiency referred to in section 7.1. Following axial flow turbine practice, the nozzle loss coefficient may be defined in the usual way by

$$\lambda_N = \frac{T_2 - T'_2}{C_2^2/2c_p}$$

Similarly, the rotor loss coefficient is given by

$$\lambda_R = \frac{T_3 - T''_3}{V_3^2/2c_p}$$

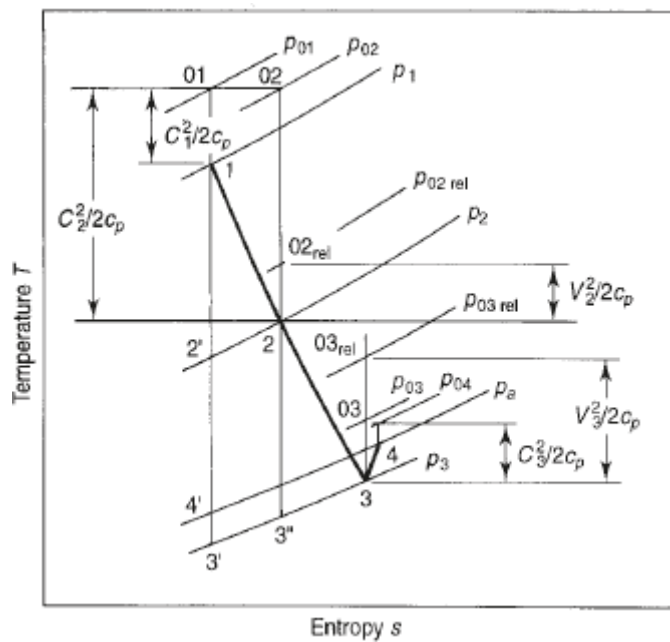


FIG. 7.47 T-s diagram for a radial flow turbine

Degree of reaction

Another useful dimensionless parameter is the "degree for reaction" or simply the "reaction" R. It may be defined for a turbine as the fraction of overall enthalpy drop (or pressure drop) occurring in the rotor

Thus,
$$R = \frac{h_2 - h_3}{h_{01} - h_{03}} \quad (14.1)$$

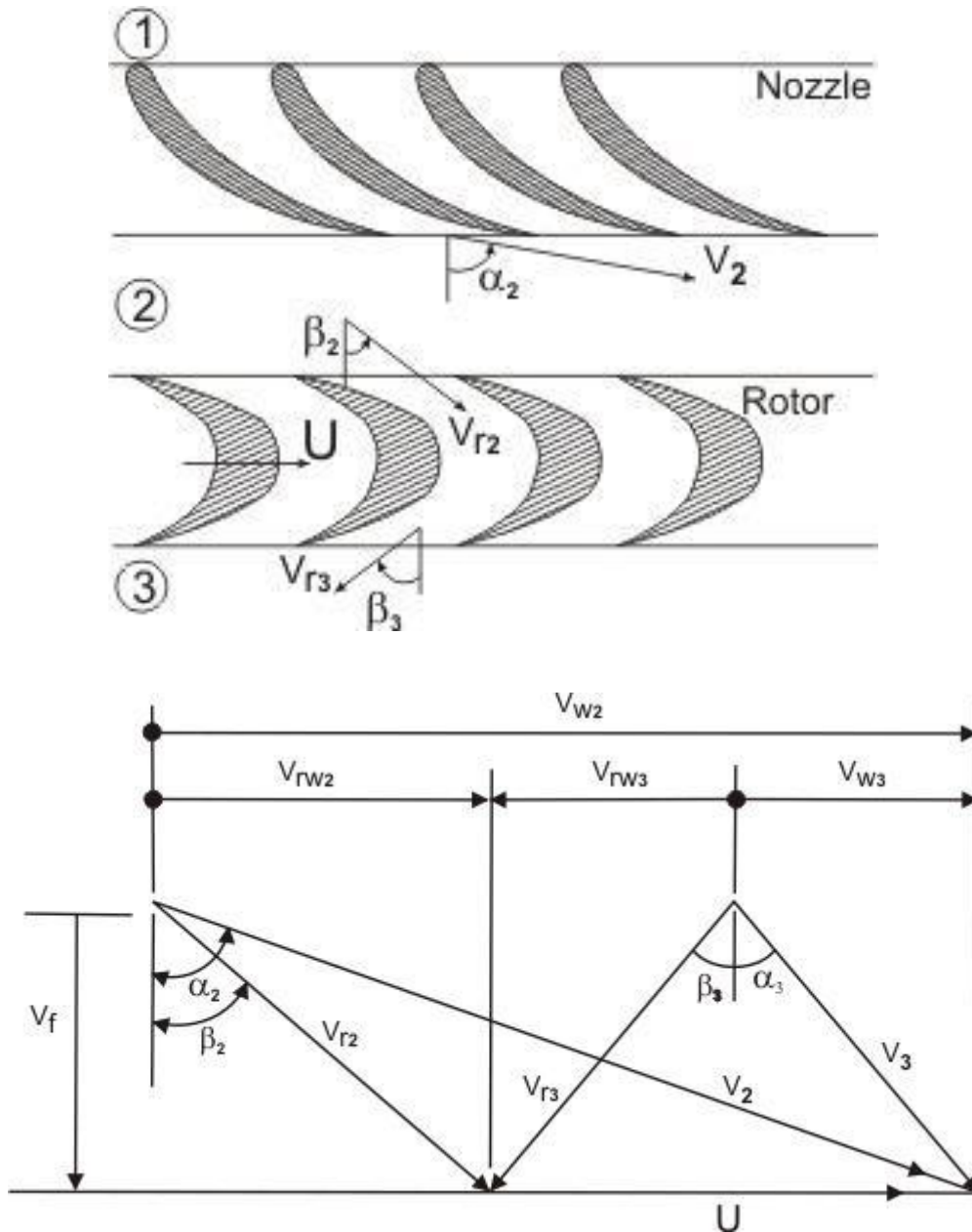
or,
$$\frac{T_2 - T_3}{T_{01} - T_{03}}$$

Turbine stage in which the entire pressure drop occurs in the nozzle are called "impulse stages". Stages in which a portion of the pressure drop occurs in the nozzle and the rest in the rotor are

called reaction stages. In a 50% reaction turbine, the enthalpy drop in the rotor would be half of the total for the stage.

An impulse turbine stage is shown in Fig14.1, along with the velocity diagram for the common case of constant axial velocity. Since no enthalpy change occurs within the rotor, the energy equation within the rotor requires that $|V_{r2}| = |V_{r3}|$. If the axial velocity is held constant, then this requirement is satisfied by

$$\beta_3 = -\beta_2$$



Impulse turbine stage with constant axial velocity

From the velocity diagram, we can see that

$$V_{r_{w3}} = -V_{r_{w2}}$$

i.e.

$$\begin{aligned} V_{w_2} - V_{w_3} &= 2V_{r_{w_2}} \\ &= 2(V_{w_2} - U) \\ &= 2U \left(\frac{V_f}{U} \tan \alpha_2 - 1 \right) \end{aligned}$$

Then,

$$\begin{aligned} \psi &= \frac{V_{w_2} - V_{w_3}}{U} \\ &= 2(\phi \tan \alpha_2 - 1) \end{aligned} \quad (14.2)$$

The Eq. (14.2) illustrates the effect of the nozzle outlet angle on the impulse turbine work output.

It is evident, then, that for large power output the nozzle angle should be as large as possible. Two difficulties are associated with very large α_2 . For reasonable axial velocities (i.e., reasonable flow per unit frontal area), it is evident that large α_2 creates very large absolute and relative velocities throughout the stage. High losses are associated with such velocities, especially if the relative velocity V_{r2} is supersonic. In practice, losses seem to be minimized for values of α_2 around 70° . In addition, one can see that for large α [$\tan \alpha_2 > (2U/V_f)$], the absolute exhaust velocity will have a swirl in the direction opposite to U .

While we have not introduced the definition of turbine efficiency as yet, it is clear that, in a turbojet engine where large axial exhaust velocity is desired, the kinetic energy associated with the tangential motion of the exhaust gases is essentially a loss. Furthermore, application of the angular momentum equation over the entire engine indicates that exhaust swirl is associated with (undesirable) net torque acting on the aircraft. Thus the desire is for axial or near-axial absolute exhaust velocity (at least for the last stage if a multistage turbine is used). For the special case of constant V_f and axial exhaust velocity $V_{w3} = 0$ and $V_{w2} = 2U$, the Eq. 14.2 becomes,

$$\psi = 2 \quad \left[\because \tan \alpha_2 = \frac{V_w}{V_f} = \frac{2U}{V_f} = 2/\phi \right]$$

For a given power and rotor speed, and for a given peak temperature, Eq. (14.2) is sufficient to determine approximately the mean blade speed (and hence radius) of a single-stage impulse turbine having axial outlet velocity. If, as is usually the case, the blade speed is too high (for stress limitations), or if the mean diameter is too large relative to the other engine components, it is necessary to employ a multistage turbine in which each stage does part of the work.

STAGE EFFICIENCY

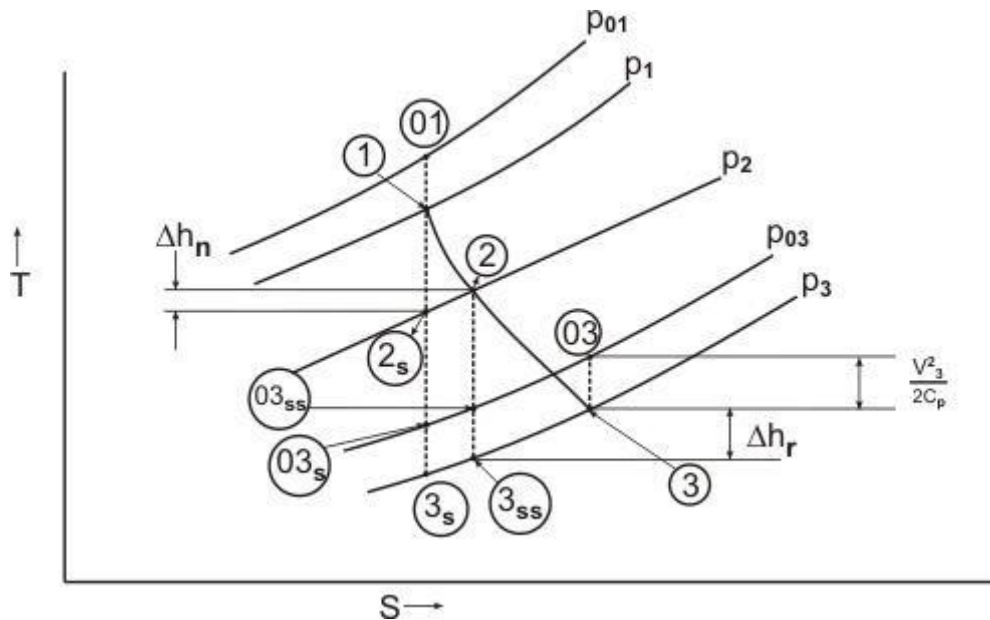
The aerodynamic losses in the turbine differ with the stage configuration, that is, the

degree of reaction. Improved efficiency is associated with higher reaction, which tends to mean less work per stage and thus a large number of stages for a given overall pressure ratio. The understanding of aerodynamic losses is important to design, not only in the choice of blading type (impulse or reaction) but also in devising ways to control these losses, for example, methods to control the clearance between the tip of the turbine blade and the outer casing wall. The choices of blade shape, aspect ratio, spacing, Reynolds number, Mach number and flow incidence angle can all affect the losses and hence the efficiency of turbine stages.

Two definitions of efficiency are in common usage: the choice between them depends on the application for which the turbine is used. For many conventional applications, useful turbine output is in the form of shaft power and the kinetic energy of the exhaust, $[(V_3)^2/2]$, is considered as a loss. In this case, ideal work would be $C_p(T_{01} - T_{3s})$ and a total-to-static turbine efficiency, η_{ts} , based on the inlet and exit static conditions, is used.

$$\text{Thus, } \eta_{ts} = \frac{T_{01} - T_{03}}{T_{01} - T_{3s}} \quad (15.1)$$

The ideal (isentropic) to actual expansion process in turbines is illustrated in Fig 15.1.



T-S diagram: expansion in a turbine

Further,

$$\begin{aligned} \eta_{ts} &= \frac{T_{01} - T_{03}}{T_{01} [1 - (P_3 / P_{01})^{(\gamma-1)/\gamma}]} \\ &= \frac{1 - (T_{03} / T_{01})}{1 - (P_3 / P_{01})^{(\gamma-1)/\gamma}} \end{aligned} \quad (15.2)$$

In some applications, particularly in turbojets, the exhaust kinetic energy is not considered a loss since the exhaust gases are intended to emerge at high velocity. The ideal work in this case is then $C_p(T_{01} - T_{03s})$ rather than $C_p(T_{01} - T_{3s})$. This requires a different definition of efficiency, the total-to-total turbine efficiency η_{tt} , defined by

$$\eta_{tt} = \frac{T_{01} - T_{03}}{T_{01} - T_{03s}} = \frac{1 - (T_{03}/T_{01})}{1 - (P_{03}/P_{01})^{(\gamma-1)/\gamma}} \quad (15.3)$$

One can compare η_{tt} & η_{ts} by making the approximation,

$$T_{03s} - T_{3s} \cong T_{03} - T_3 = V_3^2 / 2C_p,$$

and using Eqs. (15.2) and (15.3) it can be shown that

$$\eta_{tt} = \frac{\eta_{ts}}{1 - V_3^2 [2C_p (T_{01} - T_{3s})]}$$

Thus

$$\eta_{tt} > \eta_{ts}$$

The actual turbine work can be expressed as,

$$W_t = \eta_{tt} C_p T_{01} \left[1 - \left(\frac{P_{03}}{P_{01}} \right)^{(\gamma-1)/r} \right], \quad (15.4)$$

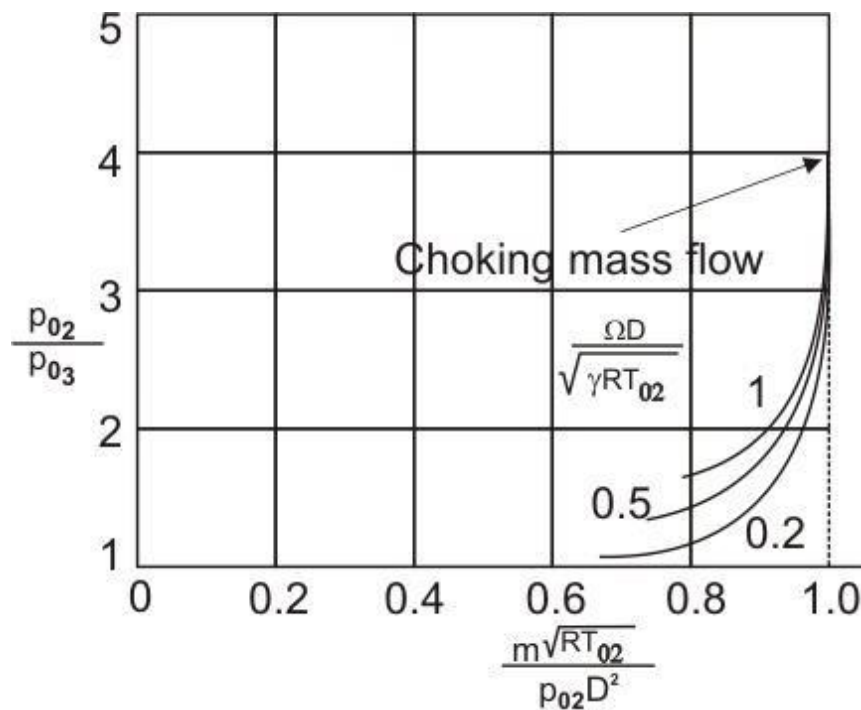
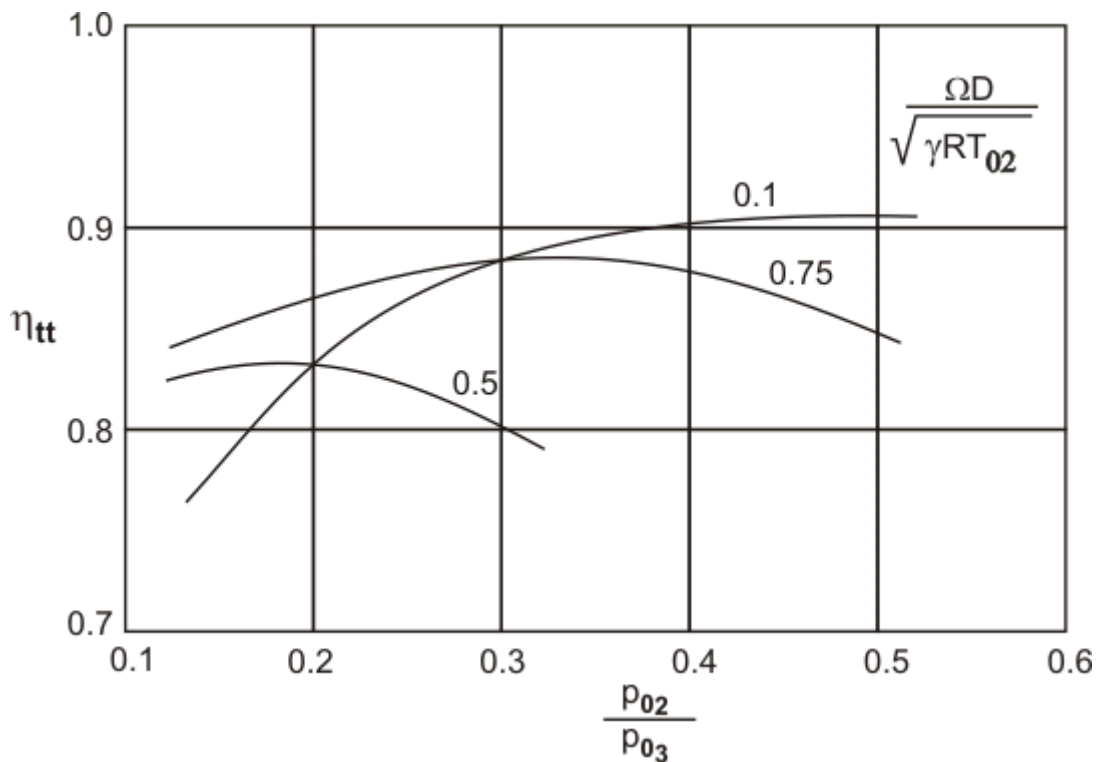
or,
$$W_t = \eta_{ts} C_p T_{01} \left[1 - \left(\frac{P_3}{P_{01}} \right)^{(\gamma-1)/r} \right].$$

Turbine Performance

For a given design of turbine operating with a given fluid at sufficiently high Reynolds member, it can be shown from the dimensional analysis as,

$$\frac{P_{02}}{P_{03}} = f \left(\frac{m \sqrt{RT_{02}}}{P_{02} D^2}, \frac{\Omega D}{\sqrt{\gamma RT_{02}}} \right),$$

where, stagnation states 02 and 03 are at the turbine inlet and outlet, respectively. Figure (15.2) shows the overall performance of a particular single-stage turbine.



Typical characteristics of a turbine stage

One can see that pressure ratios greater than those for compressor stages can be obtained with satisfactory efficiency. The performance of turbines is limited principally by two factors: compressibility and stress. Compressibility limits the mass flow that can pass through a given turbine and, as we will see, stress limits the wheel speed U . The work per stage, for example, depends on the square of the wheel speed. However, the performance of the engine depends very strongly on the maximum temperature. Of course, as the maximum temperature

increases, the allowable stress level diminishes; hence in the design of the engine there must be a compromise between maximum temperature and maximum rotor tip speed U .

For given pressure ratio and adiabatic efficiency, the turbine work per unit mass is proportional to the inlet stagnation temperature. Since, in addition, the turbine work in a jet or turboshaft engine is commonly two or three times the useful energy output of the engine, a 1% increase in turbine inlet temperature can produce a 2% or 3% increase in engine output. This considerable advantage has supplied the incentive for the adoption of fairly elaborate methods for cooling the turbine nozzle and rotor blades.

Free vortex design

- (a) the stagnation enthalpy h_0 is constant over the annulus (i.e. $dh_0/dr = 0$),
- (b) the axial velocity is constant over the annulus, and
- (c) the whirl velocity is inversely proportional to the radius,

then the condition for radial equilibrium of the fluid elements, namely equation (5.13), is satisfied. A stage designed in accordance with (a), (b) and (c) is called a free vortex stage. Applying this to the stage in Fig. 5.8, we can see that with uniform inlet conditions to the nozzles then, since no work is done by the gas in the nozzles, h_0 must also be constant over the annulus at outlet. Thus condition (a) is fulfilled in the space between the nozzles and rotor blades. Furthermore, if the nozzles are designed to give $C_{a2} = \text{constant}$ and $C_{w2}r = \text{constant}$, all three conditions are fulfilled and the condition for radial equilibrium is satisfied in plane 2. Similarly, if the rotor blades are designed so that $C_{a3} = \text{constant}$ and $C_{w3}r = \text{constant}$, it is easy to show as follows that condition (a) will be fulfilled, and thus radial equilibrium will be achieved in plane 3 also. Writing ω for the angular velocity we have

$$W_s = U(C_{w2} + C_{w3}) = \omega(C_{w2}r + C_{w3}r) = \text{constant}$$

But when the work done per unit mass of gas is constant over the annulus, and h_0 is constant at the inlet, h_0 must be constant at the outlet also: thus condition (a) is met.

It is apparent that a free vortex design is one in which the work done per unit mass of gas is constant over the annulus, and to obtain the total work output this specific value need only be calculated at one convenient radius and multiplied by the mass flow. In contrast, we may note that because the density varies from root to tip at exit from the nozzles and the axial velocity is constant, an integration over the annulus will be necessary if the continuity equation is to be used in plane 2. Thus, considering a flow dm through an annular element of radius r and width dr ,

$$\delta m = \rho_2 2\pi r \delta r C_{a2}$$

$$m = 2\pi C_{a2} \int_{r_r}^{r_t} \rho_2 r \, dr$$

With the radial variation of density determined from vortex theory, the integration can be

performed although the algebra is lengthy. For detailed calculations it would be normal to use a digital computer, permitting ready calculation of the density at a series of radii and numerical integration of equation (5.22) to obtain the mass flow. For preliminary calculations, however, it is sufficiently accurate to take the intensity of mass flow at the mean diameter as being the mean intensity of mass flow. In other words, the total mass flow is equal to the mass flow per unit area calculated using the density at the mean diameter ($r_{2m} C_{a2}$) multiplied by the annulus area (A_2). This is one reason why it is convenient to design the turbine on conditions at mean diameter (as was done in the previous example) and use the relations which will now be derived for obtaining the gas angles at other radii.

Using suffix m to denote quantities at mean diameter, the free vortex variation of nozzle angle α_2 may be found as follows:

$$C_{w2}r = rC_{a2} \tan \alpha_2 = \text{constant}$$

$$C_{a2} = \text{constant}$$

Hence α_2 at any radius r is related to α_{2m} at the mean radius r_m by

$$\tan \alpha_2 = \left(\frac{r_m}{r}\right)_2 \tan \alpha_{2m}$$

Similarly, when there is swirl at the outlet from the stage,

$$\tan \alpha_3 = \left(\frac{r_m}{r}\right)_3 \tan \alpha_{3m}$$

The gas angles at the inlet to the rotor blade, β_2 , can then be found using equation (5.1), namely

$$\tan \beta_2 = \tan \alpha_2 - \frac{U}{C_{a2}}$$

$$= \left(\frac{r_m}{r}\right)_2 \tan \alpha_{2m} - \left(\frac{r}{r_m}\right)_2 \frac{U_m}{C_{a2}}$$

similarly β_3 is given by

$$\tan \beta_3 = \left(\frac{r_m}{r}\right)_3 \tan \alpha_{3m} + \left(\frac{r}{r_m}\right)_3 \frac{U_m}{C_{a3}}$$

To obtain some idea of the free vortex variation of gas angles with radius, equations (5.23)–(5.26) will be applied to the turbine designed in the previous section. We will merely calculate the angles at the root and tip, although in practice they would be determined at several stations up the blade to define the twist more precisely. We will at the same time clear up two loose ends: we have to check that there is some positive reaction at the root radius, and that the Mach number relative to the rotor blade at the inlet, MV_2 , is nowhere higher than, say, 0.75. From the velocity triangles at the root and tip it will be seen that this Mach number is greatest at the root and it is only at this radius that it need be calculated.

The variation of gas angles with radius appears as in Fig. 5.9, which also includes the velocity triangles at the root and tip drawn to scale. That $MV_2 = V_2/U(gRT_2)$ is greatest at the root is clear from the velocity triangles: V_2 is then a maximum, and $U(gRT_2)$ is a minimum because the temperature drop across the nozzles is greatest at the root. That there is some

positive reaction at the root is also clear because $V_{3r} > V_{2r}$. Although there is no need literally to calculate the degree of reaction at the root, we must calculate $(MV_2)_r$ to ensure that the design implies a safe value. Using data from the example in section 5.1 we have

$$V_{2r} = C_{a2} \sec \beta_{2r} = 272 \sec 39.32^\circ = 352 \text{ m/s}$$

$$C_{2r} = C_{a2} \sec \alpha_{2r} = 272 \sec 62.15^\circ = 583 \text{ m/s}$$

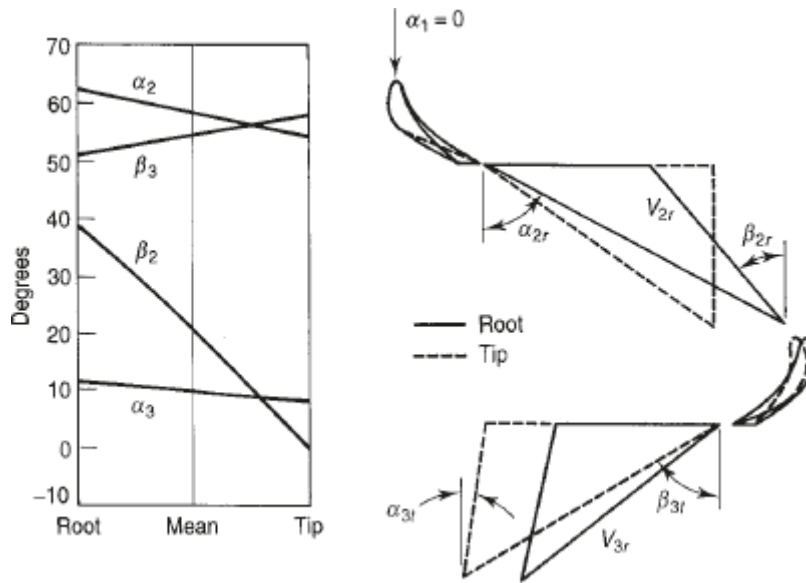


FIG. 5.9 Variation of gas angles with radius.

Constant nozzle angle design

As in the case of the axial compressor, it is not essential to design for free vortex flow. Conditions other than constant C_a and C_w may be used to give some other form of vortex flow, which can still satisfy the requirement for radial equilibrium of the fluid elements. In particular, it may be desirable to make a constant nozzle angle one of the conditions determining the type of vortex, to avoid having to manufacture nozzles of varying outlet angle. This, as will now be shown, requires particular variations of C_a and C_w .

The vortex flow equation (5.15) states that

$$C_a \frac{dC_a}{dr} + C_w \frac{dC_w}{dr} + \frac{C_w^2}{r} = \frac{dh_0}{dr}$$

Consider the flow in the space between the nozzles and blades. As before, we assume that the flow is uniform across the annulus at the inlet to the nozzles, and so the stagnation enthalpy at the outlet must also be uniform, i.e. $dh_0/dr = 0$ in plane 2. Also, if α_2 is to be constant we have

$$\frac{C_{a2}}{C_{w2}} = \cot \alpha_2 = \text{constant}$$

$$\frac{dC_{a2}}{dr} = \frac{dC_{w2}}{dr} \cot \alpha_2$$

The vortex flow equation therefore becomes

$$C_{w2} \cot^2 \alpha_2 \frac{dC_{w2}}{dr} + C_{w2} \frac{dC_{w2}}{dr} + \frac{C_{w2}^2}{r} = 0$$

$$(1 + \cot^2 \alpha_2) \frac{dC_{w2}}{dr} + \frac{C_{w2}}{r} = 0$$

$$\frac{dC_{w2}}{C_{w2}} = -\sin^2 \alpha_2 \frac{dr}{r}$$

Integrating this gives

$$C_{w2} r^{\sin^2 \alpha_2} = \text{constant}$$

And with constant α_2 , $C_{a2} C_{w2}$ so that the variation of C_{a2} must be the same, Namely

$$C_{a2} r^{\sin^2 \alpha_2} = \text{constant}$$

Normally, nozzle angles are greater than 60° , and quite a good approximation to the flow satisfying the equilibrium condition is obtained by designing with a constant nozzle angle and constant angular momentum, i.e. $\alpha_2 = \text{constant}$ and $C_{w2} r = \text{constant}$. If this approximation is made and the rotor blades are twisted to give constant angular momentum at the outlet also, then, as for free vortex flow, the work output per unit mass flow is the same at all radii. On the other hand, if equation (5.28) were used it would be necessary to integrate from root to tip to obtain the work output. We observed early in section 5.2 that there is little difference in efficiency between turbines of low radius ratio designed with twisted and untwisted blading. It follows that the sort of approximation referred to here is certainly unlikely to result in a significant deterioration of performance.

The free vortex and constant nozzle angle types of design do not exhaust the possibilities. For example, one other type of vortex design aims to satisfy the radial equilibrium condition and at the same time meet a condition of constant mass flow per unit area at all radii. That is, the axial and whirl velocity distributions are chosen so that the product $r^2 C_{a2}$ is constant at all radii. The advocates of this approach correctly point out that the simple vortex theory outlined in section 5.6 assumes no radial component of velocity, and yet even if the turbine is designed with no flare there must be a radial shift of the streamlines as shown in Fig. 5.10. This shift is due to the increase in density from root to tip in plane 2 assumption that the radial component is zero would undoubtedly be true for a turbine of constant annulus area if the stage were designed for constant mass flow per unit area. It is argued that the flow is then more likely to behave as intended, so that the gas angles will more closely match the blade angles. Further details can be found in [Ref. (1)]. In view of what has just been said about the dubious benefits of vortex blading for turbines of modest radius ratio, it is very doubtful indeed whether such refinements are more than an academic exercise.

Choice of blade profile, pitch and chord

So far in our worked example we have shown how to establish the gas angles at all radii and blade heights. The next step is to choose stator and rotor blade shapes which will accept the gas incident upon the leading edge, and deflect the gas through the required angle with the minimum loss. An overall blade loss coefficient Y (or l) must account for the following sources of friction loss

- (a) *Profile loss*—associated with boundary layer growth over the blade profile (including separation loss under adverse conditions of extreme angles of incidence or high inlet Mach number).
- (b) *Annulus loss*—associated with boundary layer growth on the inner and outer walls of the annulus.
- (c) *Secondary flow loss*—arising from secondary flows which are always present when a wall boundary layer is turned through an angle by an adjacent curved surface.
- (d) *Tip clearance loss*—near the rotor blade tip the gas does not follow the intended path, fails to contribute its quota of work output, and interacts with the outer wall boundary layer.

The profile loss coefficient Y_p is measured directly in cascade tests similar to those described for compressor blading in section 5.8. Losses (b) and (c) cannot easily be separated, and they are accounted for by a secondary loss coefficient Y_s . The tip clearance loss coefficient, which normally arises only for rotor blades, will be denoted by Y_k . Thus the total loss coefficient Y comprises the accurately measured two-dimensional loss Y_p , plus the three-dimensional loss ($Y_s + Y_k$) which must be deduced from turbine stage test results. A description of one important compilation of such data will be given in section 5.4; all that is necessary for our present purpose is a knowledge of the sources of loss.

Conventional blading

Figure 5.11 shows a conventional steam turbine blade profile constructed from circular arcs and straight lines. Gas turbines have until recently used profiles closely resembling this, although specified by aerofoil terminology

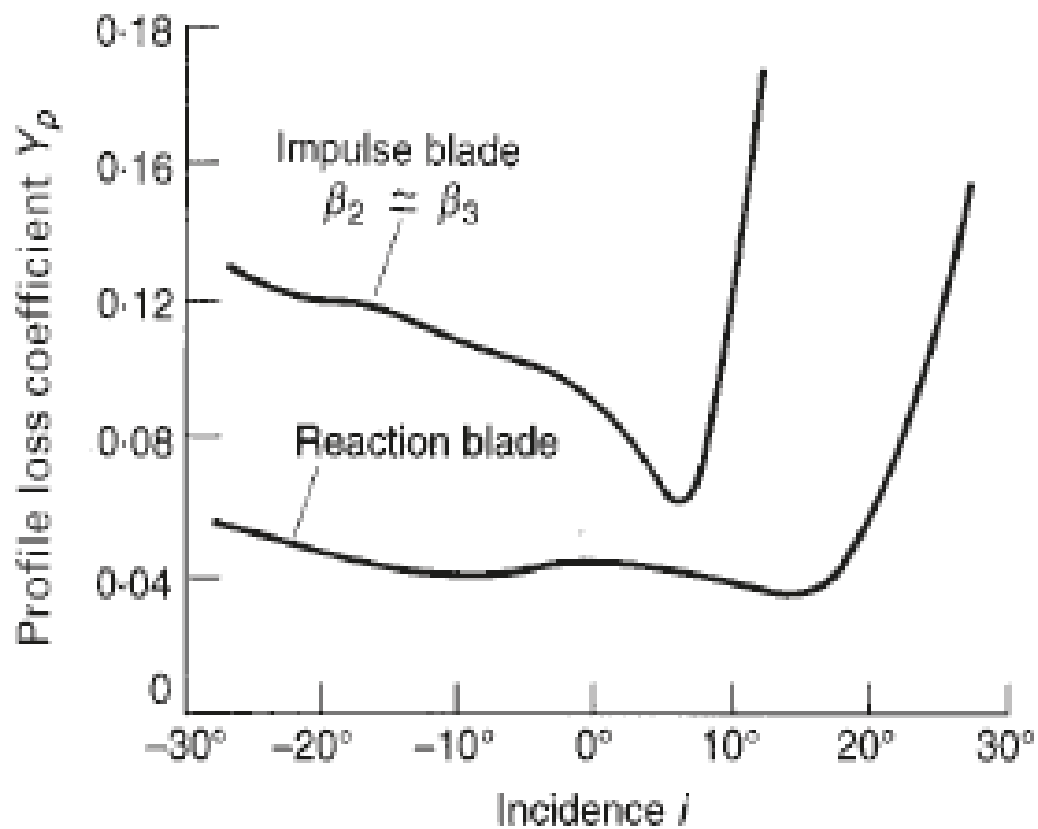
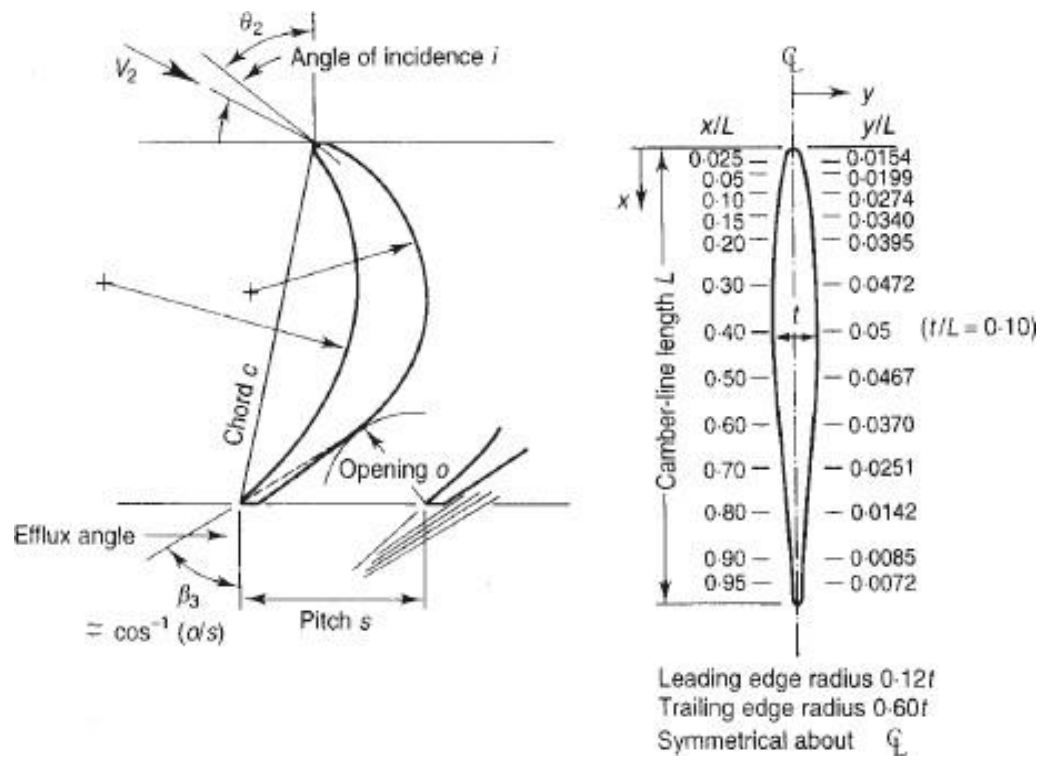


FIG. 5.12 Effect of incidence upon Y_p

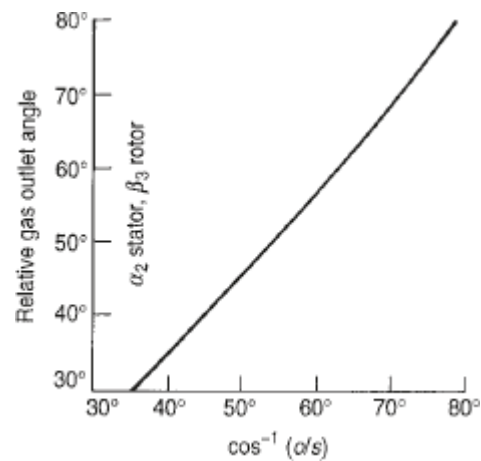


FIG. 5.13 Relation between gas and blade outlet angles

The pitch and chord have to be chosen with due regard to (a) the effect of the pitch/chord ratio (s/c) on the blade loss coefficient, (b) the effect of chord upon the aspect ratio (h/c), remembering that h has already been determined, (c) the effect of rotor blade chord on the blade stresses, and (d) the effect of rotor blade pitch upon the stresses at the point of attachment of the blades to the turbine disc. We will consider each effect in turn. FIG. 5.13 Relation between gas and blade outlet angles.

(a) 'Optimum' pitch/chord ratio

In section 5.4 (Fig. 5.20) cascade data are presented on profile loss coefficients Y_p , and from such data it is possible to obtain the useful design curves in Fig. 5.14. These curves suggest, as might be expected, that the greater the gas deflection required ($a_1 + a_2$ for a stator blade and $b_2 + b_3$ for a rotor blade), the smaller must be the 'optimum' s/c ratio to control the gas adequately. The adjective 'optimum' is in inverted commas because it is an optimum with respect to Y_p , not to the overall loss Y . The true optimum value of s/c could be found only by making a detailed estimate of stage performance (e.g. on the lines described in section 5.4) for several stage designs differing in s/c but otherwise similar. In fact the s/c value is not very critical.

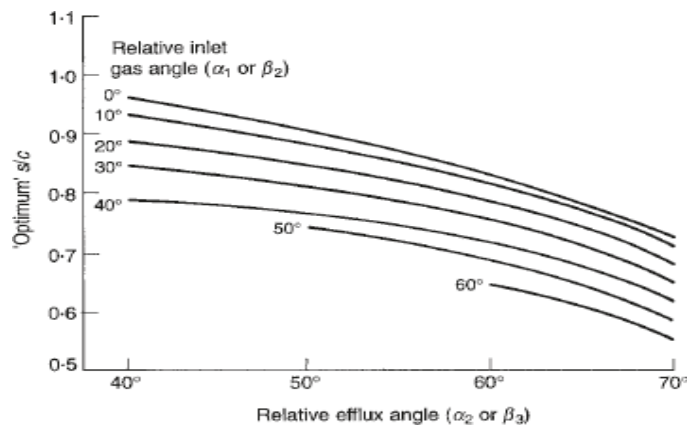


FIG. 5.14 'Optimum' pitch/chord ratio

(b) Aspect ratio (h/c)

The influence of aspect ratio is open to conjecture, but for our purpose it is sufficient to note that, although not critical, too low a value is likely to lead to secondary flow and tip clearance effects occupying an unduly large proportion of the blade height and so increasing Y_s for the nozzle row and $(Y_s + Y_k)$ for the rotor row. On the other hand, too high a value of h/c will increase the likelihood of vibration trouble: vibration characteristics are difficult to predict and depend on the damping provided by the method of attaching the blades to the turbine disc. A value of h/c between 3 and 4 would certainly be very satisfactory, and it would be unwise to use a value below 1.

(c) Rotor blade stresses

The stress analysis of rotor blades will be fully examined in Chapter 8, but at this stage it is essential to check that the stage design arrived at from an aerodynamic perspective is consistent with a permissible level of stress in the rotor blades. Simple approximate methods adequate for preliminary design calculations must be presented, because blade stresses have a direct impact on the stage design. There are three main sources of stress: (i) centrifugal tensile stress (the largest, but not necessarily the most important because it is a steady stress), (ii) gas bending stress (fluctuating as the rotor blades pass by the trailing edges of the nozzles) and (iii) centrifugal bending stress when the centroids of the blade cross-sections at different radii do not lie on a radial line (any torsional stress arising from this source is small enough to be neglected).

(d) Effect of pitch on the blade root fixing

The blade pitch s at mean diameter has been chosen primarily to be compatible with required values of s/c and h/c , and (via the chord) of permissible scb . A check must be made to see that the pitch is not so small that the blades cannot be attached safely to the turbine disc rim. Only in small turbines is it practicable to machine the blades and disc from a single forging, cast them integrally, or weld the blades to the rim, and Fig. 5.15 shows the commonly used fir tree root fixing which permits replacement of blades. The fir trees are made an easy fit in the rim, being prevented from axial movement only (e.g. by a lug on one side and peening on the other). When the turbine is running, the blades are held firmly in the serrations by centripetal force, but the slight freedom to move can provide a useful source of damping for unwanted vibration. The designer must take into account stress concentrations at the individual serrations, and manufacturing tolerances are extremely important; inaccurate matching can result in some of the serrations being unloaded at the expense of others. Failure may occur by the disc rim yielding at the base of the stubs left on the disc after broaching (at section x); by shearing or crushing of the serrations; or by tensile stress in the fir tree root itself. The pitch would be regarded as satisfactory when the root stresses can be optimized at a safe level. This need not detain us here because calculation of these centrifugal stresses is straightforward once the size of the blade, and therefore its mass, have been established by the design procedure we have outlined.

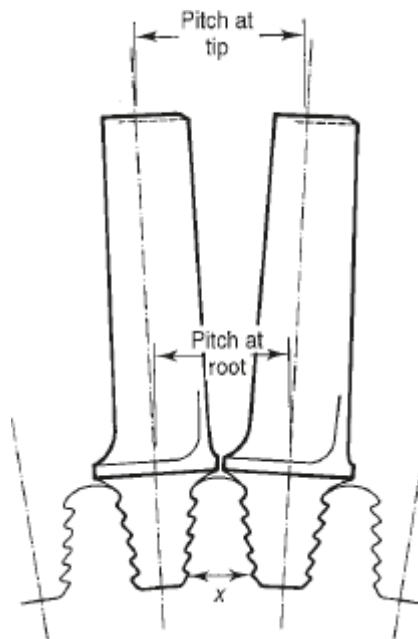


FIG. 5.15 'Fir tree' root

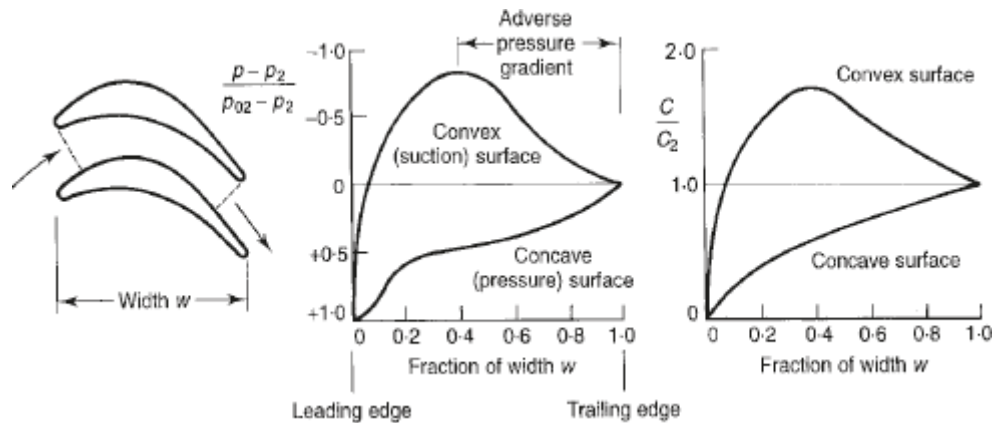


FIG. 5.16 Pressure and velocity distributions on a conventional turbine blade

Estimation of stage performance

The last step in the process of arriving at the preliminary design of a turbine stage is to check that the design is likely to result in values of nozzle loss coefficient and stage efficiency which were assumed at the outset. If not, the design calculations may be repeated with more probable values of loss coefficient and efficiency. When satisfactory agreement has been reached, the final design may be laid out on the drawing board and accurate stressing calculations can be performed.

Before proceeding to describe a method of estimating the design point performance of a stage, however, the main factors limiting the choice of design, which we have noted during the course of the worked example, will be summarized. The reason we considered a turbine for a turbojet engine was simply that we would thereby be working near those limits to keep size and weight to a minimum. The designer of an industrial gas turbine has a somewhat easier task: he or she will be using lower temperatures and stresses to obtain a longer working life, and this means lower mean blade speeds, more stages and much less stringent aerodynamic limitations. A power turbine, not mechanically coupled to the gas generator, is another case where much less difficulty will be encountered in arriving at a satisfactory solution. The choice of gear ratio between the power turbine and driven component is normally at the disposal of the turbine designer, and thus the rotational speed can be varied to suit the turbine, instead of the compressor as we have assumed here.

Limiting factors in turbine design

(a) Centrifugal stresses in the blades are proportional to the square of the rotational speed N and the annulus area: when N is fixed they place an upper limit on the annulus area.

(b) Gas bending stresses are (1) inversely proportional to the number of blades and blade section moduli, while being (2) directly proportional to the blade height and specific work output:

(1) The number of blades cannot be increased beyond a point set by blade fixing considerations, but the section moduli are roughly proportional to the cube of the blade chord which might be increased to reduce sgb. There is an aerodynamic limit on the

pitch/chord ratio, however, which if too small will incur a high loss coefficient (friction losses increase because a reduction in s/c increases the blade surface area swept by the gas).

(2) There remains the blade height, but reducing this while maintaining the same annulus area (and therefore the same axial velocity for the given mass flow) implies an increase in the mean diameter of the annulus. For a fixed N , the mean diameter cannot be increased without increasing the centrifugal disc stresses. There will also be an aerodynamic limit set by the need to keep the blade aspect ratio (h/c) and annulus radius ratio ($r_t > r_r$) at values which do not imply disproportionate losses due to secondary flows, tip clearance and friction on the annulus walls (say, not less than 2 and 1.2 respectively). The blade height might be reduced by reducing the annulus area (with the added benefit of reducing the centrifugal blade stresses) but, for a given mass flow, only by increasing the axial velocity. An aerodynamic limit on Ca will be set by the need to keep the maximum relative Mach number at the blade inlet (namely, at the root radius), and the Mach number at outlet from the stage, below the levels which mean high friction losses in the blading and jet pipe respectively.

(c) **Optimizing the design**, so that it just falls within the limits set by all these conflicting mechanical and aerodynamic requirements, will lead to an efficient turbine of minimum weight. If it proves to be impossible to meet one or more of the limiting conditions, the required work output must be split between two stages. The second design attempt would be commenced on the assumption that the efficiency is likely to be a maximum when the work, and hence the temperature drop, is divided equally between the stages.

(d) The velocity triangles, upon which the rotor blade section depends, are partially determined by the desire to work with an average degree of reaction of 50 per cent to obtain low blade loss coefficients and zero swirl for minimum loss in the jet pipe. To avoid the need for two stages in a marginal case, particularly if it means adding a bearing on the downstream side, it would certainly be preferable to design with a lower degree of reaction and some swirl. An aerodynamic limit on the minimum value of the reaction at mean diameter is set by the need to ensure some positive reaction at the blade root radius.

Turbine blade cooling

It has always been the practice to pass a quantity of cooling air over the turbine disc and blade roots. When speaking of the cooled turbine, however, we mean the application of a substantial quantity of coolant to the nozzle and rotor blades themselves. Despite potential aerodynamic losses due to coolant injection and from extraction of cooling flow from the compressor, the benefits of turbine cooling are still substantial even when these additional losses introduced by the cooling system are taken into account. Figure 5.25 illustrates the methods of blade cooling that have received serious attention and research effort in the last 25 years. Apart from the use of spray cooling for thrust boosting in turbojet engines, the liquid systems have not proved to be practicable in modern turbofan engines. There are difficulties associated with channelling the liquid to and from the blades—whether as primary coolant for forced convection or free

convection open thermosyphon systems, or as secondary coolant for closed thermosyphon systems. It is impossible to eliminate corrosion or the formation of deposits in open systems, and very difficult to provide adequate secondary surface cooling area at the base of the blades for closed systems. The only method used successfully in production engines has been internal, forced convection, air cooling. With 1.592 per cent of the air mass flow used for cooling per blade row, the blade temperature can be reduced by between 200 and 300°C. Using current alloys, this permits turbine inlet temperatures of more than 1650 K to be used with some military engines pushing over 2000 K. The blades are either cast, using cores to form the cooling passages, or forged with holes of any desired shape produced by electrochemical or laser drilling. As shown, the blade internals are cooled with multiple serpentine cooling passages and the cooling flow is ejected through film cooling holes at the blade leading edge, so-called 'shower head' cooling, as well as through film cooling holes on the pressure and suction surfaces and the tip cavity of the airfoil, and finally through trailing edge slots.

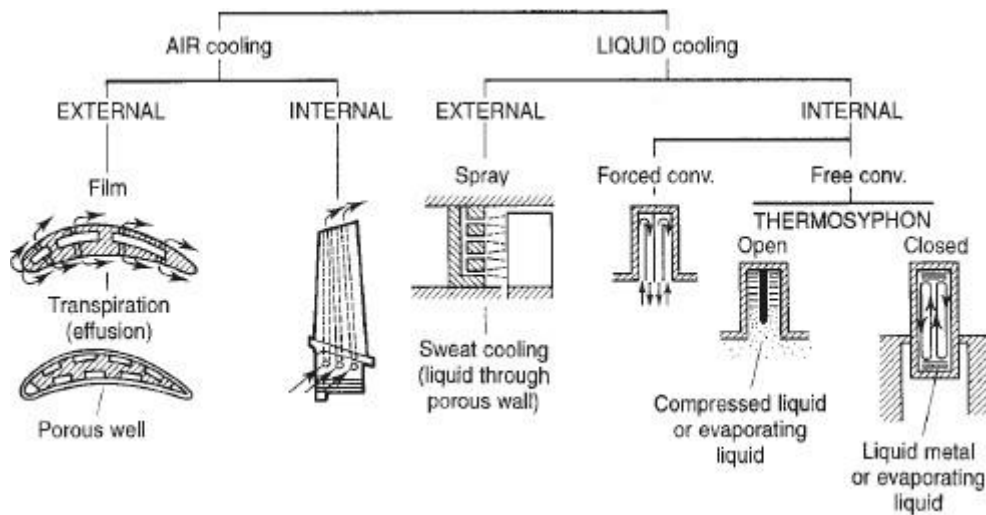


FIG. 5.25 Methods of blade cooling

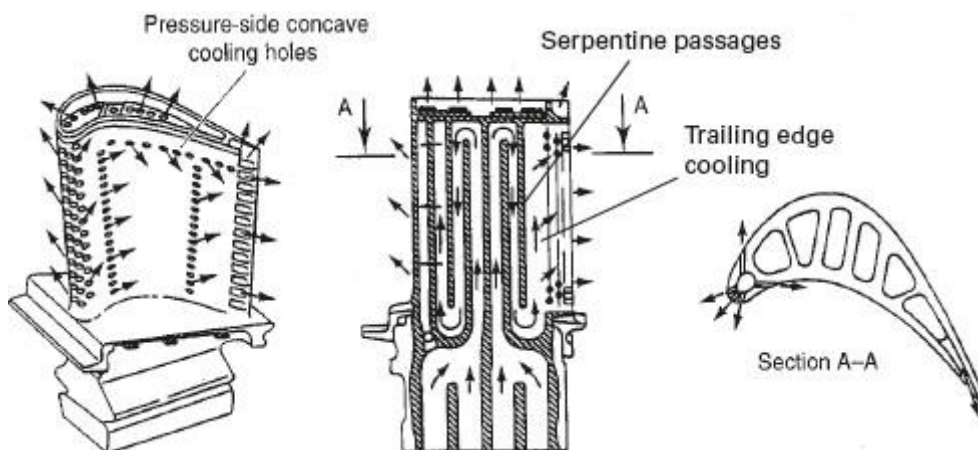


FIG. 5.26 Cooled turbine rotor blade [courtesy of GE Energy]

Figure 5.27(a) illustrates the principal features of nozzle blade cooling. The air is introduced in

such a way as to provide jet impingement cooling of the inside surface of the very hot leading edge. A large fraction of the spent air leaves through cooling holes in the blade surface (to provide film cooling), and the remainder of the air exits at the trailing edge. Trailing edge cooling is important, as this is such a thin material with high heat load. The spent air leaves through slots or holes in the blade surface (to provide some film cooling) or in the trailing edge. Figure 5.27(b) depicts a modern cast nozzle airfoil with intricate inserts forming the cooling passages. It also shows the way the annulus walls are cooled. The introduction of large high efficiency combined cycles resulted in several manufacturers developing steam-cooled systems, to reduce the significant parasitic loss due to air cooling. Most restricted their activities to cooling combustors and nozzles.

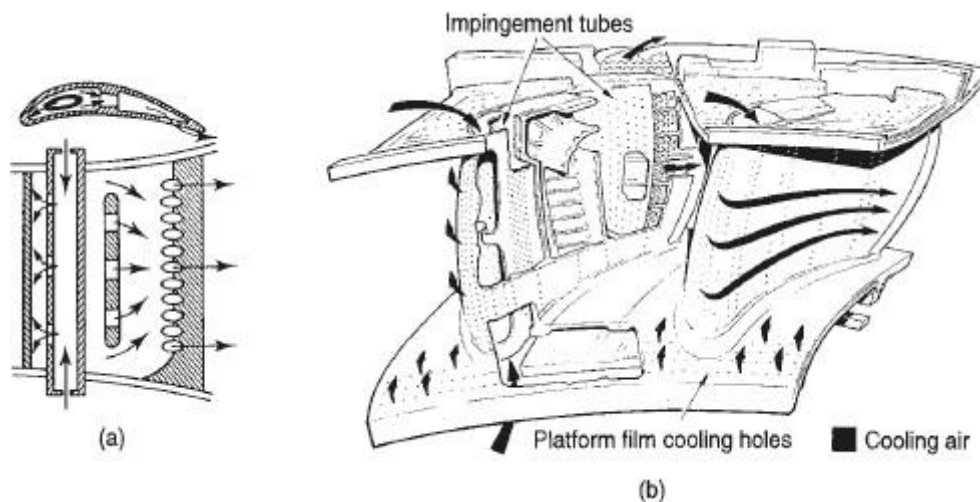


FIG. 5.27 Turbine nozzle cooling [(b) courtesy Rolls-Royce plc]

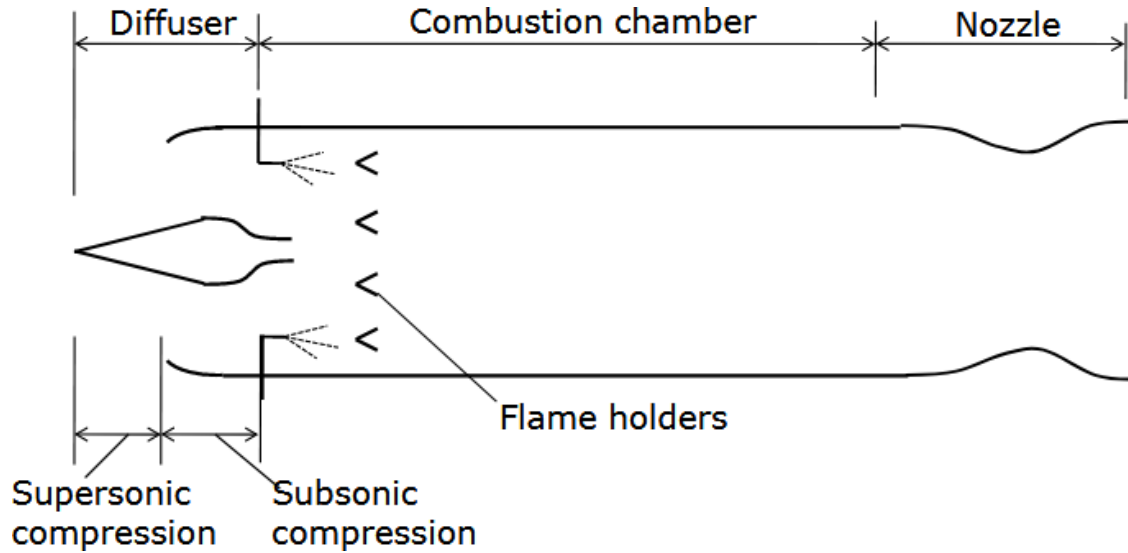
The second aspect is the effect on the cycle efficiency of losses incurred by the cooling process: a pertinent question is whether it is advantageous overall to sacrifice some aerodynamic efficiency to reduce such losses. The sources of loss are as follows:

- (a) There is a direct loss of turbine work due to the reduction in turbine mass flow.
- (b) The expansion is no longer adiabatic; and furthermore there will be a negative reheat effect in multi-stage turbines.
- (c) There is a pressure loss, and a reduction in enthalpy, due to the mixing of spent cooling air with the main gas stream at the blade tips. (This has been found to be partially offset by a reduction in the normal tip leakage loss.)
- (d) Some 'pumping' work is done by the blades on the cooling air as it passes radially outwards through the cooling passages.
- (e) When considering cooled turbines for cycles with heat-exchange, account must be taken of the reduced temperature of the gas leaving the turbine which makes the heat-exchanger less effective.

Losses (a) and (e) can be incorporated directly into any cycle calculation, while the effect of (b), (c) and (d) can be taken into account by using a reduced value of turbine efficiency. One assessment of the latter [Ref. (13)] suggests that the turbine efficiency is likely to be reduced by from 1 to 3 per cent of the uncooled efficiency, the lower value referring to near-impulse designs and the higher to 50 per cent reaction designs. The estimate for reaction

Ramjet

Ramjet is the simplest of all the air breathing engines. It consists of a diffuser, combustion chamber and a nozzle. Ramjets are most efficient when operated at supersonic speeds. When air is decelerated from a high Mach number to a low subsonic Mach number, it results in substantial increase in pressure and temperature. Hence ramjets do not need compressors and consequently no turbines as well.



Schematic of typical ramjet engine

UNIT IV

SOLID ROCKET PROPULSION

INTRODUCTION

Solid propellant motors are the simplest of all rocket designs. They consist of a casing, usually steel, filled with a mixture of solid compounds (fuel and oxidizer) that burn at a rapid rate, expelling hot gases from a nozzle to produce thrust. When ignited, a solid propellant burns from the center out towards the sides of the casing. The shape of the center channel determines the rate and pattern of the burn, thus providing a means to control thrust. Unlike liquid propellant engines, solid propellant motors cannot be shut down. Once ignited, they will burn until all the propellant is exhausted.

Salient features of solid propellant rockets:

There are two families of solids propellants: homogeneous and composite. Both types are dense, stable at ordinary temperatures, and easily storable.

Homogeneous propellants are either simple base or double base. A simple base propellant consists of a single compound, usually nitrocellulose, which has both an oxidation capacity and a reduction capacity. Double base propellants usually consist of nitrocellulose and nitroglycerine, to which a plasticiser is added. Homogeneous propellants do not usually have specific impulses greater than about 210 seconds under normal conditions. Their main asset is that they do not produce traceable fumes and are, therefore, commonly used in tactical weapons. They are also often used to perform subsidiary functions such as jettisoning spent parts or separating one stage from another.

Modern composite propellants are heterogeneous powders (mixtures) that use a crystallized or finely ground mineral salt as an oxidizer, often ammonium perchlorate, which constitutes between 60% and 90% of the mass of the propellant. The fuel itself is generally aluminum. The propellant is held together by a polymeric binder, usually polyurethane or polybutadienes, which is also consumed as fuel. Additional compounds are sometimes included, such as a catalyst to help increase the burning rate, or other agents to make the powder easier to manufacture. The final product is rubber like substance with the consistency of a hard rubber eraser.

Composite propellants are often identified by the type of polymeric binder used. The two most common binders are polybutadiene acrylic acid acrylonitrile (PBAN) and hydroxy-terminator polybutadiene (HTPB). PBAN formulations give a slightly higher specific impulse, density, and burn rate than equivalent formulations using HTPB. However, PBAN propellant is the more difficult to mix and process and requires an elevated curing temperature. HTPB binder is stronger and more flexible than PBAN binder. Both PBAN and HTPB formulations result in propellants that deliver excellent performance, have good mechanical properties, and offer potentially long burn times.

Solid propellant motors have a variety of uses. Small solids often power the final stage of a launch vehicle, or attach to payloads to boost them to higher orbits. Medium solids such as the

Payload Assist Module (PAM) and the Inertial Upper Stage (IUS) provide the added boost to place satellites into geosynchronous orbit or on planetary trajectories.

The Titan, Delta, and Space Shuttle launch vehicles use strap-on solid propellant rockets to provide added thrust at liftoff. The Space Shuttle uses the largest solid rocket motors ever built and flown. Each booster contains 500,000 kg (1,100,000 pounds) of propellant and can produce up to 14,680,000 Newtons (3,300,000 pounds) of thrust.

SELECTION CRITERIA OF SOLID PROPELLANTS:

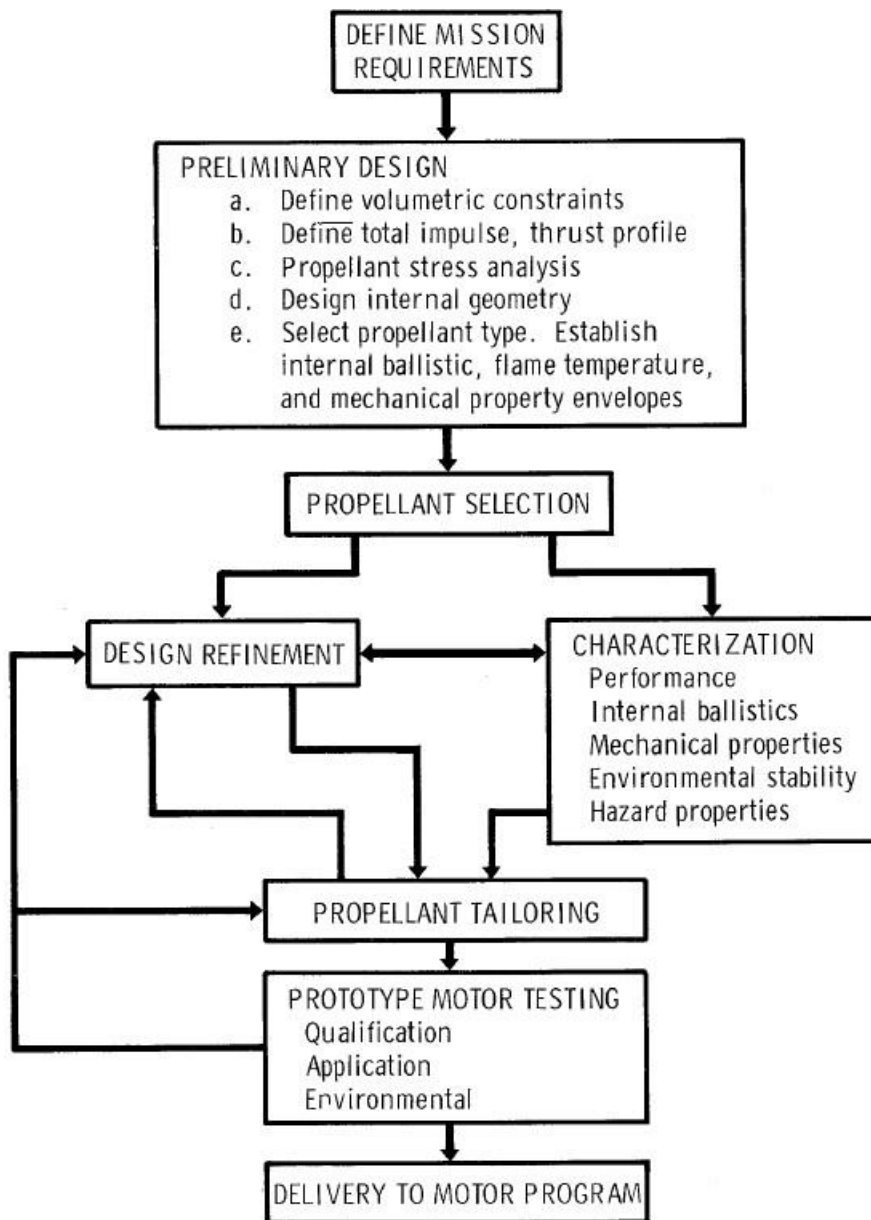


Figure 3.1 propellant selection and tailoring in design criteria

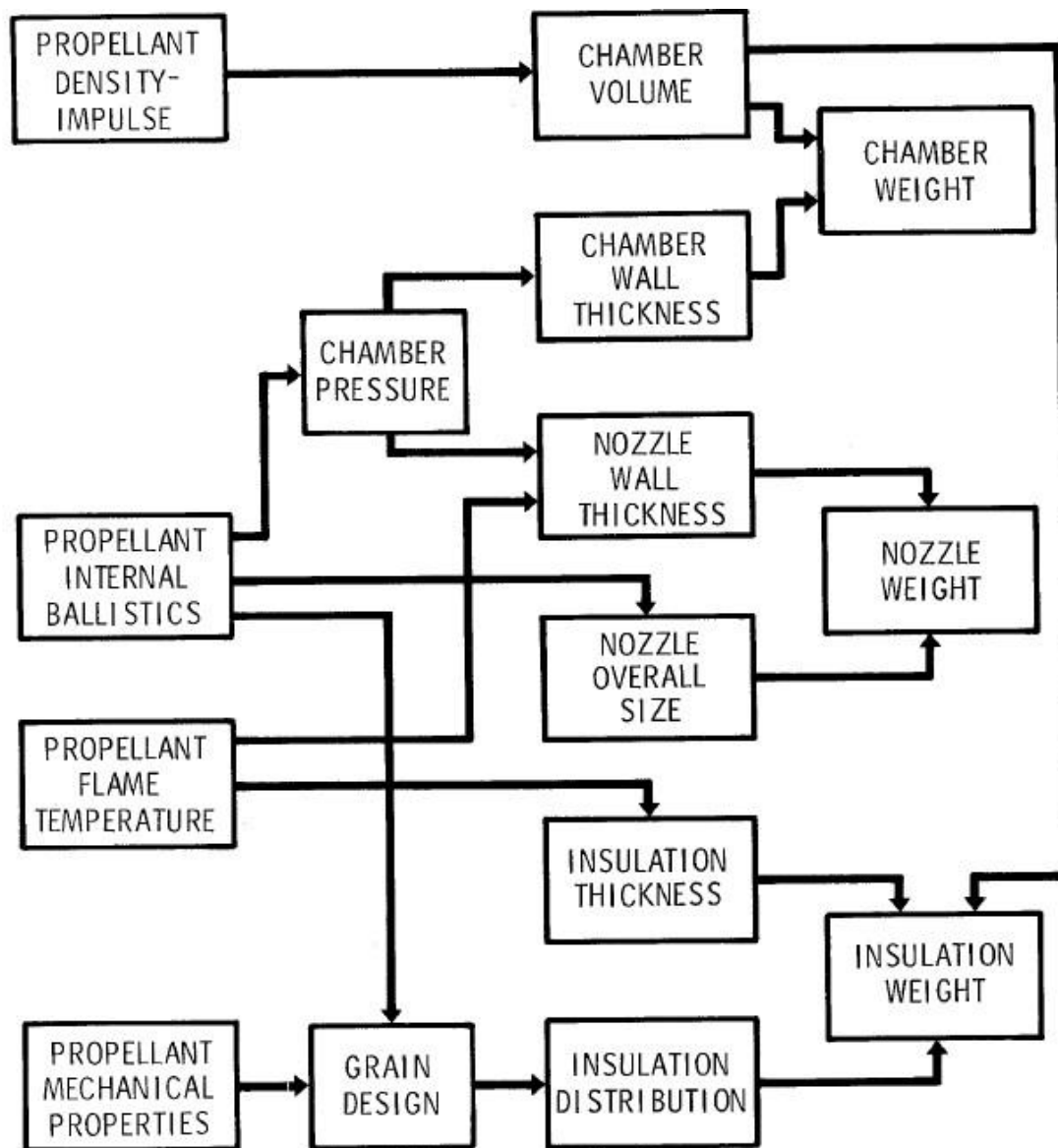


Figure 3.2: influence of propellant properties

ESTIMATION OF SOLID PROPELLANT ADIABATIC FLAME TEMPERATURE:

Adiabatic Flame Temperature: For a combustion process that takes place adiabatically with no shaft work, the temperature of the products is referred to as the adiabatic flame temperature. This is the maximum temperature that can be achieved for given reactants. Heat transfer, incomplete combustion, and dissociation all result in lower temperature. The maximum adiabatic flame temperature for a given fuel and oxidizer combination occurs with a stoichiometric mixture (correct proportions such that all fuel and all oxidizer are consumed). The amount of excess air can be tailored as part of the design to control the adiabatic flame temperature. The considerable distance between present temperatures in a gas turbine engine and the maximum adiabatic flame temperature at stoichiometric conditions is shown in Figure , based on a compressor exit temperature of 1200°F (922 K).

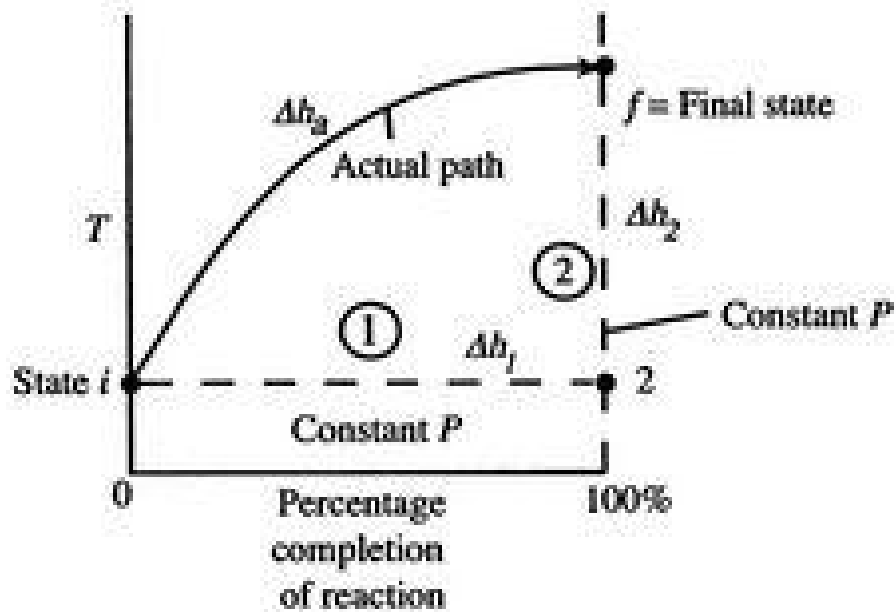


Figure 3.3: Schematic of adiabatic flame temperature

An initial view of the concept of adiabatic flame temperature is provided by examining two reacting gases, at a given pressure, and asking what the end temperature is. The process is shown schematically in Figure 3.3, where temperature is plotted versus the percentage completion of the reaction. The initial state is i and the final state is f , with the final state at a higher temperature than the initial state. The solid line in the figure shows a representation of the "actual" process.

To see how we would arrive at the final completion state the dashed lines break the state of reaction change into two parts. Process (1) is reaction at constant T and P . To carry out such a process, we would need to extract heat. Suppose the total amount of heat extracted per unit mass is q_1 . The relation between the enthalpy changes in Process (1) is

$$h_2 - h_i = -q_1 = (h_f^\circ)_{\text{unit mass}},$$

where q_1 is the "heat of reaction."

For Process (2), we put this amount back into the products to raise their temperature to the final level. For this process,

$$h_f - h_2 = q_1,$$

or, if we can approximate the specific heat as constant (using some appropriate average value)

$$c_{p,avg}(T_f - T_2) = q_1.$$

For the overall process there is no work done and no heat exchanged so that the difference in enthalpy between initial and final states is zero:

$$\Delta h_1 + \Delta h_2 = \Delta h_{adiabatic} = 0.$$

The temperature change during this second process is therefore given by (approximately)

$$(T_f - T_2) = \frac{q_1}{c_{p,avg}} = \frac{|(h_f^\circ)_{unit\ mass}|}{c_{p,avg}}. \quad (1)$$

The value of the adiabatic flame temperature given in Equation (1) is for 100% completion of the reaction. In reality, as the temperature increases, the tendency is for the degree of reaction to be less than 100%. For example, for the combustion of hydrogen and oxygen, at high temperatures the combustion product (water) dissociates back into the simpler elemental reactants. The degree of reaction is thus itself a function of temperature that needs to be computed. We used this idea in discussing the stoichiometric ramjet, when we said that the maximum temperature was independent of flight Mach number and hence of inlet stagnation temperature. It is also to be emphasized that the idea of a constant (average) specific heat, $c_{p,avg}$, is for illustration and not inherently part of the definition of adiabatic flame temperature.

PROPELLANT GRAIN DESIGN CONSIDERATIONS:

The rocket motor's operation and design depend on the combustion characteristics of the propellant, its burning rate, burning surface, and grain geometry. The branch of applied science describing these is known as internal ballistics; The burning surface of a propellant grain recedes in a direction essentially perpendicular to the surface. The rate of regression, usually expressed in cm/sec, mm/sec, or in./sec, is the burning rate r . In Fig. 3.5 we can visualize the change of the grain geometry by drawing successive burning surfaces with a constant time interval between adjacent surface contours. Figure 3.5 shows this for a two-dimensional grain with a central cylindrical cavity with five slots. Success in rocket motor design and development depends significantly on knowledge of burning rate behavior of the selected propellant under all motor operating conditions and design limit conditions.

Burning rate is a function of the propellant composition. For composite propellants it can be increased by changing the propellant characteristics:

1. Add a burning rate catalyst, often called burning rate modifier (0.1 to 3.0% of propellant) or increase percentage of existing catalyst.
2. Decrease the oxidizer particle size.
3. Increase oxidizer percentage.
4. Increase the heat of combustion of the binder and/or the plasticizer.
5. Imbed wires or metal staples in the propellant.

Aside from the propellant formulation and propellant manufacturing process, burning rate in a full-scale motor can be increased by the following:

1. Combustion chamber pressure.
2. Initial temperature of the solid propellant prior to start.
3. Combustion gas temperature.
4. Velocity of the gas flow parallel to the burning surface.

5. Motor motion (acceleration and spin-induced grain stress).

The grain is the shaped mass of processed solid propellant inside the rocket motor. The propellant material and geometrical configuration of the grain determine the motor performance characteristics. The propellant grain is a cast, molded, or extruded body and its appearance and feel is similar to that of hard rubber or plastic. Once ignited, it will burn on all its exposed surfaces to form hot gases that are then exhausted through a nozzle. A few rocket motors have more than one grain inside a single case or chamber and very few grains have segments made of different propellant composition (e.g., to allow different burning rates). However, most rockets have a single grain. There are two methods of holding the grain in the case, as seen in Fig. 3.4. Cartridge-loaded or freestanding grains are manufactured separately from the case (by extrusion or by casting into a cylindrical mold or cartridge) and then loaded into or assembled into the case. In case-bonded grains the case is used as a mold and the propellant is cast directly into the case and is bonded to the case or case insulation. Free-standing grains can more easily be replaced loaded) and a case-bonded grain.

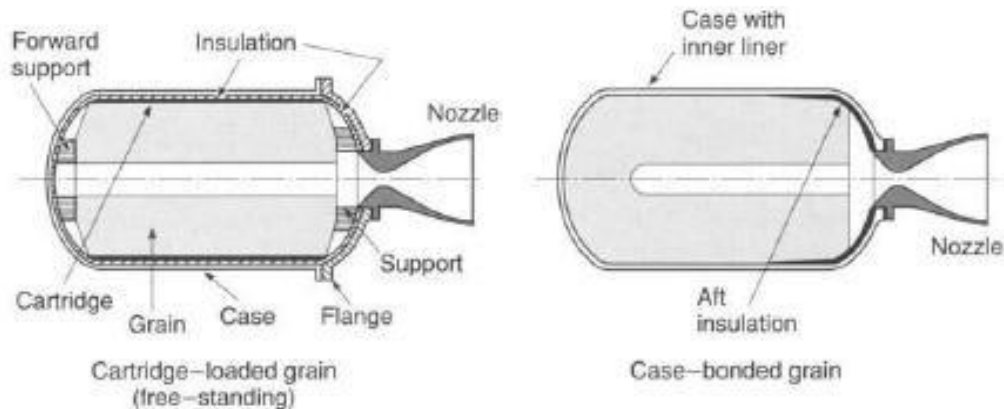


Fig. 3.4 Simplified schematic diagrams of a free-standing (or cartridge-loaded) and a case-bonded grain.

If the propellant grain has aged excessively. Aging is discussed in the next chapter. Cartridge-loaded grains are used in some small tactical missiles and a few medium-sized motors. They often have a lower cost and are easier to inspect. The case-bonded grains give a somewhat better performance, a little less inert mass (no holding device, support pads, and less insulation), a better volumetric loading fraction, are more highly stressed, and often somewhat more difficult and expensive to manufacture. Today almost all larger motors and many tactical missile motors use case bonding.

EROSIVE BURNING IN SOLID PROPELLANT ROCKETS

Definitions and terminology important to grains include:

Configuration: The shape or geometry of the initial burning surfaces of a grain as it is intended to operate in a motor.

Cylindrical Grain: A grain in which the internal cross section is constant along the axis regardless of perforation shape.

Neutral Burning: Motor burn time during which thrust, pressure, and burning

surface area remain approximately constant, typically within about +15%. Many grains are neutral burning.

Perforation: The central cavity port or flow passage of a propellant grain; its cross section may be a cylinder, a star shape, etc.

Progressive Burning: Burn time during which thrust, pressure, and burning surface area increase.

Regressive Burning: Burn time during which thrust, pressure, and burning surface area decrease

Sliver: Unburned propellant remaining (or lost--that is, expelled through the nozzle) at the time of web burnout.

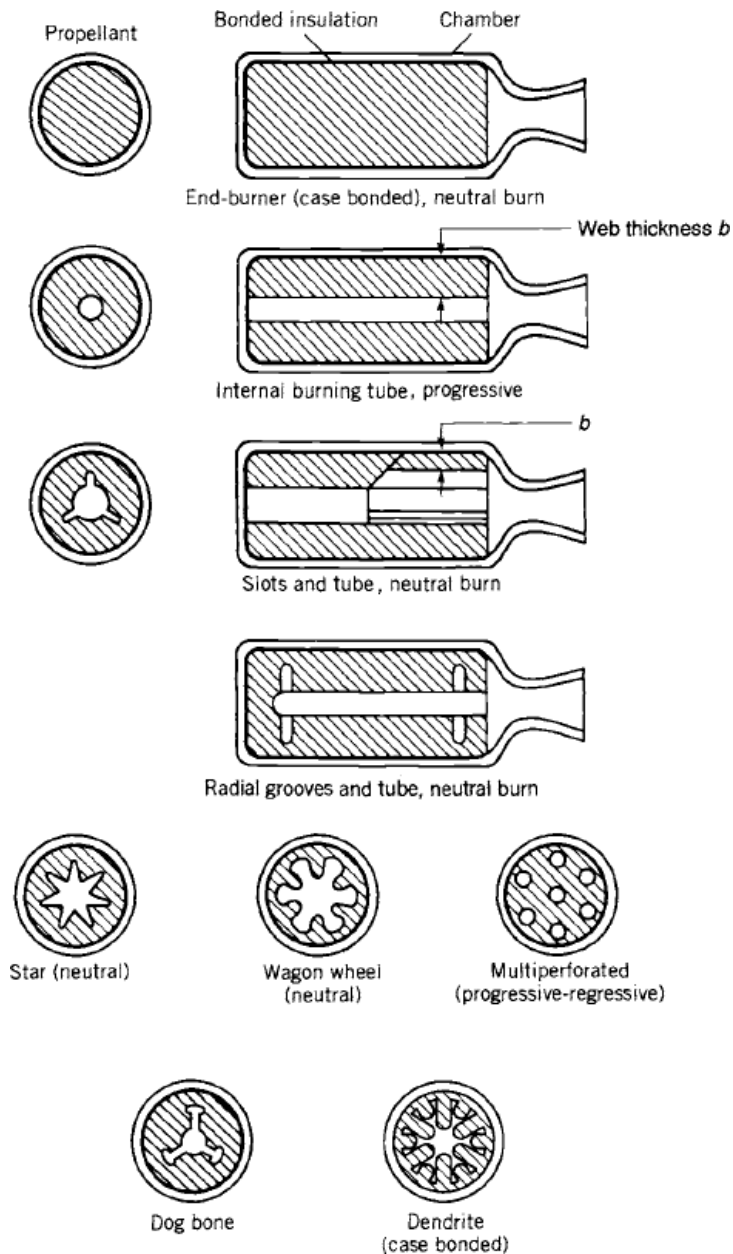


Figure 3.5 classification of grain according to their pressure-time

A grain has to satisfy several interrelated requirements:

1. From the flight mission one can determine the rocket motor requirements. They have to be defined and known before the grain can be designed. They are usually established by the vehicle designers. This can include total impulse, a desired thrust-time curve and a tolerance thereon, motor mass, ambient temperature limits during storage and operation, available vehicle volume or envelope, and vehicle accelerations caused by vehicle forces (vibration, bending, aerodynamic loads, etc.).
2. The grain geometry is selected to fit these requirements; it should be compact and use the available volume efficiently, have an appropriate burn surface versus time profile to match the desired thrust-time curve, and avoid or predictably control possible erosive burning. The remaining unburned propellant slivers, and often also the shift of the center of gravity during burning, should be minimized. This selection of the geometry can be complex.
3. The propellant is usually selected on the basis of its performance capability (e.g., characteristic velocity), mechanical properties (e.g., strength), ballistic properties (e.g., burning rate), manufacturing characteristics, exhaust plume characteristics, and aging properties. If necessary, the propellant formulation may be slightly altered or "tailored" to fit exactly the required burning time or grain geometry.
4. The structural integrity of the grain, including its liner and/or insulator, must be analyzed to assure that the grain will not fail in stress or strain under all conditions of loading, acceleration, or thermal stress. The grain geometry can be changed to reduce excessive stresses.
5. The complex internal cavity volume of perforations, slots, ports, and fins increases with burning time. These cavities need to be checked for resonance, damping, and combustion stability.
6. The processing of the grain and the fabrication of the propellant should be simple and low cost.

COMBUSTION INSTABILITY:

There seem to be two types of combustion instability: a set of acoustic resonances or pressure oscillations, which can occur with any rocket motor, and a vortex shedding phenomenon, which occurs only with particular types of grains.

Acoustic Instabilities: When a solid propellant rocket motor experiences unstable combustion, the pressure in the interior gaseous cavities (made up by the volume of the port or perforations, fins, slots, conical or radial groves) oscillates by at least 5% and often by more than 30% of the chamber pressure. When instability occurs, the heat transfer to the burning surfaces, the nozzle, and the insulated case walls is greatly increased; the burning rate, chamber pressure, and thrust usually increase; but the burning duration is thereby decreased. The change in the thrust-time profile causes significant changes in the flight path, and at times this can lead to failure of the mission. If prolonged and if the vibration energy level is high, the instability can cause damage to the hardware, such as overheating the case and causing a nozzle or case failure. Instability is a condition that should be avoided and must be carefully investigated and remedied if it occurs during a motor development program. Final designs of motors must be free of such instability.

There are fundamental differences with liquid propellant combustion behavior. In liquid propellants there is fixed chamber geometry with a rigid wall; liquids in feed systems and in injectors that are not part of the oscillating gas in the combustion chamber can interact strongly with the pressure fluctuations. In solid propellant motors the geometry of the oscillating cavity increases in size as burning proceeds and there are stronger damping factors, such as solid particles and energy-absorbing viscoelastic materials. In general, combustion instability problems do not occur frequently or in every motor development, and, when they do occur, it is rarely the cause for a drastic sudden motor failure or disintegration. Nevertheless, drastic failures have occurred. Undesirable oscillations in the combustion cavity propellant rocket motors is a continuing problem in the design, development, production, and even long-term (10 yr) retention of solid rocket missiles. While acoustically "softer" than a liquid rocket combustion chamber, the combustion cavity of a solid propellant rocket is still a low-loss acoustical cavity containing a very large acoustical energy source, the combustion process itself. A small fraction of the energy released by combustion is more than sufficient to drive pressure vibrations to an unacceptable level.

Combustion instability can occur spontaneously, often at some particular time during the motor burn period, and the phenomenon is usually repeatable in identical motors. Both longitudinal and transverse waves (radial and tangential) can occur. The pressure oscillations increase in magnitude, and the thrust and burning rate also increase. The frequency seems to be a function of the cavity geometry, propellant composition, pressure, and internal flame field. As the internal grain cavity is enlarged and local velocities change, the oscillation often abates and disappears. The time and severity of the combustion vibration tend to change with the ambient grain temperature prior to motor operation.

For a simple grain with a cylindrical port area, the resonant transverse mode oscillations (tangential and radial) correspond roughly for liquid propellant thrust chambers. The longitudinal or axial modes, usually at a lower frequency, are an acoustic wave traveling parallel to the motor axis between the forward end of the perforation and the convergent nozzle section. Harmonic frequencies of these basic vibration modes can also be excited. The internal cavities can become very complex and can include igniter cases, movable as well as submerged nozzles, fins, cones, slots, star-shaped perforations, or other shapes, as described in the section on grain geometry, determination of the resonant frequencies of complex cavities is not always easy. Furthermore, the geometry of the internal resonating cavity changes continually as the burning propellant surfaces recede; as the cavity volume becomes larger, the transverse oscillation frequencies are reduced.

The bulk mode, also known as the Helmholtz mode, L^* mode, or chuffing mode, is not a wave mode as described above. It occurs at relatively low frequencies (typically below 150 Hz and sometimes below 1 Hz), and the pressure is essentially uniform throughout the volume. The unsteady velocity is close to zero, but the pressure rises and falls. It is the gas motion (in and out of the nozzle) that corresponds to the classical Helmholtz resonator mode, similar to exciting a tone when blowing across the open mouth of a bottle. It occurs at low values of L^* , sometimes during the ignition period, and disappears when the motor internal volume becomes larger or the chamber pressure becomes higher. Chuffing is the periodic low frequency discharge of a bushy, unsteady flame of short duration (typically less than 1 sec) followed by periods of no visible flame, during which slow outgassing and vaporization of the solid propellant accumulates hot gas in the chamber. The motor experiences spurts of combustion and consequent pressure buildup followed by periods of nearly ambient pressure. This dormant period can extend for a fraction of a second to a few seconds.

A useful method of visualizing unstable pressure waves is shown in Figs. It consists of a series of Fourier analyses of the measured pressure vibration spectrum, each taken at a different time in the burning duration and displayed at successive vertical positions on a time scale, providing a map of amplitude versus frequency versus burning time. This figure shows a low-frequency axial mode and two tangential modes, whose frequency is reduced in time by the enlargement of the cavity; it also shows the timing of different vibrations, and their onset and demise.

The initiation or triggering of a particular vibration mode is still not well understood but has to do with energetic combustion at the propellant surface.

A sudden change in pressure is known to be a trigger, such as when a piece of broken-off insulation or unburned propellant flows through the nozzle and temporarily blocks all or a part of the nozzle area (causing a momentary pressure rise).

The shifting balance between amplifying and damping factors changes during the burning operation and this causes the growth and also the abatement of specific modes of vibration. The response of a solid propellant describes the change in the gas mass production or energy release at the burning surface when it is stimulated by pressure perturbations. When a momentary high pressure peak occurs on the surface, it increases the instantaneous heat transfer and thus the burning rate, causing the mass flow from that surface to also increase. Velocity perturbations along the burning surface are also believed to cause changes in mass flow. Phenomena that contribute to amplifying the vibrations, or to gains in the acoustic energy, are:

1. The dynamic response of the combustion process to a flow disturbance or the oscillations in the burning rate. This combustion response can be determined from tests of T-burners. The response function depends on the frequency of these perturbations and the propellant formulation. The

combustion response may not be in a phase with the disturbance. The effects of boundary layers on velocity perturbations have been investigated.

2. The interactions of flow oscillation with the main flow, similar to the basis for the operation of musical wind instruments or sirens.
3. The fluid dynamic influence of vortices.

Phenomena that contribute to a diminishing of vibration or to damping are energy-absorbing processes; they include the following:

1. Viscous damping in the boundary layers at the walls or propellant surfaces.
2. Damping by particles or droplets flowing in an oscillating gas/vapor flow is often substantial. The particles accelerate and decelerate by being "dragged" along by the motion of the gas, a viscous flow process that absorbs energy. The attenuation for each particular vibration frequency is an optimum at a particular size of particles; high damping for low frequency oscillation (large motors) occurs with relatively large solid particles (8 to 20 μm); for small motors or high-frequency waves the best damping occurs with small particles (2 to 6 μm). The attenuation drops off sharply if the particle size distribution in the combustion gas is not concentrated near the optimum for damping.
3. Energy from longitudinal and mixed transverse/longitudinal waves is lost out through the exhaust nozzle. Energy from purely transverse waves does not seem to be damped by this mechanism.
4. Acoustic energy is absorbed by the viscoelastic solid propellant, insulator, and the motor case; its magnitude is difficult to estimate.

The propellant characteristics have a strong effect on the susceptibility to instability. Changes in the binder, particle-size distribution, ratio of oxidizer to fuel, and burn-rate catalysts can all affect stability, often in ways that are not predictable. All solid propellants can experience instability. As a part of characterizing a new or modified propellant (e.g., determining its ballistic, mechanical, aging, and performance characteristics), many companies now also evaluate it for its stability behavior, as described below.

STRAND BURNER AND T-BURNER: In contrast with liquid rocket technology, an accepted combustion stability rating procedure does not now exist for full-scale solid rockets. Undertaking stability tests on large full-scale flight-hardware rocket motors is expensive, and therefore lower-cost methods, such as subscale motors, T-burners, and other test equipment, have been used to assess motor stability. The best known and most widely used method of gaining combustion stability-related data is the use of a T-burner, an indirect, limited method that does not use a full-scale motor. Standard T-burner has a 1.5-in. internal diameter double-ended cylindrical burner vented at its midpoint.

Venting can be through a sonic nozzle to the atmosphere or by a pipe connected to a surge tank which maintains a constant level of pressure in the burner cavity. T-burner design and usage usually concentrate on the portion of the frequency spectrum dealing with the transverse oscillations expected in a full-scale motor. The desired acoustical frequency, to be imposed on the propellant charge as it burns, determines the burner length (distance between closed ends).

The nozzle location, midway between the ends of the burner, minimizes attenuation of fundamental longitudinal mode oscillations (in the propellant grain cavity). Theoretically, an acoustic pressure node exists at the center and antinodes occur at the ends of the cavity. Acoustic velocity nodes are out of phase with pressure waves and occur at the ends of the burner. Propellant charges are often in the shape of discs or cups cemented to the end faces of the burner. The gas velocity in the burner cavity is kept intentionally low (Mach 0.2 or less) compared with the velocity in a full-scale motor. This practice minimizes the influence of velocity-coupled energy waves and allows the influence of pressure-coupled waves to be more clearly recognized.

Use of the T-burner for assessing the stability of a full-scale solid rocket presupposes valid theoretical models of the phenomena occurring in both the T-burner and the actual rocket motor; these theories are still not fully validated.

In addition to assessing solid rocket motor combustion stability, the T burner also is used to evaluate new propellant formulations and the importance of seemingly small changes in ingredients, such as a change in aluminum powder particle size and oxidizer grind method.

Once instability has been observed or predicted in a given motor, the motor design has to fix the problem. There is no sure method for selecting the right remedy, and none of the cures suggested below may work. The usual alternatives are:

1. Changing the grain geometry to shift the frequencies away from the undesirable values. Sometimes, changing fin locations, port cross-section profile, or number of slots has been successful.
2. Changing the propellant composition. Using aluminum as an additive has been most effective in curing transverse instabilities, provided that the particle-size distribution of the aluminum oxide is favorable to optimum damping at the distributed frequency. Changing size distribution and using other particulates (Zr, Al₂O₃, or carbon particles) has been effective in some cases. Sometimes changes in the binder have worked.
3. Adding some mechanical device for attenuating the unsteady gas motions or changing the natural frequency of cavities. Various inert resonance rods, baffles, or paddles have been added, mostly as a fix to an existing motor with observed instability. They can change the resonance frequencies of the cavities, introduce additional viscous surface losses, but also cause extra inert mass and potential problems with heat transfer or erosion.

Combustion instability has to be addressed during the design process, usually through a combination of some mathematical simulation, understanding similar problems in other motors, studies of possible changes, and supporting experimental work (e.g., T-burners, measuring particle-size distribution). Most solid propellant rocket companies have in-house two and three-dimensional computer programs to calculate the likely acoustic modes (axial, tangential, radial, and combinations of these) for a given grain/motor, the initial and intermediate cavity geometries, and the combustion gas properties calculated from thermochemical analysis. Data on combustion response (dynamic burn rate behavior) and damping can be obtained from T-burner tests. Data on particle sizes can be estimated from prior experience or plume measurements.

Estimates of nozzle losses, friction, or other damping need to be included. Depending on the balance between gain and damping, it may be possible to arrive at conclusions on the grain's propensity to instability for each specific instability mode that is analyzed. If unfavorable, either the grain geometry or the propellant usually has to be modified. If favorable, full-scale motors have to be built and tested to validate the predicted stable burning characteristics. There is always a trade-off between the amount of work spent on extensive analysis, subscale experiments and computer programs (which will not always guarantee a stable motor), and taking a chance that a retrofit will be needed after full-scale motors have been tested. If the instability is not discovered until after the motor is in production, it is often difficult, time consuming, and expensive to fix the problem.

APPLICATIONS AND ADVANTAGES OF SOLID PROPELLANT ROCKETS:

Major Application Categories for Solid Propellant Rocket Motors

Two general types of solid propellants are in use. The first, the so called double-base propellant, consists of nitrocellulose and nitroglycerine, plus additives in small quantity. There is no separate fuel and oxidizer. The molecules are unstable, and upon ignition break apart and rearrange themselves, liberating large quantities of heat. These propellants lend themselves well to smaller rocket motors. They are often processed and formed by extrusion methods, although casting has also been employed.

The other type of solid propellant is the composite. Here, separate fuel and oxidized chemicals are used, intimately mixed in the solid grain. The oxidizer is usually ammonium nitrate, potassium chlorate, or ammonium chlorate, and often comprises as much as four-fifths or more of the whole propellant mix. The fuels used are hydrocarbons, such as asphaltic-type compounds, or plastics. Because the oxidizer has no significant structural strength, the fuel must not only perform well but must also supply the necessary form and rigidity to the grain. Much of the research in solid propellants is devoted to improving the physical as well as the chemical properties of the fuel.

Ordinarily, in processing solid propellants the fuel and oxidizer components are separately prepared for mixing, the oxidizer being a powder and the fuel a fluid of varying consistency. They are then blended together under carefully controlled conditions and poured into the prepared rocket case as a viscous semisolid. They are then caused to set in curing chambers under controlled temperature and pressure.

Solid propellants offer the advantage of minimum maintenance and instant readiness. However, the more energetic solids may require carefully controlled storage conditions, and may offer handling problems in the very large sizes, since the rocket must always be carried about fully loaded. Protection from mechanical shocks or abrupt temperature changes that may crack the grain is essential.

UNIT V

LIQUID PROPELLANT ROCKET ENGINES

PROPELLANT TYPES

SALIENT FEATURES OF LIQUID PROPELLANT ROCKETS: The propellants, which are the working substance of rocket engines, constitute the fluid that undergoes chemical and thermodynamic changes. The term liquid propellant embraces all the various liquids used and may be one of the following:

1. Oxidizer (liquid oxygen, nitric acid, etc.)
2. Fuel (gasoline, alcohol, liquid hydrogen, etc.).
3. Chemical compound or mixture of oxidizer and fuel ingredients, capable of self-decomposition.
4. Any of the above, but with a gelling agent.

A bipropellant rocket unit has two separate liquid propellants, an oxidizer and a fuel. They are stored separately and are not mixed outside the combustion chamber. The majority of liquid propellant rockets have been manufactured for bipropellant applications.

A monopropellant contains an oxidizing agent and combustible matter in a single substance. It may be a mixture of several compounds or it may be a homogeneous material, such as hydrogen peroxide or hydrazine.

Monopropellants are stable at ordinary atmospheric conditions but decompose and yield hot combustion gases when heated or catalyzed.

A cold gas propellant (e.g., nitrogen) is stored at very high pressure, gives a low performance, allows a simple system and is usually very reliable. It has been used for roll control and attitude control.

A cryogenic propellant is liquefied gas at low temperature, such as liquid oxygen (-183°C) or liquid hydrogen (-253°C). Provisions for venting the storage tank and minimizing vaporization losses are necessary with this type.

Storable propellants (e.g., nitric acid or gasoline) are liquid at ambient temperature and can be stored for long periods in sealed tanks. Space storable propellants are liquid in the environment of space; this storability depends on the specific tank design, thermal conditions, and tank pressure. An example is ammonia.

A gelled propellant is a thixotropic liquid with a gelling additive. It behaves like a jelly or thick paint. It will not spill or leak readily, can flow under pressure, will burn, and is safer in some respects.

SELECTION OF LIQUID PROPELLANTS:

Mission Definition: Purpose, function, and final objective of the mission of an overall system are well defined and their implications well understood. There is an expressed need for the mission, and the benefits are evident. The mission requirements are well defined. The payload, flight regime, vehicle, launch environment, and operating conditions are established. The risks, as perceived, appear acceptable. The project implementing the mission must have political, economic, and institutional support with assured funding. The propulsion system requirements, which are derived from mission definition, must be reasonable and must result in a viable propulsion system.

Affordability (Cost): Life cycle costs are low. They are the sum of R&D costs, production costs, facility costs, operating costs, and decommissioning costs, from inception to the retirement of the system. Benefits of achieving the mission should appear to justify costs. Investment in new facilities should be low. Few, if any, components should require expensive materials. For

attractive. No need to hire new, inexperienced personnel, who need to be trained and are more likely to make expensive errors.

System Performance: The propulsion system is designed to optimize vehicle and system performance, using the most appropriate and proven technology. Inert mass is reduced to a practical minimum, using improved materials and better understanding of loads and stresses. Residual (unused) propellant is minimal. Propellants have the highest practical specific impulse without undue hazards, without excessive inert propulsion system mass, and with simple loading, storing, and handling. Thrust-time profiles and number of restarts must be selected to optimize the vehicle mission. Vehicles must operate with adequate performance for all the possible conditions (pulsing, throttling, temperature excursions, etc.). Vehicles should be storable over a specified lifetime. Will meet or exceed operational life. Performance parameters (e.g., chamber pressure, ignition time, or nozzle area ratio) should be near optimum for the selected mission. Vehicle should have adequate TVC. Plume characteristics are satisfactory.

Survivability (Safety): All hazards are well understood and known in detail. If failure occurs, the risk of personnel injury, damage to equipment, facilities, or the environment is minimal. Certain mishaps or failures will result in a change in the operating condition or the safe shutdown of the propulsion system. Applicable safety standards must be obeyed. Inadvertent energy input to the propulsion system (e.g., bullet impact, external fire) should not result in a detonation. The probability for any such drastic failures should be very low. Safety monitoring and inspections must have proven effective in identifying and preventing a significant share of possible incipient failures. Adequate safety factors must be included in the design. Spilled liquid propellants should cause no undue hazards. All systems and procedures must conform to the safety standards. Launch test range has accepted the system as being safe enough to launch.

Reliability: Statistical analyses of test results indicate a satisfactory high-reliability level. Technical risks, manufacturing risks, and failure risks are very low, well understood, and the impact on the overall system is known. There are few complex components. Adequate storage and operating life of components (including propellants) have been demonstrated. Proven ability to check out major part of propulsion system prior to use or launch. If certain likely failures occur, the system must shut down safely. Redundancy of key components should be provided, where effective. High probability that all propulsion functions must be performed within the desired tolerances. Risk of combustion vibration or mechanical vibration should be minimal.

Controllability: Thrust buildup and decay are within specified limits. Combustion process is stable. The time responses to control or command signals are within acceptable tolerances. Controls need to be foolproof and not inadvertently create a hazardous condition. Thrust vector control response must be satisfactory. Mixture ratio control must assure nearly simultaneous emptying of the fuel and oxidizer tanks. Thrust from and duration of afterburning should be negligible. Accurate thrust termination feature must allow selection of final velocity of flight. Changing to an alternate mission profile should be feasible. Liquid propellant sloshing and pipe oscillations need to be adequately controlled. In a zero-gravity environment, a propellant tank should be essentially fully emptied.

Maintainability: Simple servicing, foolproof adjustments, easy parts replacement, and fast, reliable diagnosis of internal failures or problems. Minimal hazard to service personnel. There must be easy access to all components that need to be checked, inspected, or replaced. Trained maintenance personnel are available. Good access to items which need maintenance.

Geometric Constraints: Propulsion system fits into vehicle, can meet available volume, specified length, or vehicle diameter. There is usually an advantage for the propulsion system that has the smallest volume or the highest average density. If the travel of the center of gravity has to be controlled, as is necessary in some missions, the propulsion system that can do so with minimum weight and complexity will be preferred.

Prior Related Experience: There is a favorable history and valid, available, relevant data of similar propulsion systems supporting the practicality of the technologies, manufacturability, performance, and reliability. Experience and data validating computer simulation programs are available. Experienced, skilled personnel are available.

Operability: Simple to operate. Validated operating manuals exist. Procedures for loading propellants, arming the power supply, launching, igniter checkout, and so on, must be simple. If applicable, a reliable automatic status monitoring and check-out system should be available. Crew training needs to be minimal. Should be able to ship the loaded vehicle on public roads or railroads without need for environmental permits and without the need for a decontamination unit and crew to accompany the shipment. Supply of spare parts must be assured. Should be able to operate under certain emergency and overload conditions.

Producibility: Easy to manufacture, inspect, and assemble. All key manufacturing processes are well understood. All materials are well characterized, critical material properties are well known, and the system can be readily inspected. Proven vendors for key components have been qualified. Uses standard manufacturing machinery and relatively simple tooling. Hardware quality and propellant properties must be repeatable. Scrap should be minimal. Designs must make good use of standard materials, parts, common fasteners, and off-the-shelf components. There should be maximum use of existing manufacturing facilities and equipment. Excellent reproducibility, i.e., minimal operational variation between identical propulsion units. Validated specifications should be available for major manufacturing processes, inspection, parts fabrication, and assembly.

Schedule: The overall mission can be accomplished on a time schedule that allows the system benefits to be realized. R&D, qualification, flight testing, and/or initial operating capability are completed on a preplanned schedule. No unforeseen delays. Critical materials and qualified suppliers must be readily available.

Environmental Acceptability: No unacceptable damage to personnel, equipment, or the surrounding countryside. No toxic species in the exhaust plume. No serious damage (e.g., corrosion) due to propellant spills or escaping vapors. Noise in communities close to a test or launch site should remain within tolerable levels. Minimal risk of exposure to cancer-causing

chemicals. Hazards must be sufficiently low, so that issues on environmental impact statements are not contentious and approvals by environmental authorities become routine. There should be compliance with applicable laws and regulations. No unfavorable effects from currents generated by an electromagnetic pulse, static electricity, or electromagnetic radiation.

Reusability: Some applications (e.g., Shuttle main engine, Shuttle solid rocket booster, or aircraft rocket assisted altitude boost) require a reusable rocket engine. The number of flights, serviceability, and the total cumulative firing time then become key requirements that will need to be demonstrated. Fatigue failure and cumulative thermal stress cycles can be critical in some of the system components. The critical components have been properly identified; methods, instruments, and equipment exist for careful check-out and inspection after a flight or test (e.g., certain leak tests, inspections for cracks, bearing clearances, etc.). Replacement and/or repair of unsatisfactory parts should be readily possible. Number of firings before disassembly should be large, and time interval between overhauls should be long.

Other Criteria: Radio signal attenuation by exhaust plume to be low. A complete propulsion system, loaded with propellants and pressurizing fluids, can be storable for a required number of years without deterioration or subsequent performance decrease. Interface problems are minimal. Provisions for safe packaging and shipment are available. The system includes features that allow decommissioning (such as to deorbit a spent satellite) or disposal (such as the safe removal and disposal of over-age propellant from a refurbishable rocket motor).

INJECTOR: The functions of the injector are similar to those of a carburetor of an internal combustion engine. The injector has to introduce and meter the flow of liquid propellants to the combustion chamber, cause the liquids to be broken up into small droplets (a process called atomization), and distribute and mix the propellants in such a manner that a correctly proportioned mixture of fuel and oxidizer will result, with uniform propellant mass flow and composition over the chamber cross section. This has been accomplished with different types of injector designs and elements; several common types are shown in Fig. 4.1 and complete injectors are shown in Fig. 4.2.

The injection hole pattern on the face of the injector is closely related to the internal manifolds or feed passages within the injector. These provide for the distribution of the propellant from the injector inlet to all the injection holes. A large complex manifold volume allows low passage velocities and good distribution of flow over the cross section of the chamber. A small manifold volume allows for a lighter weight injector and reduces the amount of "dribble" flow after the main valves are shut. The higher passage velocities cause a more uneven flow through different identical injection holes and thus a poorer distribution and wider local gas composition variation. Dribbling results in afterburning, which is an inefficient irregular combustion that gives a little "cutoff" thrust after valve closing. For applications with very accurate terminal vehicle velocity requirements, the cutoff impulse has to be very small and reproducible and often valves are built into the injector to minimize passage volume.

Impinging-stream-type, multiple-hole injectors are commonly used with oxygen-hydrocarbon and storable propellants. For *unlike doublet* patterns the propellants are injected through a number of separate small holes in such a manner that the fuel and oxidizer streams

The non-impinging or shower head injector employs non impinging streams of propellant usually emerging normal to the face of the injector. It relies on turbulence and diffusion to achieve mixing. The German World War II V-2 rocket used this type of injector. This type is now not used, because it requires a large chamber volume for good combustion. Sheet or spray-type injectors give cylindrical, conical, or other types of spray sheets; these sprays generally intersect and thereby promote mixing and atomization. By varying the width of the sheet (through an axially moveable sleeve) it is possible to throttle the propellant flow over a wide range without excessive reduction in injector pressure drop. This type of variable area concentric tube injector was used on the descent engine of the Lunar Excursion Module and throttled over a 10:1 range of flow with only a very small change in mixture ratio.

The coaxial hollow post injector has been used for liquid oxygen and gaseous hydrogen injectors by most domestic and foreign rocket designers. It is shown in the lower left of Fig. 4.1. It works well when the liquid hydrogen has absorbed heat from cooling jackets and has been gasified. This gasified hydrogen flows at high speed (typically 330 m/sec or 1000 ft/sec); the liquid oxygen flows far more slowly (usually at less than 33 m/sec or 100 ft/sec) and the differential velocity causes a shear action, which helps to break up the oxygen stream into small droplets. The injector has a multiplicity of these coaxial posts on its face. This type of injector is not used with liquid storable bipropellants, in part because the pressure drop to achieve high velocity would become too high.

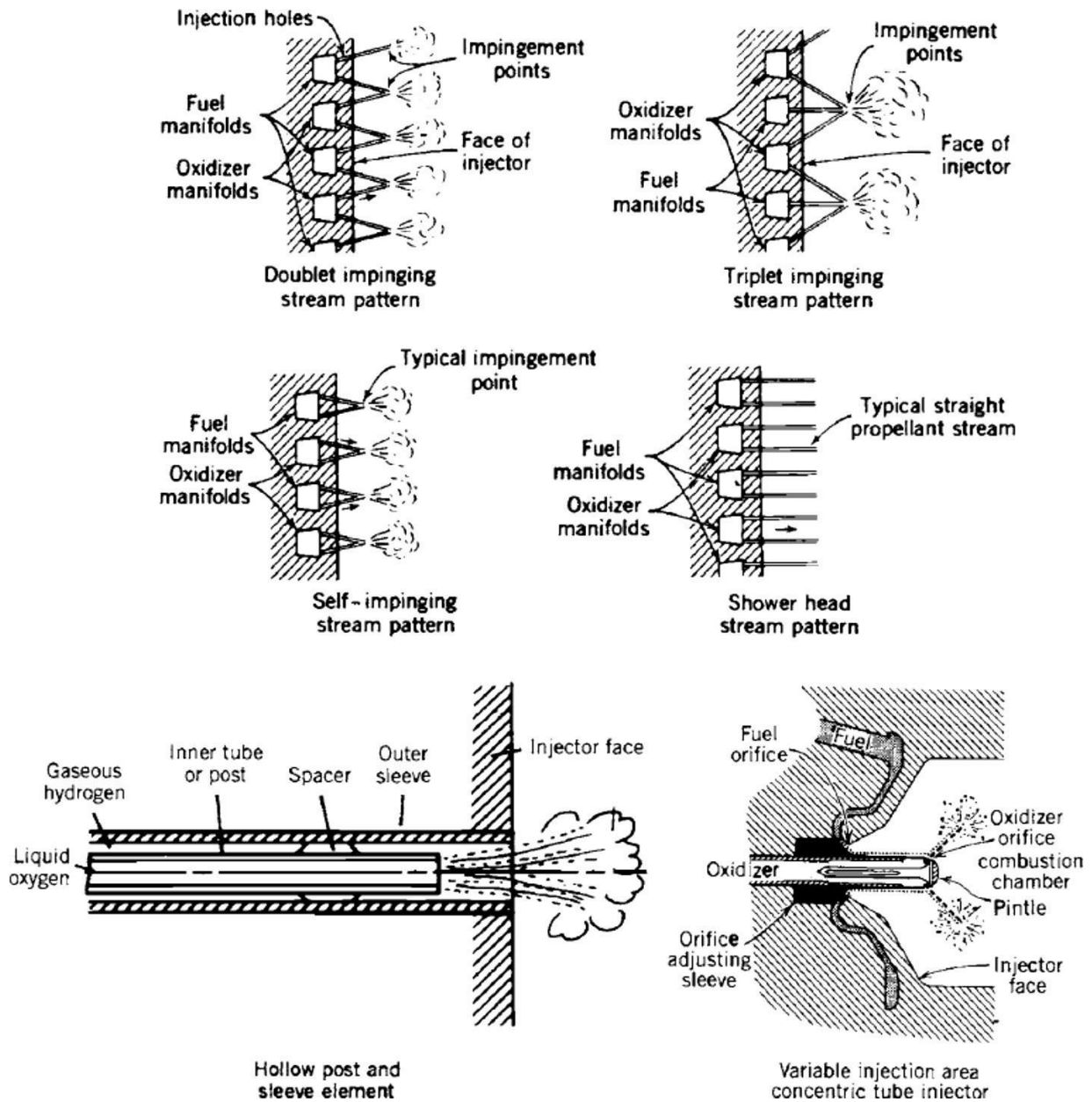


Figure 4.1 Schematic diagrams of several injector types. The movable sleeve type variable thrust injector

The SSME injector uses 600 concentric sleeve injection elements; 75 of them have been lengthened beyond the injector face to form cooled baffles, which reduce the incidence of combustion instability.

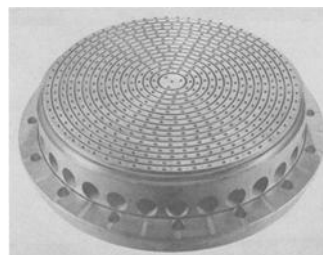
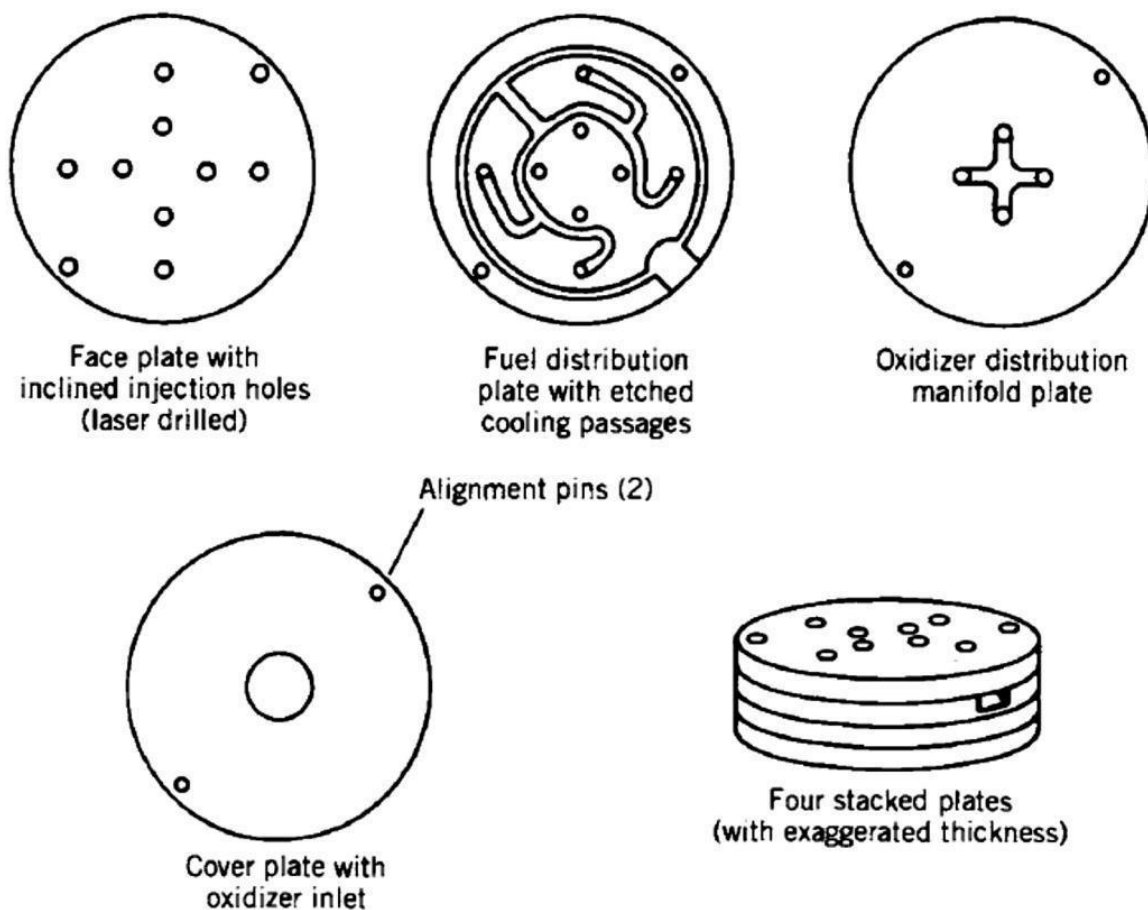


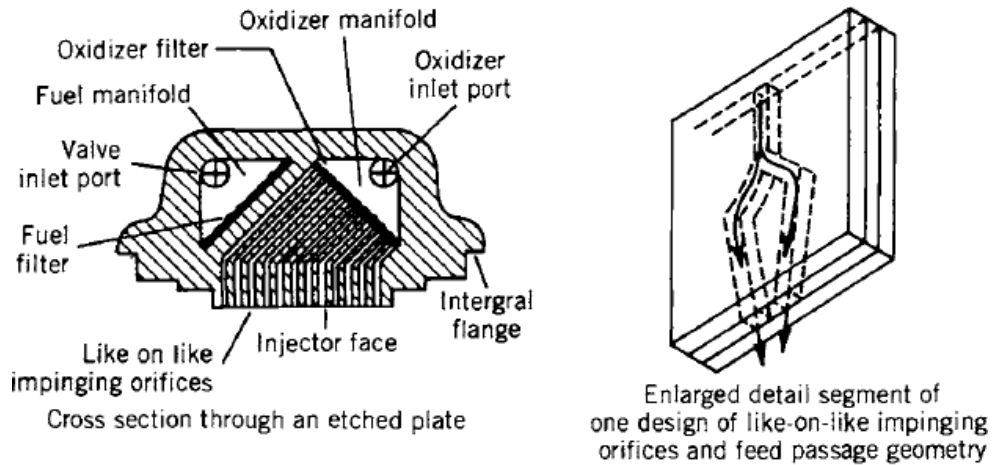
Figure 4.2: injector

Figure 4.2 Injector with 90° self-impinging (fuel-against-fuel and oxidizer-against oxidizer) - type countersunk doublet injection pattern. Large holes are inlets to fuel manifolds. Pre-drilled rings are brazed alternately over an annular fuel manifold or groove and a similar adjacent oxidizer manifold or groove.

The original method of making injection holes was to carefully drill them and round out or chamfer their inlets. This is still being done today. It is difficult to align these holes accurately (for good impingement) and to avoid burrs and surface irregularities. One method that avoids these problems and allows a large number of small accurate injection orifices is to use multiple etched, very thin plates (often called platelets) that are then stacked and diffusion bonded together to form a monolithic structure as shown in Fig.4. 3. The photo-etched pattern on each of the individual plates or metal sheets then provides not only for many small injection orifices at the injector face, but also for internal distribution or flow passages in the injector and sometimes also for a fine-mesh filter inside the injector body. The platelets can be stacked parallel to or normal to the injector face. The finished injector has been called the platelet injector and has been patented by the Aero jet Propulsion Company.



(a)



(b)

Figure 4.3 Simplified diagrams of two types of injector using a bonded platelet construction technique: (a) injector for low thrust with four impinging unlike doublet liquid streams; the individual plates are parallel to the injector face; (b) Like-on-like impinging stream injector with 144 orifices; plates are perpendicular to the injector face.

PROPELLANT FEED SYSTEMS:

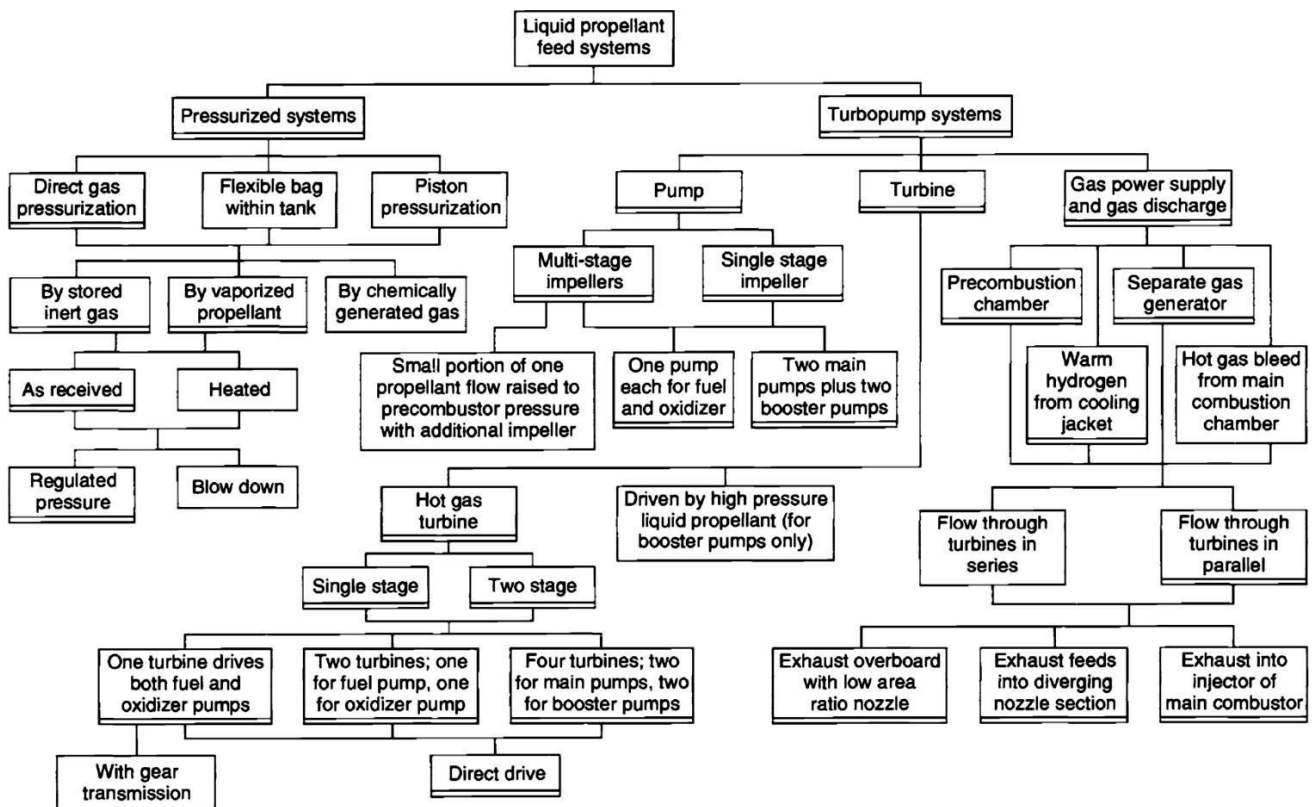


Figure 4.4 Design options of feed systems for liquid propellant rocket engines. The more common types are designated with a double line at the bottom of the box.

The propellant feed system has two principal functions: to raise the pressure of the propellants and to feed them to one or more thrust chambers. The energy for these functions comes either from a high- pressure gas, centrifugal pumps, or a combination of the two. The selection of a particular feed system and its components is governed primarily by the application of the rocket, duration, number or type of thrust chambers, past experience, mission, and by general requirements

of simplicity of design, ease of manufacture, low cost, and minimum inert mass. A classification of several of the more important types of feed system is shown in Fig. 4.4 and some are discussed in more detail below. All feed systems have piping, a series of valves, provisions for filling and removing (draining and flushing) the liquid propellants, and control devices to initiate, stop, and regulate their flow and operation.

In general, a pressure feed system gives a vehicle performance superior to a turbo pump system when the total impulse or the mass of propellant is relatively low, the chamber pressure is low, the engine thrust-to-weight ratio is low (usually less than 0.6), and when there are repeated short-duration thrust pulses; the heavy-walled tanks for the propellant and the pressurizing gas usually constitute the major inert mass of the engine system. In a turbo pump feed systems the propellant tank pressures are much lower (by a factor of 10 to 40) and thus the tank masses are much lower (again by a factor of 10 to 40).

Turbo pump systems usually give a superior vehicle performance when the total impulse is large (higher Au) and the chamber pressure is higher. The pressurized feed system can be relatively simple, such as for a single operation, factory-preloaded, simple unit (with burst diaphragms instead of some of the valves), or quite complex, as with multiple restartable thrusters or reusable systems. If the propulsion system is to be reusable or is part of a manned vehicle (where the reliability requirements are very high and the vehicle's crew can monitor and override automatic commands), the feed system becomes more complex (with more safety features and redundancies) and more expensive.

The pneumatic (pressurizing gas) and hydraulic (propellant) flows in a liquid propellant engine can be simulated in a computer analysis that provides for a flow and pressure balance in the oxidizer and the fuel flow paths through the system. Some of these analyses can provide information on transient conditions (filling up of passages) during start, flow decays at cutoff, possible water hammer, or flow instabilities.

THRUST CONTROL COOLING IN LIQUID PROPELLANT ROCKETS AND THE ASSOCIATED HEAT TRANSFER PROBLEMS:

Liquid rocket engines developed for space missions encompass a wide spectrum of performance and structural requirements.

Thrust levels may vary from a few Newtons to many thousands of Newtons, with burning time from fraction of a second to hours. In all these engines, the energy released by the propellants must be contained inside the thrust chamber and accelerated through the nozzle to extract the thrust. Extremely high heat flux levels and temperature gradients are present not only in the immediate vicinity of the injector head, but also in the nozzle throat region.

It is seen that the maximum heat flux occurs in the close proximity to nozzle throat, and an effective cooling of the throat area is crucial for enhanced reliability and reusability. Regenerative cooling is the standard cooling system for almost all modern main stage, booster, and upper stage engines. Different cooling techniques such as film cooling, transpiration cooling, ablative cooling, radiation cooling, heat sink cooling and dump cooling have been developed in the past to reduce regenerative cooling load and propellant requirements. Film cooling can be employed either at the combustion chamber or at the nozzle of a rocket engine.

Liquid film cooling with fuel or oxidizer as the coolant can be employed in the combustion chambers of gas generator/expander/staged combustion cycle engines. In case of gas generator cycle, the turbine exhaust gas can be used as a gaseous film coolant in the combustion chamber or nozzle sections. It is found that all these methods lead to reduced wall temperatures. The mechanism by which film cooling maintains a lower combustor wall temperature is considerably different from that of convective cooling. Film cooling is accomplished by interposing a layer of coolant fluid between the surface to be protected and the hot gas stream. The fluid is introduced directly into the combustion

chamber through slots or holes and is directed along the walls (Figure 4.5). A typical temperature distribution from the hot combustion gases to the exterior of the chamber wall in a film cooled

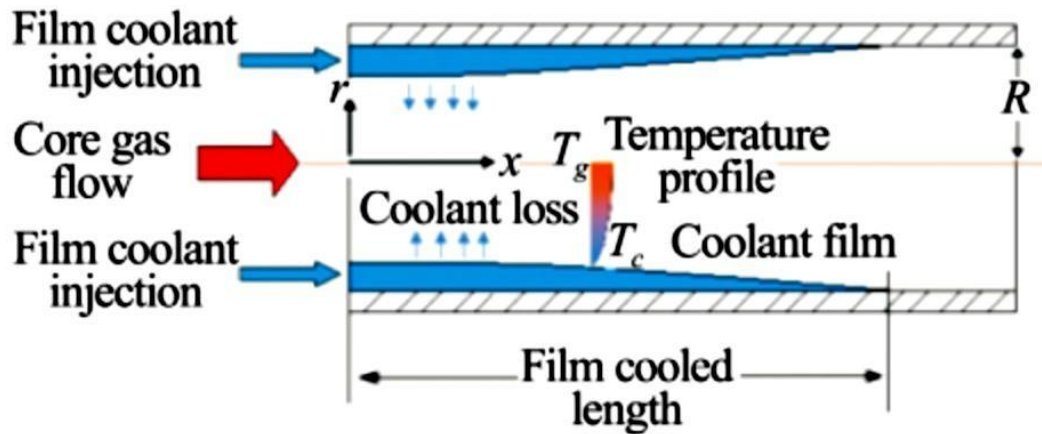


Figure 4.5: Schematic of the physical system

Combustion chamber is shown in Figure 4.6. It can be observed that the coolant film produces a thermal insulation effect and reduces the chamber wall temperature. Coolant film may be generated by injecting liquid fuel or oxidizer through wall slots or holes in the combustion chamber, or through the propellant injector. The cooling effect will persist up to the throat region in the case of a shorter combustion chamber. In a fully film-cooled design, injection points are located at incremental distances along the wall length.

In liquid film cooling, the vaporized film coolant does not diffuse rapidly into the main gas stream but persists as a protective layer of vapor adjacent to the wall for an appreciable distance downstream from the terminus of the liquid film. The film coolant also forms a protective film which restricts the transport of the combustion products to the wall, thus reducing the rate of oxidation of the walls.

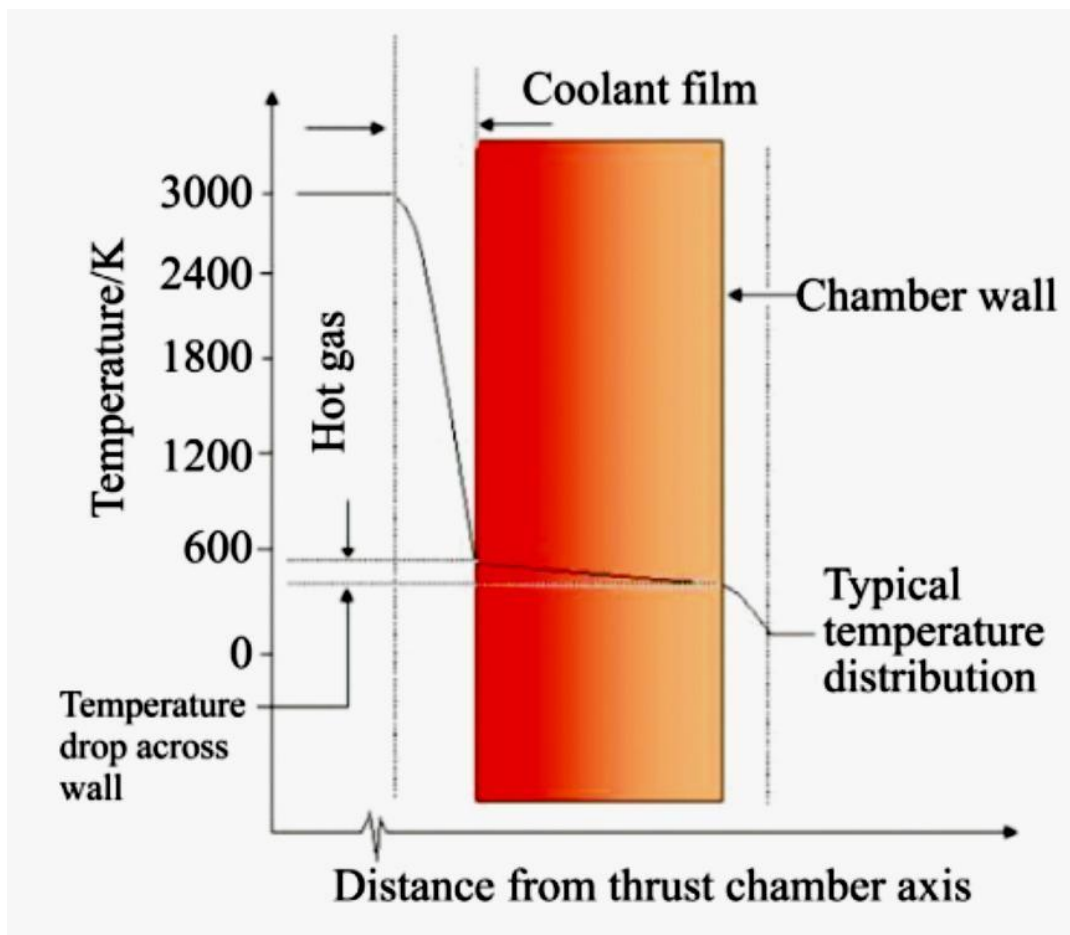


Figure 4.6 Typical temperature distribution of combustion chamber across wall

COMBUSTION INSTABILITY IN LIQUID PROPELLANT ROCKETS:

If the process of rocket combustion is not controlled (by proper design), then combustion instabilities can occur which can very quickly cause excessive pressure vibration forces (which may break engine parts) or excessive heat transfer (which may melt thrust chamber parts). The aim is to prevent occurrence of this instability and to maintain reliable operation.

Although much progress has been made in understanding and avoiding combustion instability, new rocket engines can still be plagued by it.

Table below lists the principal types of combustion vibrations encountered in liquid rocket thrust chambers. Admittedly, combustion in a liquid rocket is never perfectly smooth; some fluctuations of pressure, temperature, and velocity are always present. When these fluctuations interact with the natural frequencies of the propellant feed system (with and without vehicle structure) or the chamber acoustics, periodic superimposed oscillations, recognized as instability, occur. In normal rocket practice smooth combustion occurs when pressure fluctuations during steady operation do not exceed about $\pm 5\%$ of the mean chamber pressure. Combustion that gives greater pressure fluctuations at a chamber wall location which occur at completely random intervals is called rough combustion. Unstable combustion, or combustion instability, displays organized oscillations occurring at well-defined intervals with a pressure peak that may be maintained, may increase, or may die out. These periodic peaks, representing fairly large concentrations of vibratory energy, can be easily recognized against the random-noise background in fig 4.7.

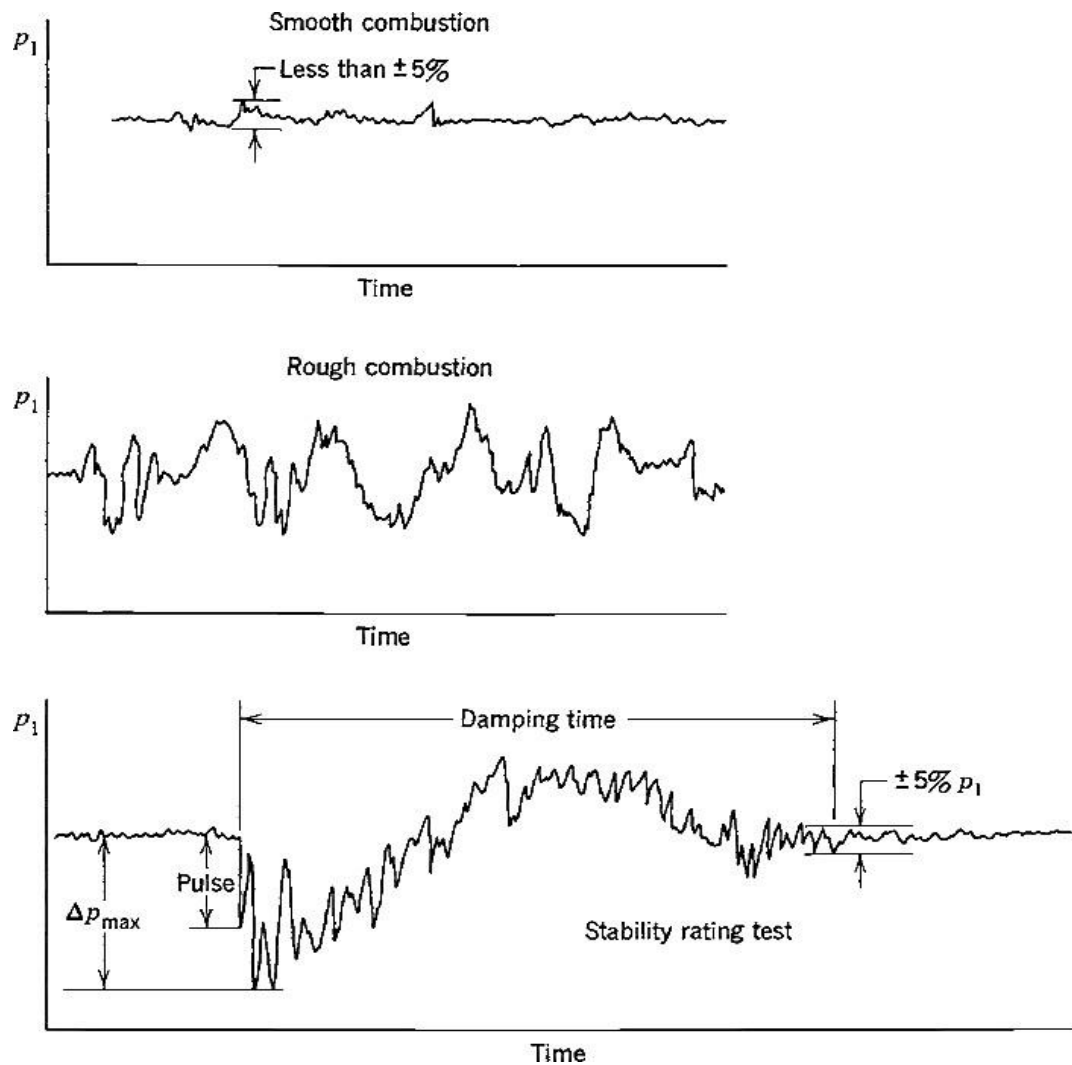


Fig. 4.7 Typical oscillograph traces of chamber pressure P_1 with time for different combustion events.

PRINCIPAL TYPES OF COMBUSTION INSTABILITY:

Type and word description	Frequency	Cause relationship
Low frequency, called chugging or feed system instability	10-400	Linked with pressure interactions between propellant feed system, if not the entire vehicle, and combustion chamber
Intermediate frequency, called acoustic, a buzzing, or entropy waves	400-1000	Linked with mechanical vibrations of propulsion structure, injector manifold, flow eddies, fuel/oxidizer ratio fluctuations, and propellant feed system resonances
High frequency, called screaming, screeching, or squealing	Above 1000	Linked with combustion process forces (pressure waves) and chamber acoustical resonance properties

PROBLEMS ASSOCIATED WITH OPERATION OF CRYOGENIC ENGINES:

Peculiar problems associated with operation of cryogenic engines. The thrust comes from the rapid expansion from liquid to gas with the gas emerging from the motor at very high speed. The energy needed to heat the fuels comes from burning them, once they are gasses. Cryogenic engines are the highest performing rocket motors. Cryogenic engines are fundamentally different from electric motors because there isn't anything rotating in them. They're essentially reaction engines. By 'reaction' I'm referring to Newton's law: "to every action there is an equal and opposite reaction. "The cryogenic (or rocket) engine throws mass in one direction, and the reaction to this is a thrust in the opposite direction. Therefore, to get the required mass flow rate, the only option was to cool the propellants down to cryogenic temperatures (below $-183\text{ }^{\circ}\text{C}$ [90 K], $-253\text{ }^{\circ}\text{C}$ [20 K]), converting them to liquid form. Hence, all cryogenic rocket engines are also, by definition, either liquid-propellant rocket engines or hybrid rocket engines

Introduction to hybrid rocket propulsion-standard and reverse hybrid systems-combustion mechanism in hybrid propellant rockets applications and limitations.

INTRODUCTION TO HYBRID ROCKET PROPULSION:

Rocket propulsion concepts in which one component of the propellant is stored in liquid phase while the other is stored in solid phase are called hybrid propulsion systems. Such systems most commonly employ a liquid oxidizer and solid fuel. Various combinations of solid fuels and liquid oxidizers as well as liquid fuels and solid oxidizers have been experimentally evaluated for use in hybrid rocket motors. Most common is the liquid oxidizer-solid fuel concept shown in Fig. 4.8. Illustrated here is a large pressure-fed hybrid booster configuration. The means of pressurizing the liquid oxidizer is not an important element of hybrid technology and a turbo pump system could also perform this task. The oxidizer can be either a non-cryogenic (storable) or a cryogenic liquid, depending on the application requirements.

In this hybrid motor concept, oxidizer is injected into a pre combustion or vaporization chamber upstream of the primary fuel grain. The fuel grain contains numerous axial combustion ports that generate fuel vapor to react with the injected oxidizer. An aft mixing chamber is employed to ensure that all fuel and oxidizer are burned before exiting the nozzle.

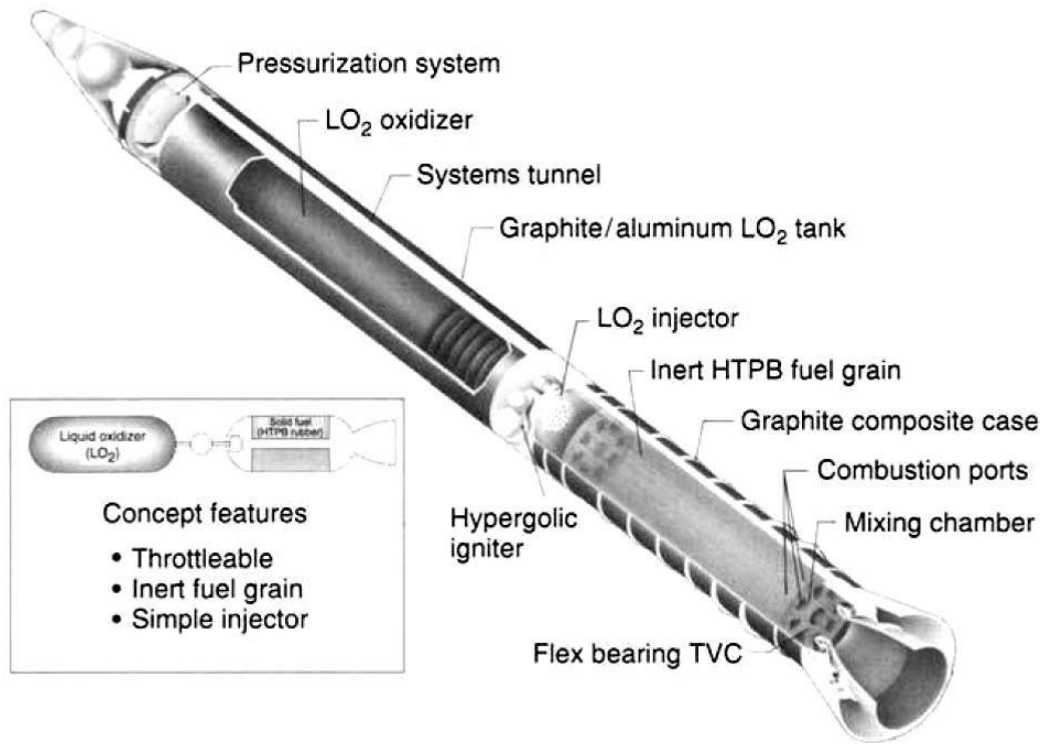
The main advantages of a hybrid rocket propulsion system are:

- (1) Safety during fabrication, storage, or operation without any possibility of explosion or detonation;
- (2) start-stop-restart capabilities;
- (3) Relatively low system cost;
- (4) Higher specific impulse than solid rocket motors and higher density-specific impulse than liquid bipropellant engines; and
- (5) The ability to smoothly change motor thrust over a wide range on demand.

The disadvantages of hybrid rocket propulsion systems are:

- (1) Mixture ratio and, hence, specific impulse will vary somewhat during steady-state operation and throttling;
- (2) lower density-specific impulse than solid propellant systems;
- (3) some fuel sliver must be retained in the combustion chamber at end-of burn, which slightly reduces motor mass fraction; and
- (4) Unproven propulsion system feasibility at large scale.

STANDARD AND REVERSE HYBRID SYSTEMS :



- Concept features
- Throttleable
 - Inert fuel grain
 - Simple injector

Figure 4.8. Large hybrid rocket booster concept capable of boosting the Space Shuttle. It has an inert solid fuel grain, pressurized liquid oxygen feed system, and can be throttled.

: HYBRID ROCKET CONFIGURATION:

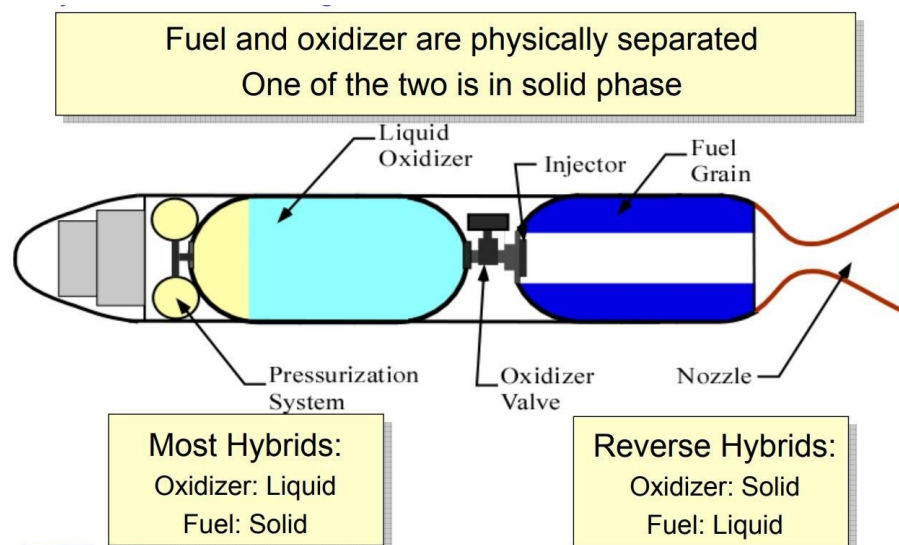


Figure 4.9 hybrid rocket

The hybrid is inherently safer than other rocket designs. The idea is to store the oxidizer as a liquid and the fuel as a solid, producing a design that is less susceptible to chemical explosion than conventional solid and bi-propellant liquid designs. The fuel is contained within the rocket combustion chamber in the form of a cylinder with a circular channel called a port hollowed out along its axis. Upon ignition, a diffusion flame forms over the fuel surface along the length of the port. The combustion is sustained by heat transfer from the flame to the solid fuel causing continuous fuel vaporization until the oxidizer flow is turned off. In the event of a structural failure, oxidizer and fuel cannot mix intimately leading to a catastrophic explosion that might endanger personnel or destroy a launch pad.

The hybrid rocket requires one rather than two liquid containment and delivery systems. The complexity is further reduced by omission of a regenerative cooling system for both the chamber and nozzle. Throttling control in a hybrid is simpler because it alleviates the requirement to match the momenta of the dual propellant streams during the mixing process. Throttle ratios up to 10 have been common in hybrid motors. The fact that the fuel is in the solid phase makes it very easy to add performance enhancing materials to the fuel such as aluminum powder. In principle, this could enable the hybrid to gain an I_{sp} advantage over a comparable hydrocarbon fueled liquid system.

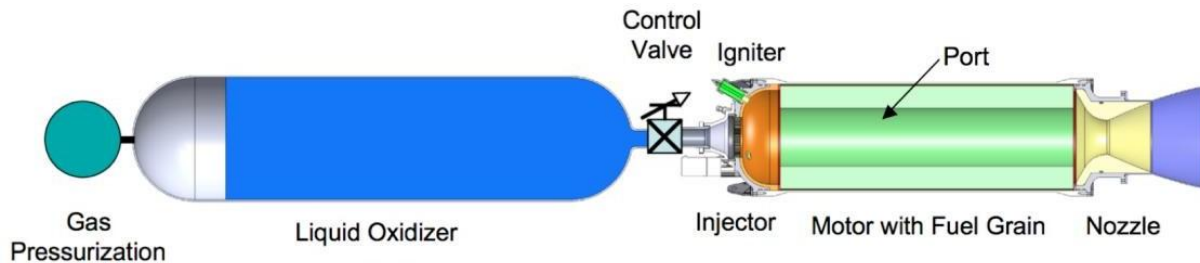


Fig. 4.10 Schematic of a hybrid rocket motor.

: COMBUSTION MECHANISM IN HYBRID PROPELLANT ROCKETS

The process in a hybrid rocket combustion chamber over a large portion of the chamber constitutes the diffusive combustion in the boundary layer very close to the regressing fuel surface. The initial part is dominated by processes of impingement of the liquid oxidizer (which is sprayed by an injector) on the fuel surface and its vaporisation. Since the process is essentially diffusion-dominated, chemical kinetics, and therefore pressure, have a relatively smaller effect. It is the flux of hot gases (consisting of the products of combustion and oxidizer not yet utilised) past the fuel surface which primarily affects the regression of the fuel. The regression rate law can be deduced from the boundary layer considerations as was first accomplished by Marxman & Gilbert (1963). The law reads that $rh=aG^n$, where G is the mass flux of hot gases past the surface, a and n are constants; typically a 0.01--0.03 cm/s (flux) n , $n=0.5$ for laminar flow and 0.8 for turbulent flow.

Now it is possible to explain some features of hybrid engines. First, the O/F of a hybrid engine is not necessarily constant throughout the firing. Using the expression, we can express O/F in terms of the inner diameter of the cylindrical fuel block burning from inside outwards as

$$O/F \simeq d^{2n-1} (m_{ox}/\pi)^{1-n} / \rho_p a L,$$

Where d =inner diameter of the port and L is the length of the fuel block. If $n=0.5$, as in the case of laminar flow, O/F is a constant and does not change during the firing; and if $n=0.8$, as in the case of turbulent flow, the value of O/F increases during the firing, showing that the products become oxidiser-rich. This, in fact, causes changes in the specific impulse of the system during the firing. There are ways of combating this problem (see Anon 1964). One of these is to fix the initial operating point on a slightly fuel-rich side so that when the operating point moves to the oxidiser-rich side, the specific impulse does not vary by more than 1-2%. Another technique which maintains a constant O/F level is to use two oxidiser injection points, one near the head end and the other near the aft end. In the early part of the firing the burning is fuel-rich and aft end injection is used to optimize it.

During the later part of the firing the products of combustion from the end of the fuel block tend towards oxidiser-richness and so aft-end injection is reduced to maintain the same O/F level.

The second feature concerns the low explosion hazard during storage, transportation and firing. That the explosion and fire hazard are small compared to that for a solid rocket is easy to appreciate because the solid rocket has the fuel and oxidizer imbedded in the same matrix whereas the hybrid has the solid fuel and liquid oxidizer separately stored. And in the event of an accidental initiation, the former can burn by itself, whereas the fuel in the hybrid rocket has to receive oxidiser for its combustion.

The fire hazard of the hybrid is smaller than of liquids because, in the event of an explosion, the liquids of a liquid rocket can flow, widely spread and get mixed up, while the fuel and oxidiser in the hybrid have greater resistance to large scale mixing since the fuel is in the form of a solid.

We can further argue that a crack or a tiny hole in the fuel block of a hybrid causes little or no change in the performance, whereas the same crack or hole in a solid propellant may cause explosion. To appreciate this we notice that the regression of the fuel occurs under the action of a heat flux from the diffusion flame. Thus any area of the fuel which receives less heat flux will regress less. The tiny hole represents a zone which is farther away from the flame and hence receives less heat flux and so will regress less. This means that the tiny hole evens out instead of becoming larger as in a solid rocket and the perturbation due to changed mass flow becomes small as burning progresses.

The third feature concerns the sensitivity of the regression rate to the nature of fuel. It has already been noted that addition of even a small amount of some compounds can disastrously alter the burning rate of a solid propellant. The situation is quite the opposite in the case of hybrids. The regression rate is negligibly dependent on the nature of fuels, even when they are as different as polystyrene and natural rubber or polybutadiene. The reason for this lies in the counter-balancing effect called 'blowing effect'. This effect is simply that the burning rate does not linearly scale with the ratio of the input heat flux to heat of phase transformation at the surface, but less (in fact, much less) strongly dependent on it. If we invoke the heat balance at the surface of the burning fuel, we have

$$\rho_p r_h = \dot{q}'' / (\Delta h)_s,$$

where $(\Delta h)_s$ is the heat of phase change at the surface (including that needed for degradation) and \dot{q}'' , the heat flux into the surface. Now, if by some mechanism r_h increases by decrease of $(\Delta h)_s$, this increase in r_h causes an increase in boundary layer thickness, hence, reduction in gradients at the surface and in heat flux. The net result is of course, an increase in regression rate but much less than is to be expected from the linear relation. This effect is so significant that a 10% increase in \dot{q}'' leaves r_h virtually unaltered. Even a 35% increase in \dot{q}'' causes only a 10% increase in the regression rate (Marxman & Gilbert 1963).

Similar arguments can be used to explain why the initial temperature change causes much less change in the regression rate of a hybrid fuel than in the burning rate of a solid propellant.

- The purpose is to predict the regression rate.

Assumptions:

- Steady-state operation.
- Simple grain configuration (flat plate).
- No exothermic reactions in the solid grain (No oxidizer in solid phase).
- Oxidizer enters the port as a uniform gas.

- $Le = Pr = 1$ ($Le = k/D$)
- No heat transfer to the ambient air through the walls of the rocket.
- All kinetic effects are neglected (Characteristic times for all chemical rxns \ll characteristic times for diffusion processes).
- Flame zone is infinitely thin. (Flame sheet). No oxidizer beneath the flame.
- Boundary layer is turbulent.

- Energy balance at the fuel surface: (Steady-state)

$$\dot{Q}_w = \dot{m}_f h_v = \rho_f \dot{r} h_v = (\rho v)_w h_v$$

\dot{Q}_w = Total heat flux to the wall

h_v = Effective heat of gasification (Heating of the solid fuel grain + Heat of evaporation and melting + Heat of reaction for degradation of the polymer)

- End result:

$$\dot{r}(x) = AG^{0.8} x^{-0.2}$$

- Space time averaged regression rate ($n \sim 0.5-0.8$)

$$\bar{\dot{r}} = aG_o^n$$

Limitations of the Theory:

Each propellant combination has an upper and lower limit for the mass flux beyond which the model is not applicable.

- High mass fluxes Kinetic effects (Pressure dependency via the gas phase rxn rates)
- Low mass fluxes Radiation effects (Pressure dependency via the radiation effects)
- Transition to laminar boundary layer
- Cooking of the propellant (at very low regression rates)
- Dilution of the oxidizer

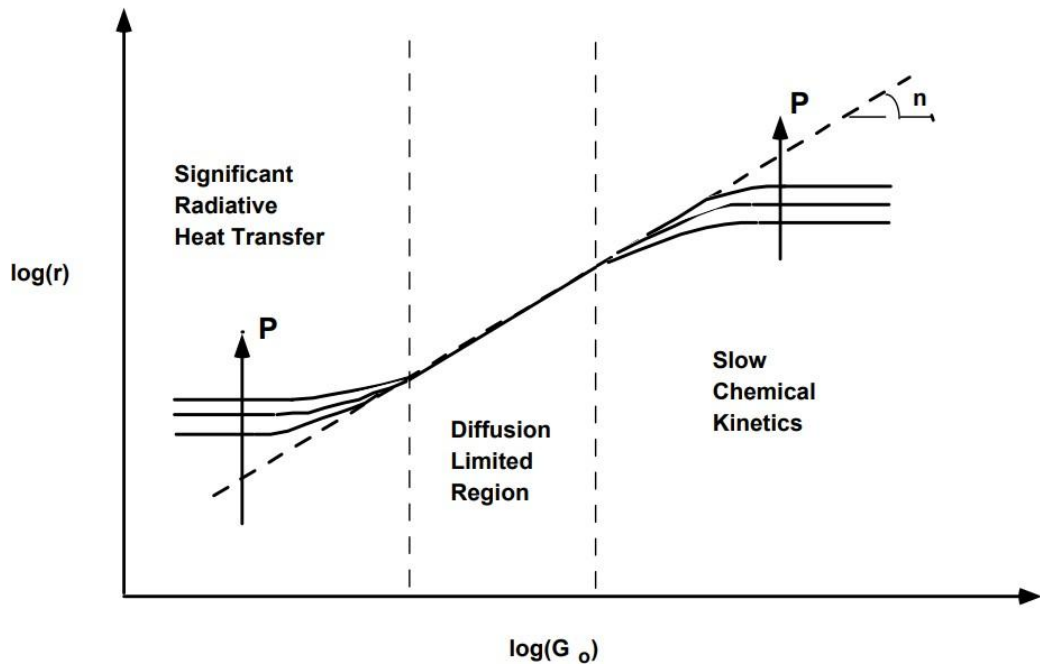


Figure 4.11 Effect of Pressure on the Regression Rate

- The heat conduction equation in the solid in reference of frame fixed to the regressing surface

$$\kappa \equiv \lambda_f / \rho_f C_{pf}$$

- During Steady state operating this expression can be integrated to yield

$$T(x) = (T_s - T_a)e^{-x/\delta_T} + T_a$$

- Here the characteristic thermal thickness can be given as

$$\delta_T = \kappa / \dot{r}$$

- Similarly the characteristics time is

$$\tau_T = \kappa / \dot{r}^2$$

- During typical operation of a polymeric hybrid fuel

$$\delta_T = 10^{-6} / 10^{-3} = 10^{-3} \text{ m} \quad \tau_T = 10^{-6} / 10^{-6} = 1 \text{ sec}$$

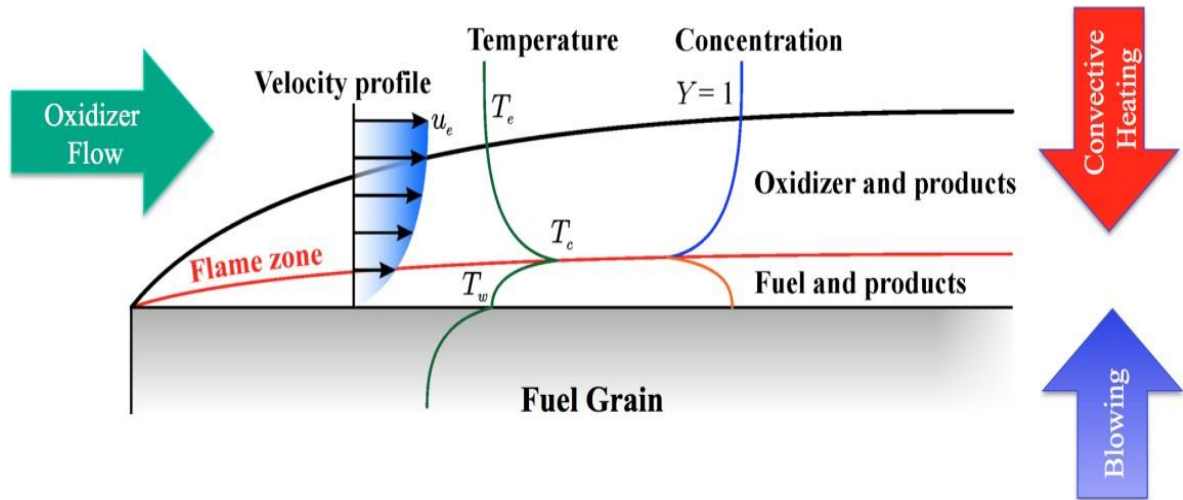
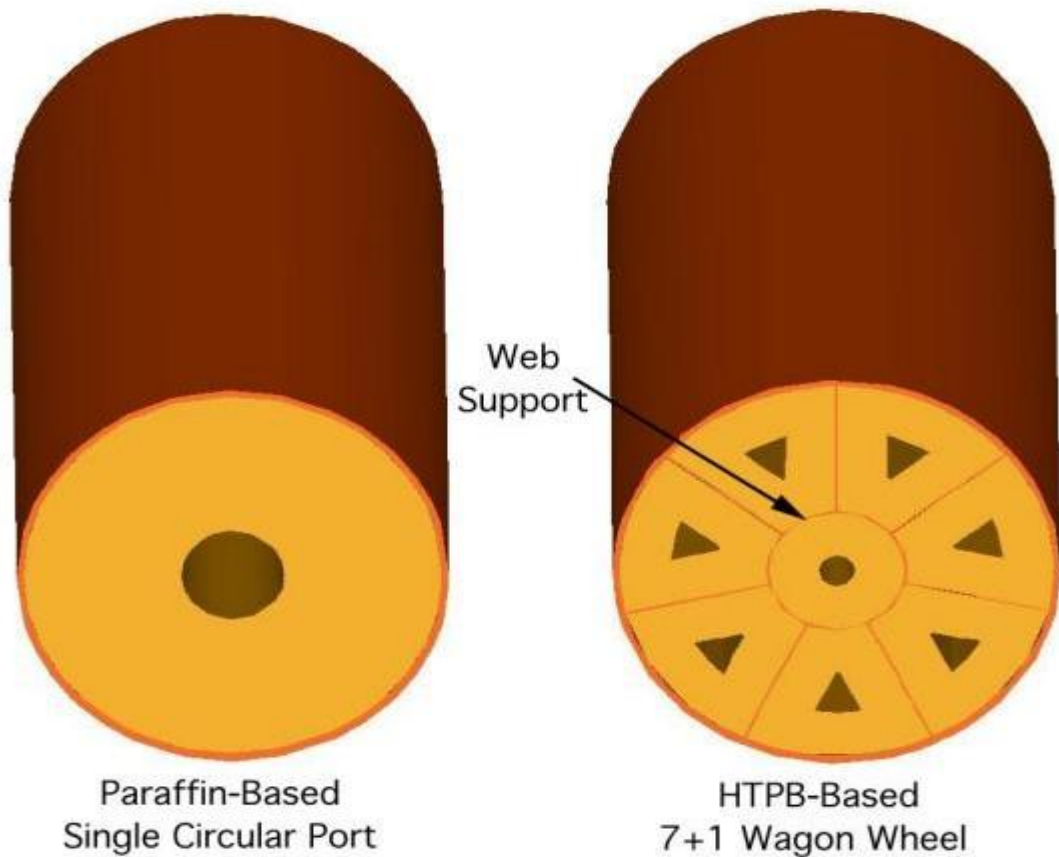


Fig. 4.12 Boundary layer combustion.

Disadvantage of Classical Hybrids:

Low Burning Rates --> Multi-port design

- Issues with multi-port design
- Excessive unburned mass fraction (i.e. typically in the 5% to 10% range).
- Complex design/fabrication, requirement for a web support structure.
- Compromised grain structural integrity, especially towards the end of the burn.
- Uneven burning of individual ports.
- Requirement for a substantial pre combustion chamber or individual injectors for each port.



APPLICATIONS:

Hybrid propulsion is well suited to applications or missions requiring throttling, command shutdown and restart, long-duration missions requiring storable nontoxic propellants, or infrastructure operations (manufacturing and launch) that would benefit from a non-self-deflagrating propulsion system.

Such applications would include primary boost propulsion for space launch vehicles, upper stages, and satellite maneuvering systems.

Many early hybrid rocket motor developments were aimed at target missiles and low-cost tactical missile applications (Ref. 15-1). Other development efforts focused on high-energy upper-stage motors. In recent years development efforts have concentrated on booster prototypes for space launch applications.

ADVANTAGES OF HYBRID PROPELLANTS:

Compared to	Solids	Liquids
Simplicity	<ul style="list-style-type: none"> ○ Chemically Simpler ○ Tolerant to processing errors 	<ul style="list-style-type: none"> ○ Mechanically Simpler ○ Tolerant to fabrication errors
Safety	<ul style="list-style-type: none"> ○ Reduced Chemical Explosion hazard ○ Thrust termination and Abort possibility 	<ul style="list-style-type: none"> ○ Reduced fire hazard ○ Less prone to hard starts
Performance Related	<ul style="list-style-type: none"> ○ Better Isp Performance ○ Throttling/Restart capability 	<ul style="list-style-type: none"> ○ Higher fuel density ○ Easy inclusion of solid performance additives (Al, Be)
Other	<ul style="list-style-type: none"> ○ Reduced Environmental impact 	<ul style="list-style-type: none"> ○ Reduced number and mass of liquids
Cost	<ul style="list-style-type: none"> ○ Reduced Development costs are expected ○ Reduced recurring costs are expected 	